SEISMIC RESPONSE MAPPING OF SAINT LOUIS COUNTY

Richard W. Stephenson and John D. Rockaway

University of Missouri, Rolla
Rolla, Missouri 65401

USGS CONTRACT NO. 14-08-0001-G518
Supported by the EARTHQUAKE HAZARDS REDUCTION PROGRAM

OPEN-FILE NO.81-382

U.S. Geological Survey
OPEN FILE REPORT

Seismic Response Mapping of Saint Louis County

Sponsored by the

United States Geological Survey

NO. 14-08-0001-G-518

($50,398.00)

Effective Date of Contract - March 10, 1978
Termination Date of Contract - June 1, 1980

Gordon Greene - Technical Officer

by

Richard W. Stephenson and John D. Rockaway

The University of Missouri-Rolla

Rolla, Missouri 65401

November 1980

SUMMARY

The greater St. Louis area of Missouri and Illinois, one of the largest population centers in the Midwest, is located within 200 miles of one of the most seismically active regions in the United States. Since the destructive New Madrid earthquakes of 1811 and 1812, there have been 13 other earthquakes of Modified Mercalli Intensity VII or greater in the area. In addition to the active seismic record of the area, other geologic factors exist to add to the potential for damage from earthquakes. Central United States earthquakes characteristically have larger areas of perceptibility of ground motion and greater duration and amplitude than West Coast earthquakes. The potential for damage is compounded because urban expansion has extended onto the thick lacustrine and alluvial deposits flanking the Mississippi and Missouri Rivers as well as onto the deep loess deposits that extend back from the bluffs above their valleys. These deep deposits of unconsolidated materials, which tend to amplify earthquake ground motion, occasion greater intensities and damage at the surface.

This report presents seismic hazard mapping procedures, which are based on the dynamic response of the local soil deposits. From these procedures, a simple and rational method was developed to assess the relative levels of individual seismic hazards. The method was then applied to the Creve Coeur Quadrangle, Missouri. The hazard analysis is based on state-of-the-art engineering procedures for analyzing ground motion, liquefaction, and slope stability; the results are presented as computer-generated earthquake hazards maps. The maps delineate areas of potential slope failure, liquefaction, and relative structural damage from ground motion in the event that a maximum predicted earthquake were to occur. The hazards maps are intended for the use of engineers, architects, and those persons involved in land-use planning.

ACKNOWLEDGMENTS

The authors of this report acknowledge with thanks the work of the following former University of Missouri-Rolla graduate students whose efforts have been instrumental in conducting much of the research reported herein: Michael Simac, Frederick Bauhof and Dr. Jerry Higgins. In addition, the contributions of Daniel Dickey, Ken Haas, Donald Foster, Sharon Rickman, and Jama Allison have been most helpful in the successful completion of the work.

Consultation and advice were provided by David Barr and Shamsher Prakash of the University of Missouri-Rolla, Otto Nuttli and Robert Herrmann of St. Louis University, Gregory Hempen and Michael Klosterman of the St. Louis District, United States Army Corps of Engineers, Eugene Brucker of Brucker and Associates, and Ray Limeback of the Missouri State Highway Department.

CONTENTS

ILLUSTRATIONS

Figure		Page

TABLES

INTRODUCTION

Definition of the Problem

The greater St. Louis area of Missouri and Illinois, one of the largest population centers in the Midwest, is located within 200 miles of one of the most seismically active regions in the United States. This seismic region encompasses a portion of southeastern Missouri, southwestern Illinois, western Kentucky, and northwestern Tennessee and was the location of the greatest sequence of earthquakes in North American history--the New Madrid earthquakes of 1811 and 1812. The earthquakes caused topographic changes over 50,000 square miles and were felt over two-thirds of the United States. Structural damage was reported as far away as Ohio, South Carolina, and Georgia (Fuller, 1912). Since the events of 1811 and 1812, at least 85 earthquakes of Modified Mercalli Intensity (MMI) V or greater (13 earthquakes of MMI VII or greater) have been recorded within 200 miles of the New Madrid area.

The New Madrid fault zone is buried deep beneath thick sediments of the Mississippi embayment, and its specific location and characteristics are as yet undetermined. The U. S. Geological Survey (1979) has defined a portion of the fault zone in northwest Arkansas with the aid of oil-exploration seismic reflection techniques (Fig. 1). The fault is believed to be a rupture in the basement rocks along the middle of a rift that measures approximately 30 miles (50 km) in width and 120 miles (190 km) in length. About half a dozen associated faults are included within the rift zone. Vertical displacement has been measured up to 3300 feet (1000 m). Most of the movement occurred over 100 million years ago, although younger overlying sediments have been displaced.

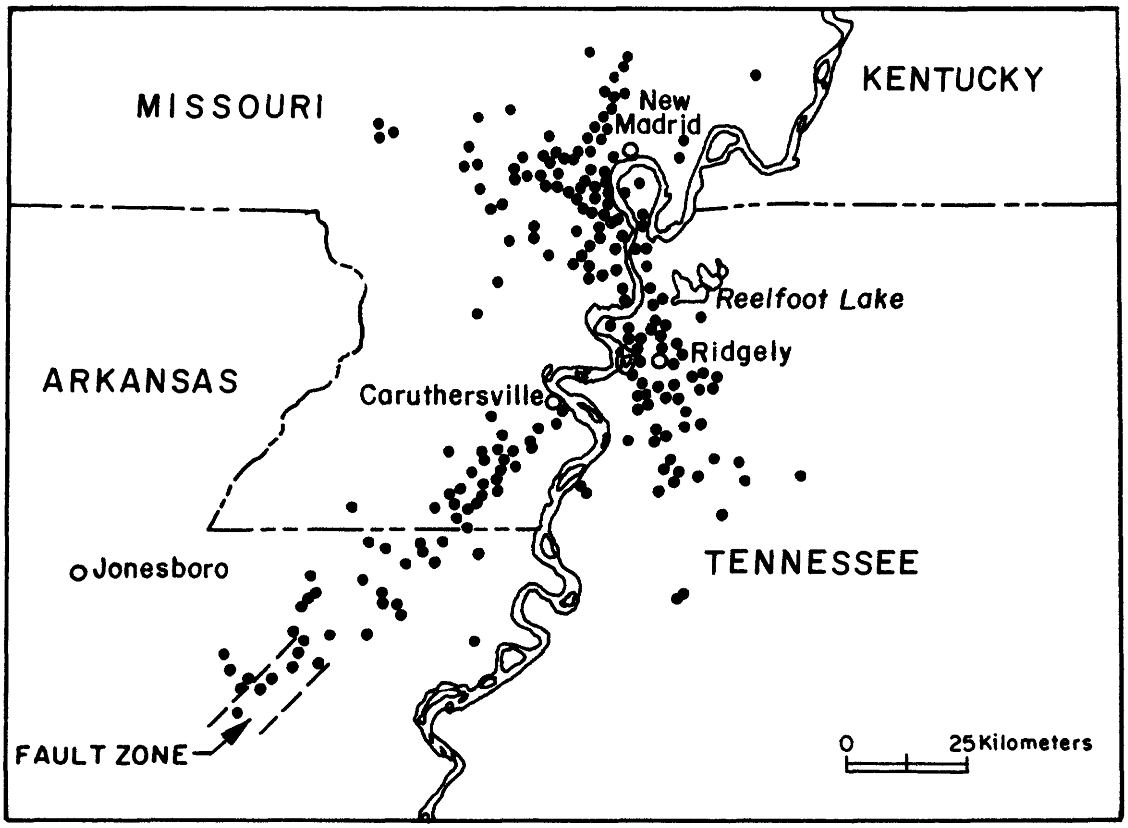

Figure 1. A Portion of the New Madrid Fault Zone and Associated Earthquake Epicenters (after U.S. Geological Survey, 1979).

In a recent interview with Time magazine (November 19, 1979, pp.66-67), St. Louis University seismologist Dr. Otto Nuttli indicated that he believes stresses are continuing to build along the fault, because small earthquakes are frequently recorded in the area. Because of this, he feels a moderately large earthquake will occur in the future.

In addition to the proximity of the St. Louis area to an active seismic region, other geologic factors exist that can add to the potential for earthquake damage. First, one of the distinguishing features of Central United States earthquakes is their large area of perceptibility of ground motion. The extent of this effect is more widespread and of greater duration and amplitude than that experienced on the West Coast (Nuttle, 1972). Second, urban expansion has encroached upon the thick lacustrine and alluvial deposits along the Mississippi and Missouri Rivers and their tributaries as well as upon the thick loess deposits on the uplands. Deep deposits of unconsolidated materials, which tend to amplify earthquake-induced ground motion, occasion greater intensities and damage at the surface. As an example of urban expansion, it has been proposed that a large commercial complex be developed on the Missouri River flood plain in the area of Creve Coeur Lake, St. Louis County. A large outdoor sports stadium, extensive industrial parks, commercial hotels, and manufacturing warehousing are planned. The floodplain deposits of the area consist of over 100 feet of sandy sediment, and the water table lies within ten feet of the surface. This type of saturated deposit not only tends to amplify the ground motion from earthquakes but is subject to serious ground failure and subsidence through liquefaction.

As a result, if a large earthquake were to occur with today's dense population, there would be a far greater loss of life and property than experienced by the scattered inhabitants of 1811 and 1812. A recent study of potential earthquake destruction for an earthquake equivalent to the maximum New Madrid event (Liu and Hsieh, 1979) shows that for a night-time occurrence the death rate could exceed 370, and the total monetary damages could reach 3.2 billion dollars in the St. Louis area alone.

Scope and Objectives

In 1978, the United States Geological Survey awarded a research grant to the University of Missouri-Rolla for the purpose of conducting a pilot study to analyze the potential of earthquake-induced geologic hazards in a portion of the Creve Coeur Quadrangle in St. Louis County, Missouri (Fig. 2). The primary objective of this project was to develop mapping procedures that would be based on the dynamic response of local soil columns rather than on a conventional geologic classification of soil deposits. For microzonation or seismic response mapping, the subjects of major interest have been the modification of bedrock motion by overlying soil deposits and the resulting surface response. It is this dynamic response that can be used as a basis for evaluating seismic hazards, i.e., potential for liquefaction and slope failure, and for determining the potential for damaging structures.

Classically, microzonation has been based on the geologic classification of soil units, and it has been assumed that the seismic response varies for each deposit. However, considering the interrelated effects of the base motion, the dynamic properties of the individual soils composing a deposit, and the thickness of

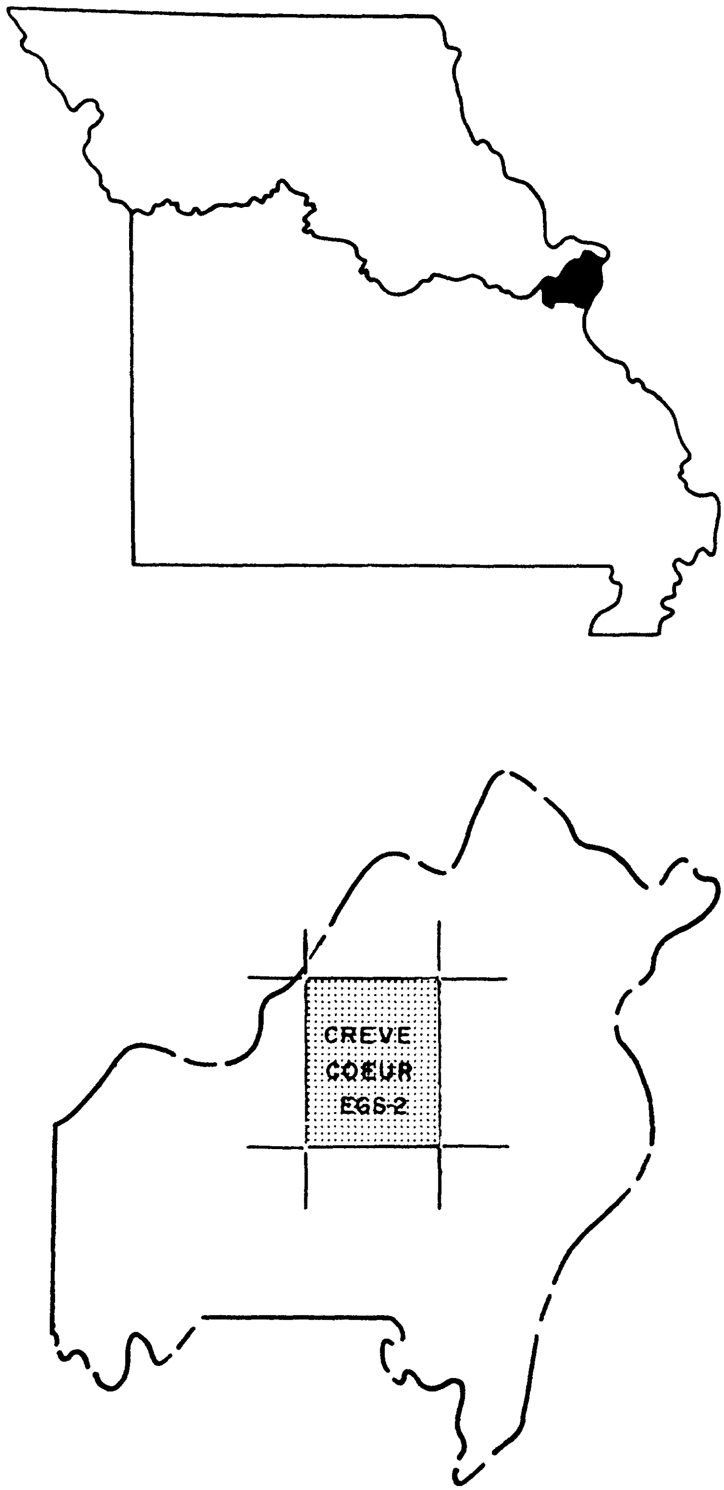

Figure 2. The Location of St. Louis County and the Creve Coeur Quadrangle, Missouri.

the deposit, geologically different deposits may exhibit very similar dynamic responses. Because the evaluation of seismic hazards as well as the effects on structures is based on the dynamic response of the soil columns and not necessarily on the geology, it is suggested that the most reasonable basis for a microzonation map is the dynamic response of the soil columns. This report presents seismic hazard mapping procedures that are based on this concept and utilizes the Creve Coeur area to demonstrate this new approach.

Additional objectives of the research were to provide an appraisal of the relative levels of individual seismic hazards in the form of zoning maps at detailed scales and to assess the significant seismic hazards for the study area. The format of the zoning maps was to be useful to engineers and architects as well as to government officials, planners, and others involved in land-use planning.

Conventional zoning maps are usually constructed on the basis of geology or empirical procedures with little or no consideration given to the engineering properties of the soil deposits. Engineering analyses for determining the factor of safety against failure are not commonly considered for regional mapping purposes. This report presents procedures of seismic hazard assessments that are based on state-of-the-art engineering analyses and techniques, and it demonstrates these procedures by presenting an assessment of the level of seismic hazards in the Creve Coeur area.

As a part of the pilot study, a review of the regional geology and seismicity and an estimate of bedrock motions from expected earthquakes of maximum magnitude in the surrounding region were made. The design earthquakes chosen consist of a near field, high frequency, Ozark Uplift source earthquake and a far field, low frequency, New Madrid region source earthquake. These design earthquakes were selected to represent the maximum bedrock motion expected at the study site in terms of peak horizontal acceleration, peak horizontal velocity, predominant period, and bracketed duration. Existing acceleration time-histories were modified to match these ground motion parameters to produce the design earthquake accelerograms. A field exploration program also was undertaken to establish the soil stratigraphy, depth to bedrock, and depth to ground water and to collect quality soil samples for laboratory analyses of the engineering properties.

A computer program, PACTT, was developed for cyclic triaxial test control and data acquisition. The program was designed to provide control over the methods of testing and of the recording of data. In addition, it generated immediate feedback to aid in adjusting the testing program so that all the necessary information desired could be obtained for analysis. The SHAKE (Schnable, et al., 1972) computer program, which was used in the ground response analysis, was modified to accept more materials of the same type. This modification allowed for the use of a less generalized soil column model and yielded a truer account of dynamic behavior for similar types of material.

For this study, the appraisal of the relative levels of individual seismic hazards was accomplished by inputting the selected design earthquakes and the static and dynamic properties of the soil deposits into the SHAKE computer analysis. This was done to determine the modification of the ground response of the various soil deposits at the study site. The resulting ground response data, combined with the static and dynamic material properties and with the information on thickness, topography, and groundwater levels, were used to determine the susceptibility of the unconsolidated units to seismically induced geologic hazards. The relative potential for failure of these units was evaluated on the basis of computed factors of safety for the different levels of ground motion. A schematic outline illustrating the production of the earthquake hazards maps is included in Figure 3.

The outcome of the above is the set of maps that shows the response of the various soil deposits to the design base motion and the potential for slope failure, liquefaction, and damage to structures in the event that an earthquake of maximum strength was to occur. Because the maps are based on state-of-the-art analytical methods and engineering hazard evaluations, they should be useful in the planning, development, and design of new structures in the rapidly growing Creve Coeur area. In addition, the research, based on the dynamic response of the local soil deposits, has led to the development of systematic techniques, which can be used for the appraisal of individual seismic hazards. All of these procedures of seismic hazard analysis and mapping are believed to be improvements over existing procedures, because they incorporate both quantitative engineering data and qualitative geologic data. They also have a wide range of applicability and can be applied to seismic zoning studies in areas other than St. Louis.

Computer Mapping Procedures

The digital image processing system of the University of

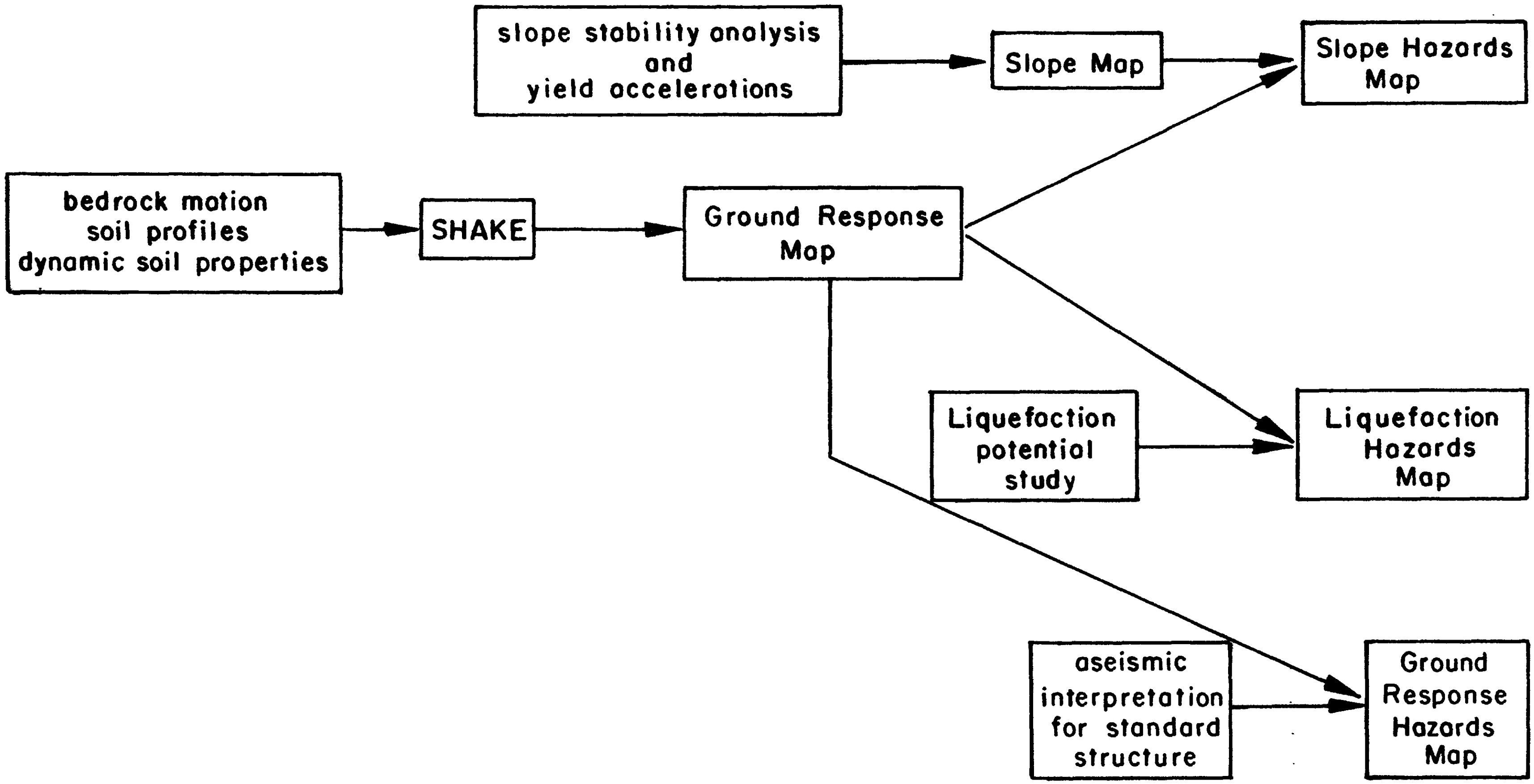

Figure 3. Schematic Outline Illustrating Production of Earthquake Hazards Maps.

Missouri-Rolla's Geological Engineering Department was used to evaluate and map the earthquake hazards. The computer program that was used was modified from an existing seismic mapping program developed at the Nevada Bureau of Mines and Geology (Bell, *et al.*, 1978).

Equipment.

The digital image processing facility is a part of the University of Missouri-Rolla's remote sensing laboratory. The system consists of a minicomputer-driven Comtal interactive graphics terminal and appurtenant equipment (Figs. 4 and 5).

An interactive data base management program is part of the operating system, which allows one to compute the algorithm that best explains the end product of the interaction of the data files.

Computer Program.

The mapping program that was used is a modified version of the hazard model for the Reno, Nevada, area (Bell, *et al.*, 1978). The program originally was developed to evaluate earthquake hazards and assess seismic risk for large-scale areas of investigation. It is based on phenomenologic and probabilistic data incorporating available geologic and engineering information. The program assessments are based on major factors that influence seismic induced hazards, which include properties of the unconsolidated geologic units, depth to bedrock, slope of terrain, and depth to ground water. These parameters are evaluated for a geographic area based on a matrix with a cell as the fundamental unit of evaluation and digitization. The basic data digitized for each cell represents the predominant condition in that cell. The parameters for each cell are assigned integer values to represent their relative magnitude, and these values are digitized for the

Figure 4. Comtal Interactive Graphics Terminal.

Figure 5. Sperry-Univac V-77-602 Minicomputer.

matrix. The individual hazards maps are constructed by algebraic summation of the digitized values in the seismic response classification with each of the other basic data files. The hazard assessment is aided by the fact that each parameter in the data base can be ranked individually according to its contributing effect on the total seismic hazard. Modifications were made to the program so that some slightly different parameters could be used and different hazards maps constructed.

Methodology.

Parameters digitized to form the basic data files for this study included the maximum horizontal acceleration response, the velocity response spectrum, areas of saturated sandy deposits susceptible to liquefaction, and the slope of the terrain. The digitization of these parameters was based on assigned integer values, which represent the relative magnitude of the predominant condition within a 400- x 400-foot cell (160,000 square-foot area). The cell size was chosen on the basis of the desired detail of the individual data files and was considered small enough to provide a realistic representation of the seismic hazards at a map scale of 1:24,000. The matrix for the study area is composed of a total of 4500 cells.

Ground Response.

Digitization of the ground response was based on the maximum acceleration response (computed by analytical methods) of generalized soil profiles, which were constructed to represent the soil stratigraphy of the study area. The response depended on the properties of the soils composing the unconsolidated deposits, the deposit thickness, and the characteristics of the base motion;

therefore, each soil profile had characteristic responses to each design earthquake. The soil profiles were assigned integer values for digitization on the basis of their relative magnitude of response to the base motion, i.e., 1 represented the lowest magnitude response and 8 the highest. The relative ground response for the maximum acceleration or the velocity response needed to be digitized only once, because after it was put in the data base, the relative values could be manipulated to represent the responses from additional base motions. The input of ground response actually produced two maps: a maximum acceleration map to provide data for calculating the factors of safety against liquefaction and slope instability and a damage potential map based on the velocity spectrum for a given range of fundamental periods.

The data image for the ground response was displayed on the Comtal screen. Then, areas of similar acceleration response and velocity response were grouped by use of a color table (Figs. 6-9), labeled, and inscribed on a magnetic tape for generating a gray scale plot.

Liquefaction Potential.

Areas of saturated sandy deposits with a high water table and low relative densities were digitized into a liquefaction susceptibility data file (Fig. 10). The digitization was based on the magnitude of horizontal accelerations needed to cause liquefaction, i.e., low integers represented high accelerations and high integers low accelerations. The liquefaction susceptibility data file was then superimposed on the maximum acceleration data file. Where horizontal accelerations equaled or exceeded those calculated to cause liquefaction, the area was delineated as having a liquefaction hazard. Areas of greater potential

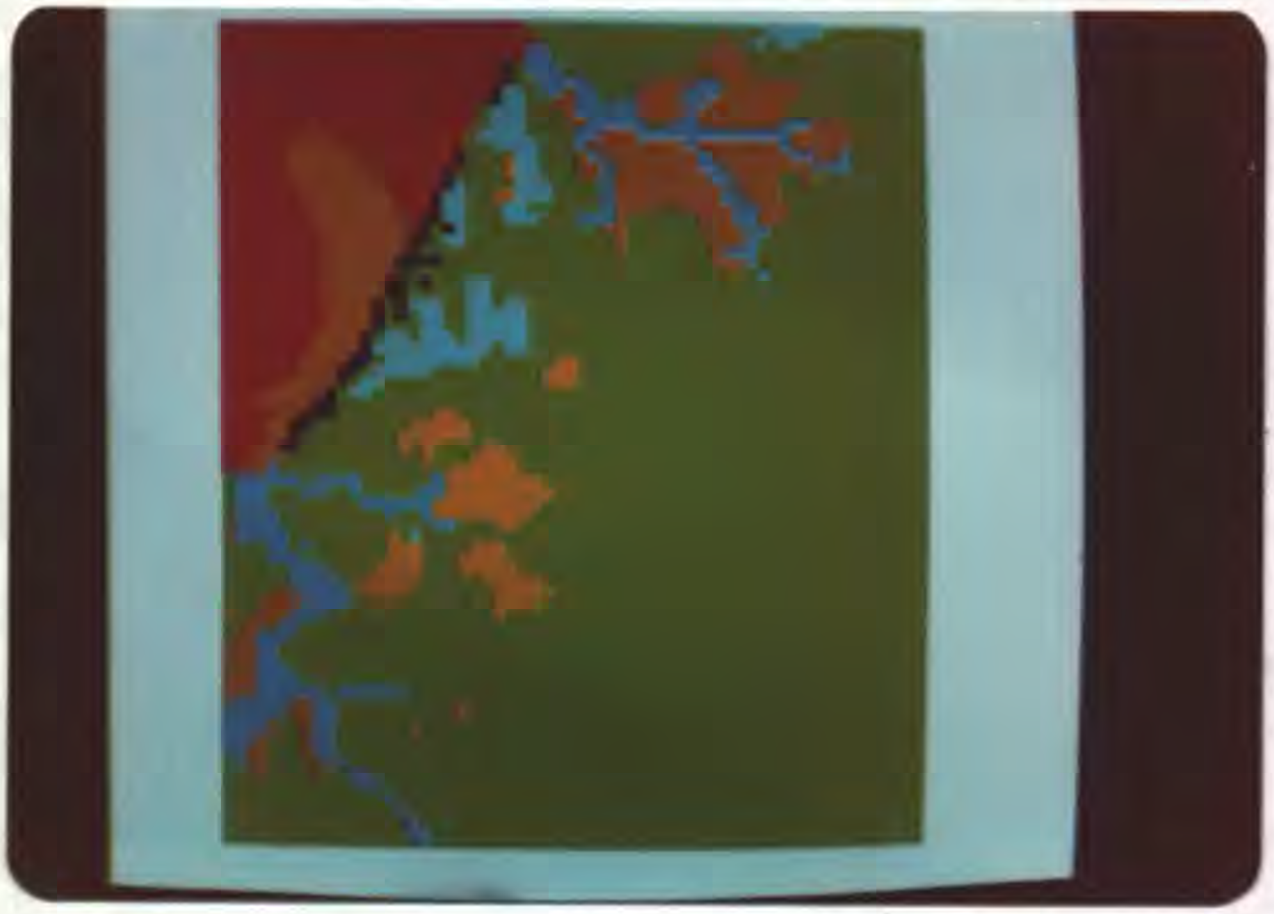

Figure 6. Data Image of Relative Acceleration Response for the Near Field Earthquake, Creve Coeur Quadrangle.

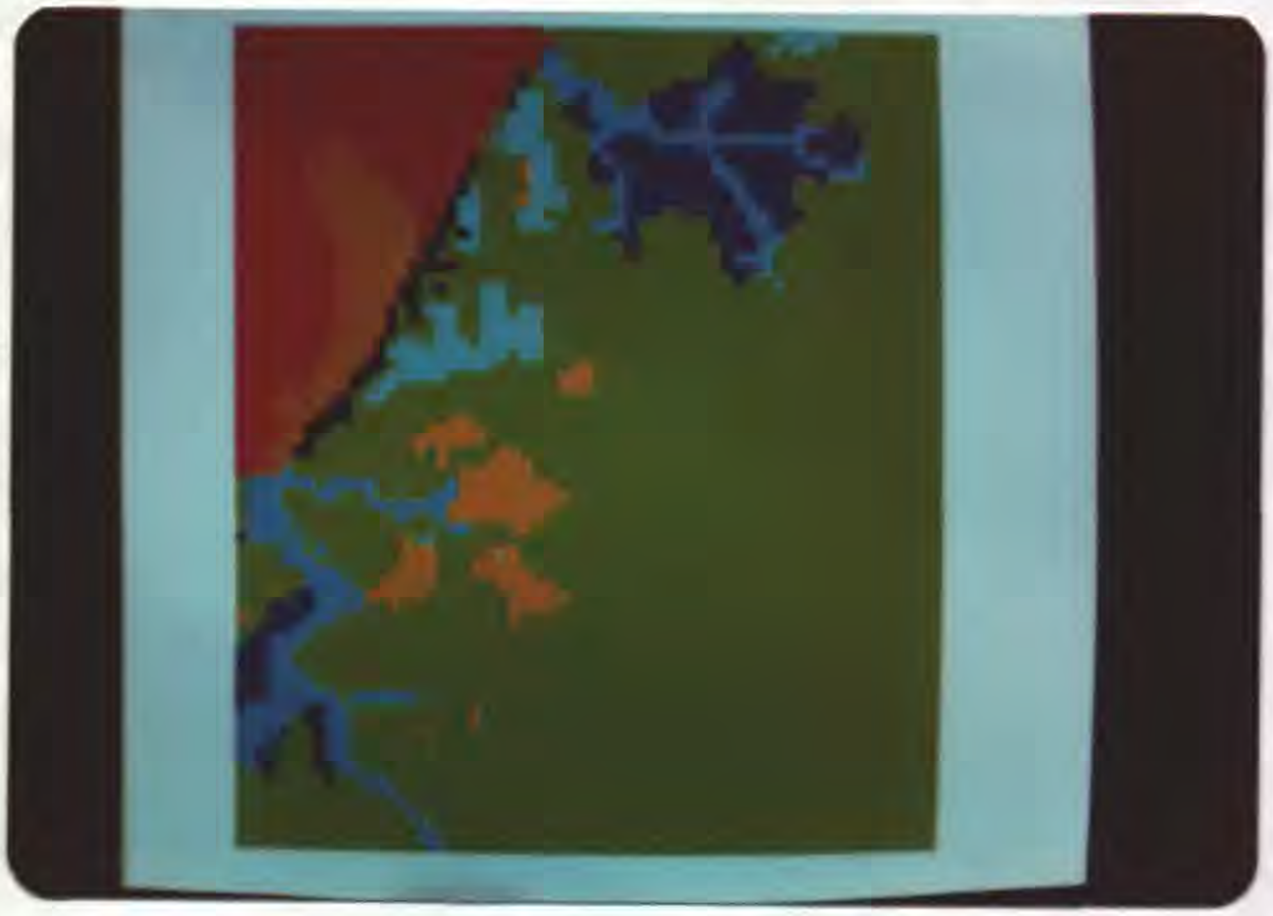

Figure 7. Data Image of Relative Acceleration Response for the Far Field Earthquake, Creve Coeur Quadrangle.

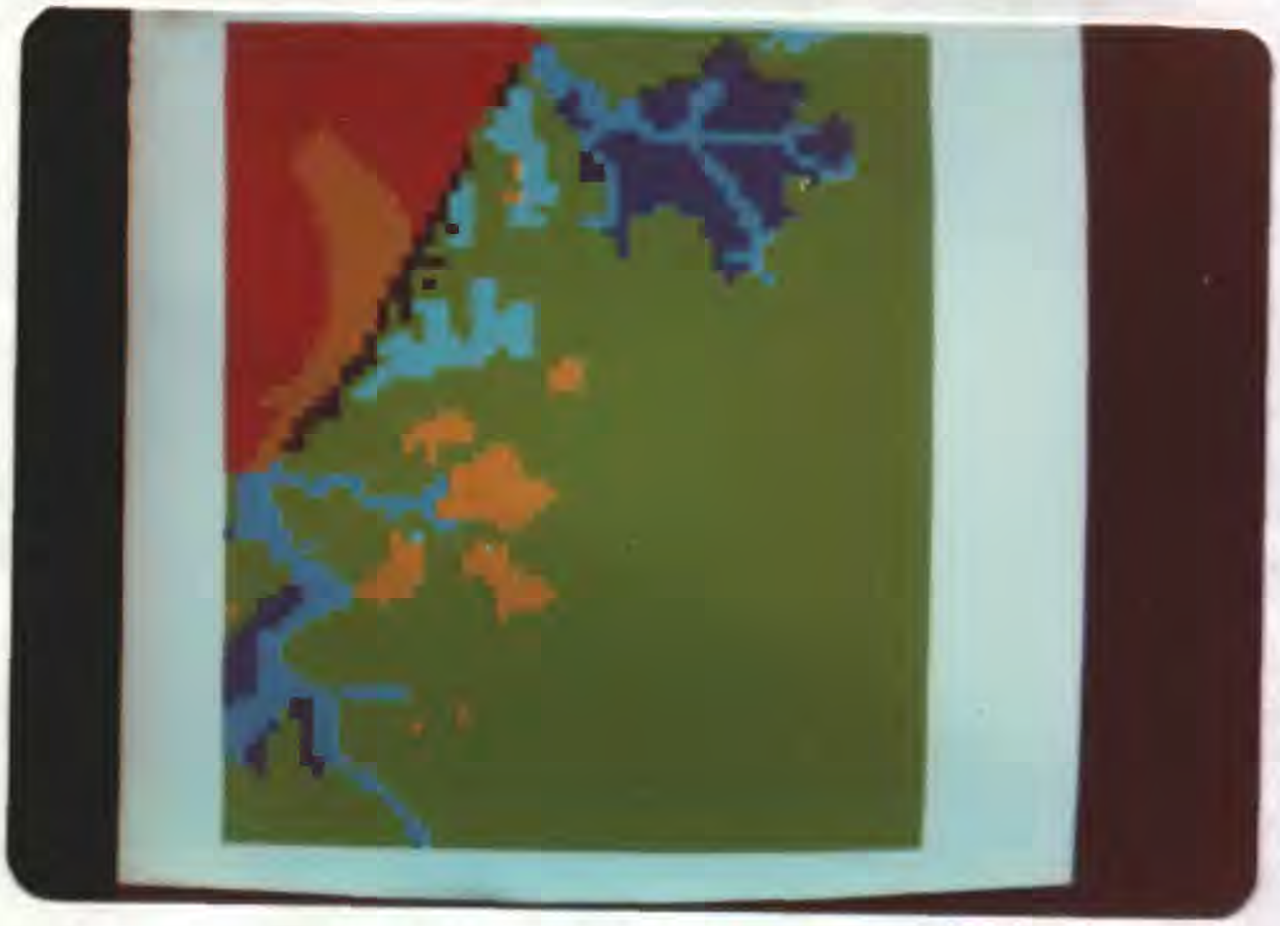

Figure 8. Data Image of Relative Velocity Response for One- to Two-Story Structures for the Near Field Earthquake, Creve Coeur Quadrangle.

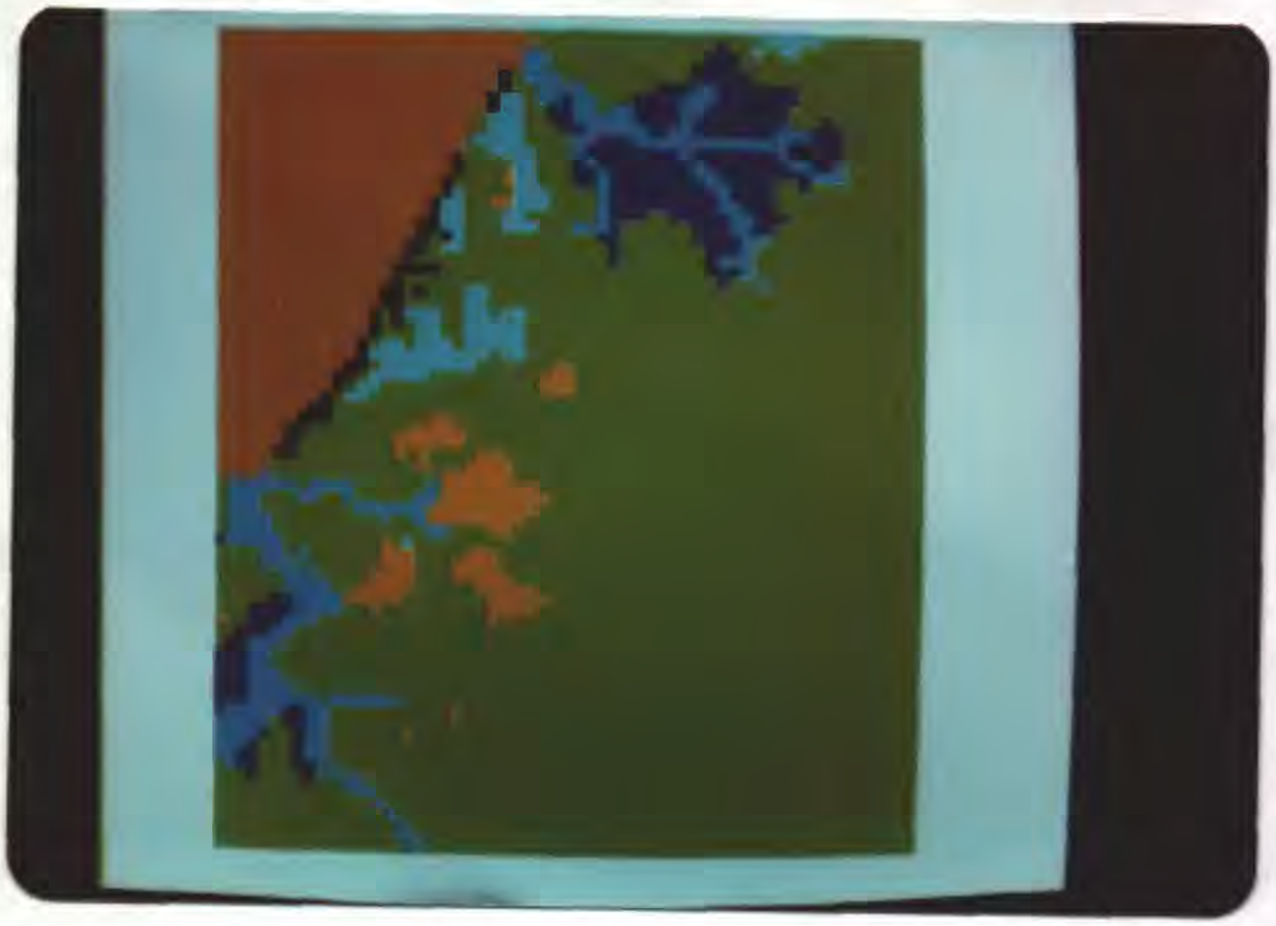

Figure 9. Data Image of Relative Velocity Response for One- to Two-Story Structures for the Far Field Earthquake, Creve Coeur Quadrangle.

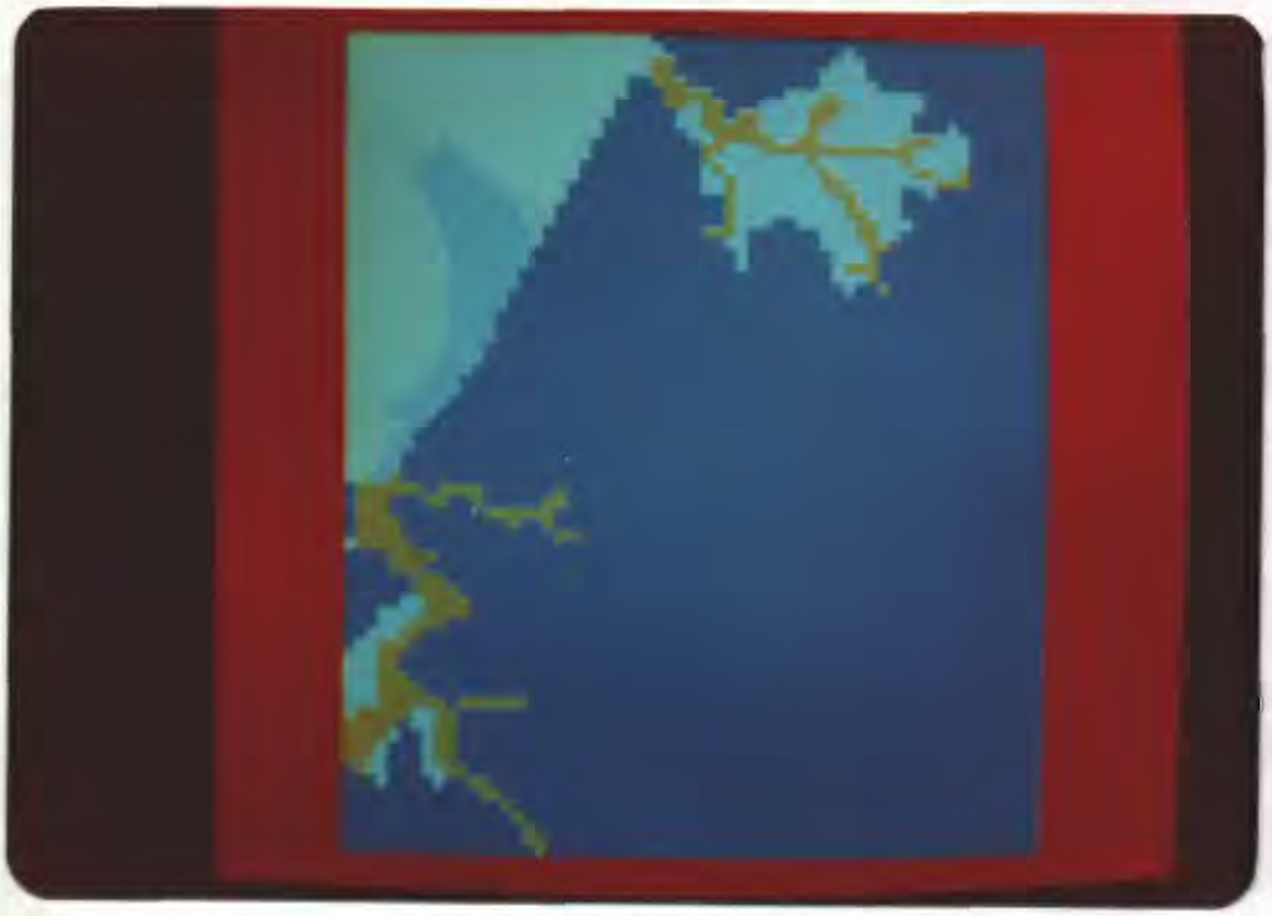

Figure 10. Data Image of Relative Susceptibility of Saturated Sandy Deposits to Liquefaction, Creve Coeur Quadrangle.

(higher total value of cells) were separated from areas of lesser potential. For this study, all the susceptible areas were rated in the high potential category, and all were classified together. The liquefaction potential was assessed on the Comtal screen, and areas of similar liquefaction potential were grouped by use of a color table (Fig. 11), assigned similar symbols, and inscribed on magnetic tape for plotting.

Slope Analyses.

For the potential slope hazards evaluation, the degree of slope was digitized into a gridded data file on the basis of a range of slope and corresponding yield accelerations (Fig. 12). The slope file was superimposed on the maximum acceleration data file to form a slope hazards map. Areas where yield accelerations were equaled or exceeded were assessed on the Comtal screen, identified by the use of a color table (Figs. 13 and 14), assigned symbols, and inscribed on magnetic tape for gray scale plotting.

Hazards Maps.

With the completion of the hazard assessment, the maps were recalled from the tape and plotted at a scale of 1:48,000 on the Varian printer-plotter (Figs. 18-25). The resulting maps delineate areas of geologic hazards and levels of ground response from earthquakes similar in magnitude to the design earthquakes. The maps are predictive in nature and are based on field exploration, laboratory testing, and state-of-the-art engineering assessments of response and ground instability.

The computer mapping program addresses the major factors which influence earthquake-induced hazards. Each parameter in the data base can be ranked individually according to its contributing effect on the total seismic hazard. The computer system

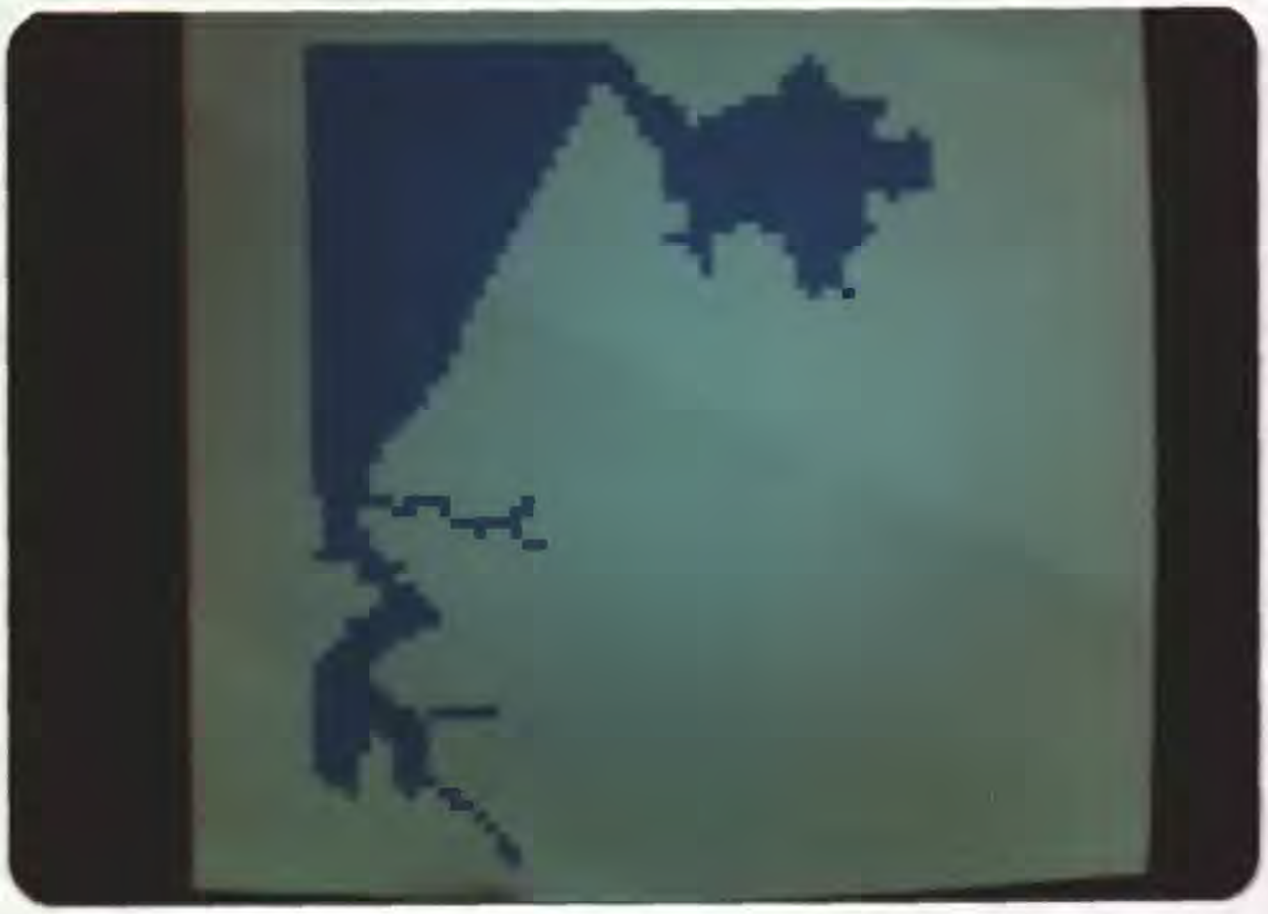

Figure 11. Data Image of Relative Liquefaction Hazard for the Far Field and Near Field Design Earthquakes, Creve Coeur Quadrangle.

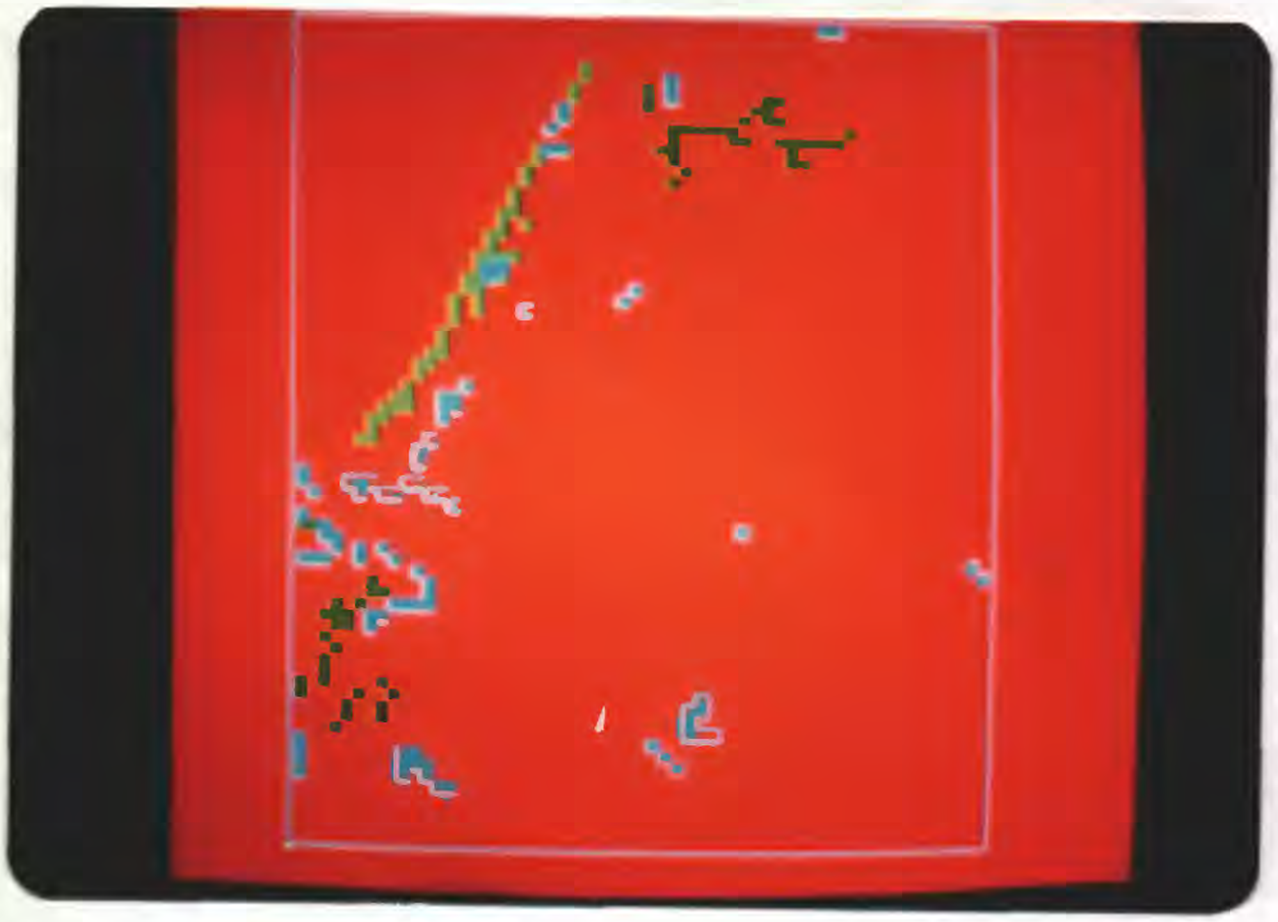

Figure 12. Data Image of Yield Accelerations and Slope, Creve Coeur Quadrangle.

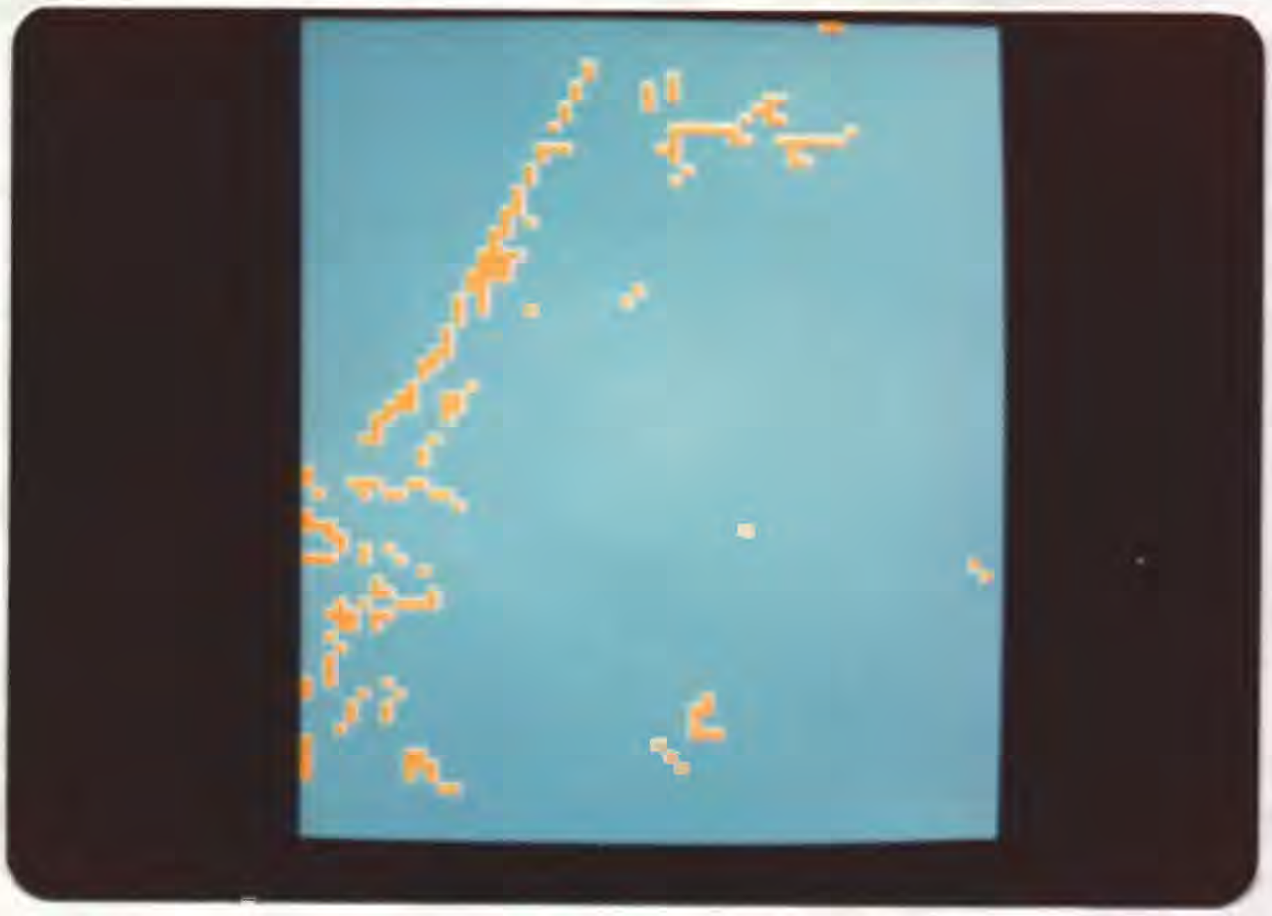

Figure 13. Data Image of Slope Hazards for the Near Field Earthquake, Creve Coeur Quadrangle.

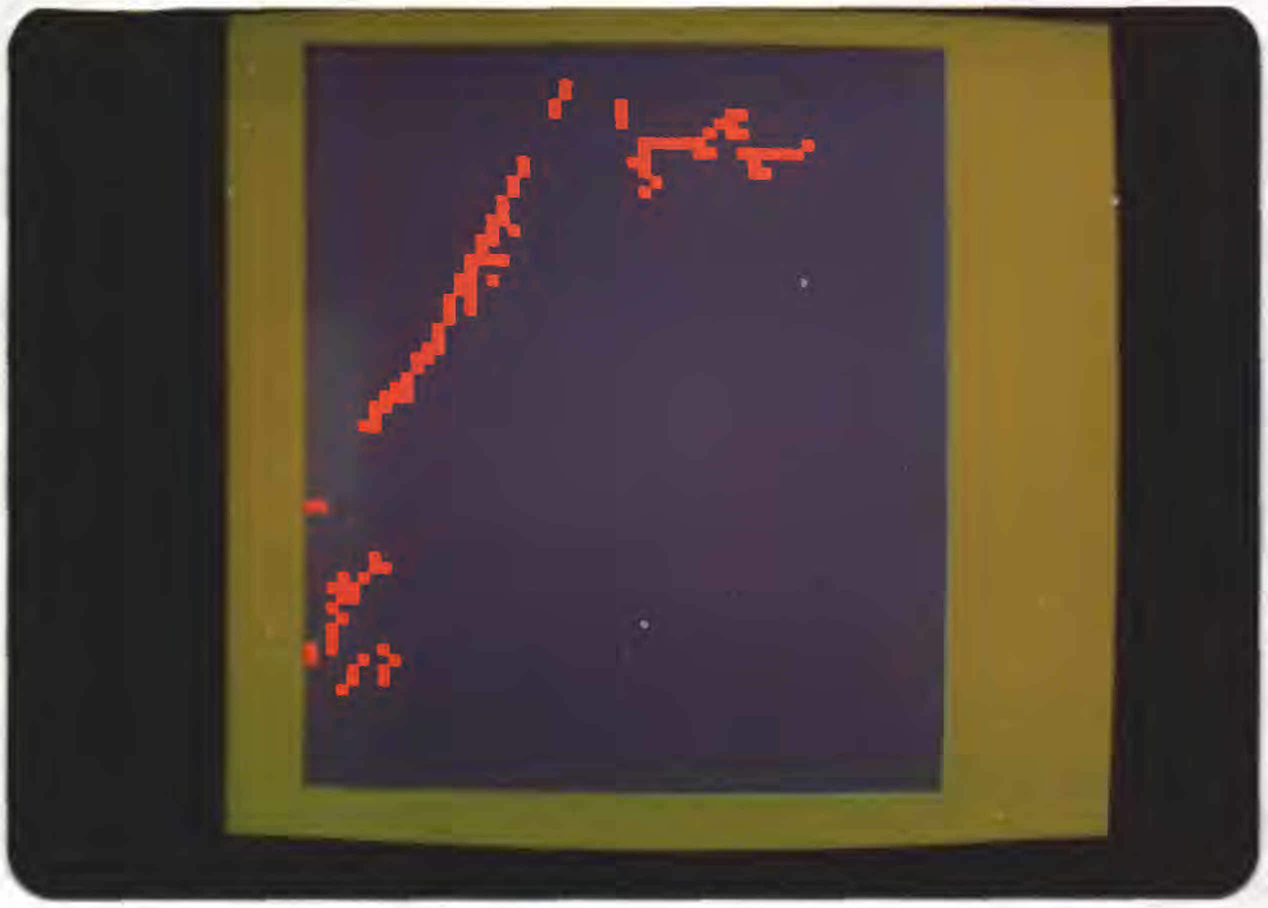

Figure 14. Data Image of Slope Hazards for the Far Field Earthquake, Creve Coeur Quadrangle.

allows the maximum degree of freedom in assessing or delineating each specific hazard or combination of hazards for a given area because of its format and the versatility allowed by the Comtal interactive graphic console. With the operator having the advantage of observing the data base files and manipulating the data (separating or grouping), hazard classifications may be modified or updated easily for different earthquakes or new information as well as be adjusted to reflect the relative magnitude of hazard. In addition, with the mapped response represented by an area (cell) that reflects the predominant condition within that area, the map should be less likely to be misinterpreted than a conventional map showing sharp line boundaries between hazards or geologic conditions.

The accuracy of the map obviously depends upon the map scale and the cell size. For this reason, the limitations of the computer map, with respect to scale and detail, depend chiefly upon the resources available to the developer, and the map can be updated and improved as additional information is assimilated.

RESEARCH PROGRAM

Prior Investigations

Zoning and Microzoning.

The mapping or zoning of potential earthquake effects has become a highly accepted procedure in the United States in recent years; however, the scale at which the zoning is done and the philosophy, data base, and procedures used to develop the zoning depend upon the interests of the investigators. Gaus and Sherif (1972) discussed the individual interests of the many groups involved in zonation and their effect on the final product. Government officials and urban planners are interested principally in the use of seismic zoning as a guide in establishing regulations concerning public safety and proper land-use planning. Engineers and architects, on the other hand, are interested in seismic zoning data that provides the information they need to prepare adequate aseismic designs. Seismic zonation, therefore, ideally should furnish quantitative data concerning the potential dynamic motions and forces to which a strucure may be subjected as well as data concerning earthquake-related geologic phenomena that may influence the performance or stability of a structure. Consequently, the seismic zonation of an area should be designed to satisfy the needs of many users.

The size of the zone ideally should be determined by the needs of the ultimate users. In the past, maps were constructed to designate zones that would experience various intensities of shaking (Algermissen *et al.*, 1969; Richter, 1959). These maps depicted large areas and were not in such detail as to be adequate for structural design. Recognition of the amplification of ground motion, which can occur in local regions during large earthquakes, however, stressed the need for zoning at a more detailed scale (microzonation). Ideally, microzonation of an area should provide the general guidelines that need to be followed in the development of that area and should form the basis for building regulations.

Seismic Hazards Mapping.

It is now generally recognized that seismic land-use planning is needed to reduce the loss of life and damage to property in seismically active areas. The implementation of plans by local, state, and Federal governments in the form of ordinances or building codes (Kochelman and Brabb, 1978) and the need for basic and interpretive data concerning seismic hazards that can be used as a basis for establishing such ordinances have accelerated geologic mapping related to seismic hazards. In addition, the requirements of the Nuclear Regulatory Commission for the aseismic design of nuclear power plants have strongly influenced the development of zonation methodology.

Radbrush-Hall (1978) reviewed the research reports and data on seismic hazards and zonation that have been published in the past 15 years. The results of his study illustrate that many interrelated factors have been integrated into the seismic zonation investigations. These include the location of active faults, recurrence intervals of movements on active faults, earthquake-induced ground failure, and the seismic response of different earth materials. In addition, many studies of damage have been made after the occurrence of major earthquakes. These studies have increased the store of knowledge of earthquake-related geologic and engineering phenomena and have added to the data and experience needed for sound engineering judgment. The data have been presented in various formats, usually as specific maps showing individual seismic hazards or, in some cases, as comprehensive seismic hazards maps. Most of these maps present existing geologic or geotechnic parameters that are related to seismic studies, including studies made after the occurrence of major earthquakes (basic data maps), but some maps define the relative potential for hazards affected by earthquake activity (interpretive maps).

Basic Data Maps. Compilations of the effects of recent earthquakes, such as surface ruptures and landslides, have been presented in a number of published maps and reports. The National Academy of Sciences (1971) published a comprehensive report on the 1964 Alaska earthquake. This report includes an examination of the relations between the geology and the effects of the earthquake on the region as well as generalized seismic slope stability maps for the Anchorage vicinity. In addition, detailed engineering evaluations of specific failures that developed during the Alaska earthquake have been published. As an example, Seed and Wilson (1967) investigated the damage from and causes of the Turnagain Heights landslide from which much was learned concerning the magnitude of the slope failure hazard occasioned by the liquefaction of the underlying loose granular materials.

A study of building damage caused by the 1967 Caracas, Venezuela, earthquake (Seed and Whitman, 1972) is one of the best documented examples of the degree of influence of local soil conditions on the intensity of ground shaking and, therefore, on structural damage. Similar studies of the relationship between soil conditions and ground shaking intensity were made for the 1906 San Francisco earthquake (Lawson, *et al.*, 1908). The data from these studies were reexamined to evaluate the liquefaction potential (Youd and House, 1976). As a result of these and similar studies, soils engineers and geologists have begun to devote careful attention to the influence of local soil conditions on shaking intensity and damage hazard. Many of the papers presented in the First and Second International Conferences on Microzonation (1972, 1978) reflect this knowledge.

One of the best documented earthquakes in the United States was the 1971 San Fernando, California, event (U.S Geological Survey, 1971). The large network of geophysical instruments located in structures as well as on soil and rock provided some of the best and most complete ground and building response data to date. Also, the U.S. Geological Survey carried out many detailed studies concerning the resulting geologic hazards.

A number of basic maps showing the locations of earthquakes, the location and amount of creep, and the location of microseisms along active faults have been published by the U.S. Geological Survey. An example is the 1:250,000 scale map of the Los Angeles, California, area (Wentworth, et al., 1970) that shows landslide areas of known historic surface subsidence and areas of soft rock and sediment that may experience strong seismic shaking. The map also includes the location, pattern, and displacement recency of faults.

Many known active faults in California have been mapped at different scales. The scales of the maps range from the 1:125,000 scale of Dibblee's (1973) regional geology map of the San Andreas fault system to the 1:24,000 scale of more detailed maps. The detailed maps are exemplified by Radbrush-Hall's (1974), map, which delineates recent breaks as indicated by physiographic and geologic evidence as well as offset man-made structures. It also contains information from historic records. Brown (1972) mapped bands of associated fracture zones along major active faults.

Interpretive Maps. Interpretive maps, which are predictive in nature, depict areas of potential slope instability and liquefaction, regions that may be subject to future seismic activity, areas of relative levels of shaking intensity occasioned by future earthquakes, and recurrence intervals along active faults.

Interpretive maps of predicted earthquake intensity were developed for the San Francisco Bay region by Borcherdt, et al. (1975) who used comparative measurements of the amount of ground shaking in different geologic units that was produced by a 1957 earthquake and nuclear explosions in Nevada.

Relative slope stability maps for the San Francisco Bay area were prepared by Brabb, et al. (1972) and Nilsen and Brabb (1975). Keefer, et al. (1978) made a preliminary map showing zones highly susceptible to seismically-induced landslides. Their information was based on studies of slope failures that occurred during historic earthquakes. Wilson (1979) and Wieczorek, et al. (1979) prepared an experimental map of areas susceptible to earthquake-induced landslides for the La Honda Quadrangle, San Mateo County, California. Their work was based on slopes, geology, and calculated factors of safety. Displacements of the landslide masses also were calculated on the basis of acceleration time-history.

Bingler (1974) prepared an earthquake hazards map for the Reno, Nevada, area in which he included fault traces with inferred maximum ages since the last movements and a classification of rock and soil types according to inferred seismic response. Bell, *et al.* (1978) developed a computer-simulated composite earthquake hazards map based on data from Bingler's maps. The computer map expressed the seismic hazards in terms of relative potentials for liquefaction, slope stability, and ground breakage occasioned by faulting. Van Horn and Van Driel (1977) developed a computer composite earthquake hazards map of the Sugar House Quadrangle, Utah, which showed inferred relative stability of the land surface during earthquakes. The final composite map was based on four source maps consisting of relative slope stability, thickness of loosely consolidated materials, texture or grain size, and depth to the groundwater table.

The Santa Cruz County, California, Board of Supervisors (1975), as a part of the county's seismic safety element of their general plan, included maps showing liquefaction potential, landslide deposits, faults, and other related features. The potential for liquefaction, however, appeared to be based only on age and type of unconsolidated geologic deposit.

A preliminary microzonation map of the City of Santa Barbara, California, was developed by Olsen (1972). The microzonation was based on a correlation of the geologic information and on a detailed study of observed intensities from a destructive earthquake that took place in 1925. The geologic analysis included an examination of the bedrock exposures, stratigraphy, depth to ground water, and location of major faults within the city. This information provided data that were used to predict anticipated intensity differences in the area. The geologically based predictions were correlated with actual intensities experienced during a 1925 earthquake and were used as the foundation for constructing the microzonation map. The map divided the city into areas of maximum, intermediate, and lowest intensity of shaking.

Basic data maps from the previously mentioned seismic-response studies of the San Francisco Bay region (Borcherdt, *et al.*, 1975) were used to prepare a map of predicted regional maximum earthquake intensities for a large part of the area (Borcherdt, *et al.*, 1975). The predicted maximum intensities were determined by using an average intensity computed for generalized geologic units, an empirical intensity *vs*. distance relationship (derived from intensity data recorded for the 1906 San Francisco earthquake), and a generalized geologic map. The U.S. Geological Survey (Borcherdt, *et al.*, 1978) undertook a program to determine detailed seismic velocity characteristics (logs of P- and S- waves) and geologic profiles for a large number of sites in all major geologic units in the Bay region to develop an improved data base for more quantitative predictions of ground motion on a regional scale. New estimates of ground response were predicted in the form of amplification and intensity increments for the local geologic units. A liquefaction potential mapping methodology was developed from the Bay region research (Youd, *et al.*, 1978). The map shows areas where conditions may be favorable for the development of liquefaction and incorporates assessments of age and type of sedimentary deposits, depth to ground water, and expected seismicity.

Preliminary maps of relative ground response were constructed for the Salt Lake City area by Hays, *et al.* (1978) who used nuclear-explosion ground motion data. The ground response maps were prepared on the basis of dominant trends in the velocity spectral ratios at various sites and were adjusted for high strain level effects by empirical methods. The resulting maps show ground response values relative to rock for two period bands: 1) 0.1-0.2 second (the upper) end of the range of the natural period of the fundamental mode of response for one- to two-story structures) and 2) 0.2-0.7 second (the natural period range for three- to seven-story structures).

Much of the research and resulting seismic response mapping and zoning has been useful in land-use planning; however, only a few of the more recent studies actually are based on quantitative data suitable for engineering analyses. Considerable research is still needed to develop techniques for quantitatively evaluating and mapping regions in a form useful to planners and developers and those engineers and architects who are concerned with aseismic design.

Considerations for Evaluation of Site Response.

A number of factors must be considered by anyone making a meaningful evaluation of the seismic response of an area. The level of seismic hazards for a given area is a function of seismicity, soil type, water table elevation, and geology (Gaus and Sherif, 1972).

Seismicity. Seismicity is determined by the magnitude and frequency of seismic events, distribution and location of faults in relation to the area under consideration, and the historic seismic trends of the area.

Records of seismic history indicate seismically active areas where a loss of life and property would result from earthquake occurrences. From these records, a credible earthquake magnitude is chosen as a basis of design. The distribution and number of the faults and extent of faulting provide some indication of the seismic and tectonic activity in a region and delineate areas where possible ground failure can occur.

Soil Type. The soil type must be considered when the seismic hazards of a site are evaluated, because earthquake-induced ground motion may cause some soils to undergo liquefaction, a loss of strength, or densification.

Liquefaction is a phenomenon in which saturated cohesionless soils completely lose their strength as a result of a buildup of hydrostatic pressures from dynamic excitation and thereby behave as a liquid. The potential for a soil to undergo liquefaction during an earthquake is a function of many factors, especially the confining pressure, water table elevation, relative density, and soil type.

Loss of strength is experienced in many cohesive soils when they are subjected to repetitive dynamic loading. The strength loss is greatest for overly consolidated soils and increases with increasing dynamic stress levels. Soils at or near the surface are most prone to strength reduction during earthquakes (Sherif, _et al._, 1972).

Densification from dynamic loads may occur in granular soils if the soil densities are less than the critical density. The amount of settlement that may occur depends on the thickness of the granular deposit as well as the dynamic loading. The potential for densification decreases with increasing confining pressure and increasing depths below the ground surface; therefore, surface and near-surface soils tend to be most susceptible to densification.

Depth to Ground Water. The intensity of seismic shaking tends to be increased if the depth to the water table is less than approximately ten meters in unconsolidated deposits (Medvedev, 1965). A high groundwater table also tends to increase the potential for liquefaction during an earthquake.

Geology. The intensity of earthquake-induced ground motion is influenced by the type and nature of the consolidated and unconsolidated deposits as well as by the regional geology. The rock types and geologic structure of a region affects the attenuation of maximum acceleration values with increasing distance from the epicentral region. The modification of base motions by an unconsolidated deposit is influenced by the amplitude and frequency characteristics of the motions, the dynamic properties of the deposit's material, and the deposit's thickness. The base motions may be amplified or attenuated by an unconsolidated deposit (Seed and Schnabel, 1972; Gaus and Sherif, 1972).

Seismicity

As stated previously, seismicity refers to and is determined by the magnitude and frequency of seismic events, distributions, and historic seismic trends of the area.

In the Central United States, the identification of active faults and the correlation of earthquake epicenters with individual faults is difficult. However, major zones of seismic activity have been identified for the Central United States by two different methods: seismotectonic regions established by the Nuclear Regulatory Commission and seismic source zones established by Nuttli and Herrmann (1978).

Seismotectonic Regions.

Seismotectonic regions define major zones of seismic activity that are related to regional tectonic regimes. The purpose of seismotectonic regionalization is to describe the distribution of historic seismic activity in relation to geologic structures and tectonic provinces and to characterize this neotectonic activity (Hadley and Devine, 1974; Schell, 1978). The basis of seismotectonic zonation is the coincidence of uniform seismic activity and tectonic conditions (Schell, 1978), although geologic, geophysical, and seismological data should also be used, when available, to refine the zonation.

The seismotectonic region is based on a broader data base than the tectonic province. Seismic activity in tectonic provinces is generally nonuniform and varies within the province (Hadley and Devine, 1974) and seismotectonic regions do not necessarily coincide with regional structural features.

In engineering practice, a maximum earthquake is defined for the seismotectonic region and then is assumed to be capable of occurring anywhere within the boundaries. The design earthquake is then assumed to occur at the closest point of the region to the site under consideration. Suitable attenuation curves are then used to estimate the ground motion at the site.

The Central United States has been zoned into seismotectonic regions for definition of the safe shutdown earthquake used in the design of nuclear power plants. The seismotectonic map of the upper Mississippi Valley for the Callaway Nuclear Power Plant site is shown in Fig. 15 (Union Electric Company, 1973). Delineation of the seismotectonic boundaries was based on a comparison of historical seismicity, geological structure, and fault plane solutions. The boundaries of the New Madrid seismotectonic region were based also on a comparison of gravity, magnetics, ERTS imagery, and geomorphologic data. The MMI of the maximum historical earthquake of each region is summarized in Table I.

Earthquake Source Zones.

The most recent zonation work in the Central United States has been done by Nuttli and Herrmann (1978) (Fig. 16). Zonation of the Central United States into earthquake source zones was based

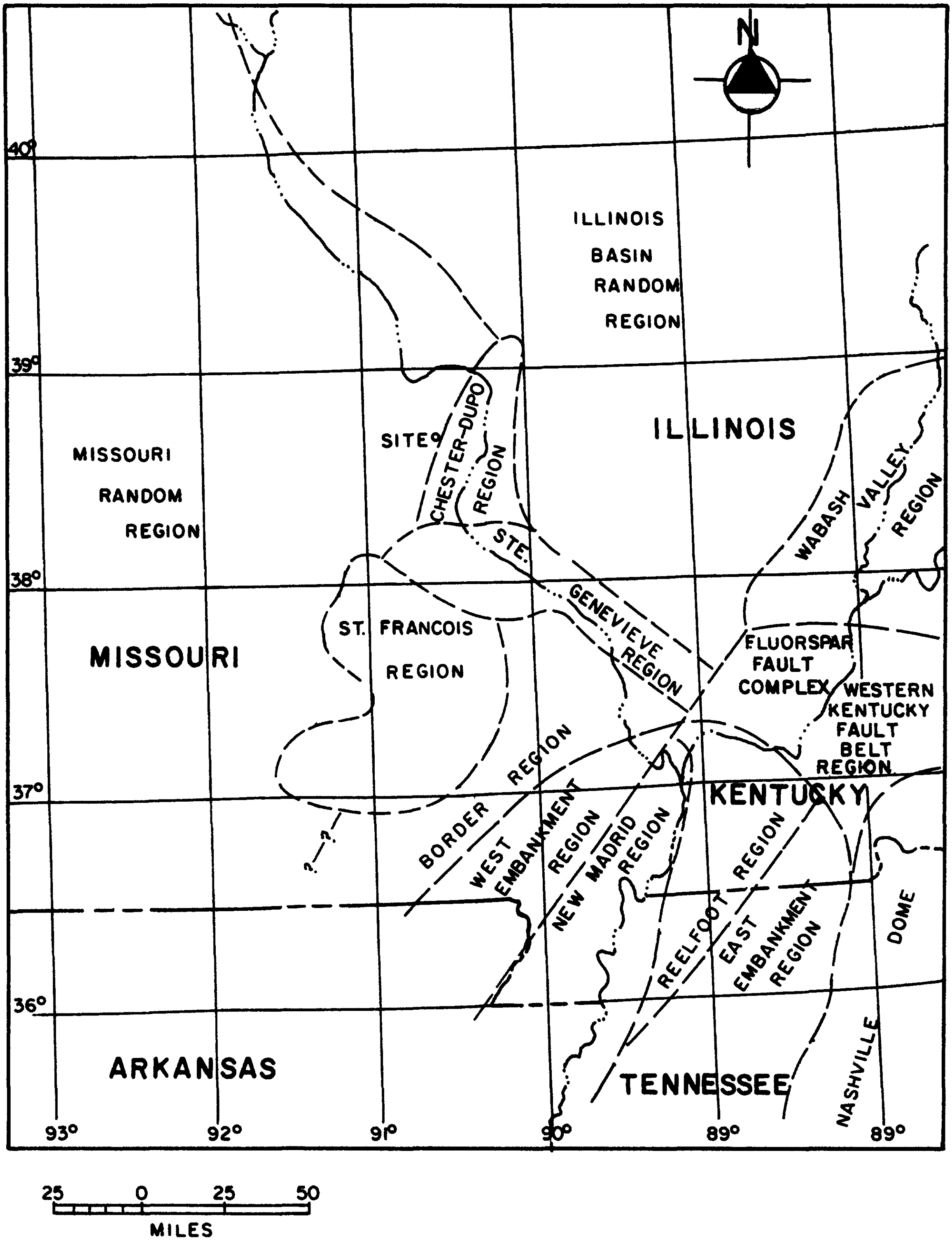

Figure 15. Seismotectonic Map of the Regional Study Area (after Union Electric Company, 1973).

TABLE I

MAXIMUM HISTORICAL EARTHQUAKES IN THE SEISMOTECTONIC REGIONS OF THE CENTRAL UNITED STATES (CALLAWAY NUCLEAR POWER PLANT STUDY)

Region	Maximum Historical Earthquake
New Madrid Region	XI
Reelfoot Region	VII
West Embayment Region	VI
East Embayment Region	<V
Nashville Dome	<V
Fluorspar Fault Complex and Western Kentucky Faulted Belt	V
Wabash Valley Region	VII
Border Region	<V
Illinois Basin Random Region	VII
Missouri Random Region	V
Chester-Dupo Region	VII
Ste. Genevieve Region	VI
St. Francois Region	VI

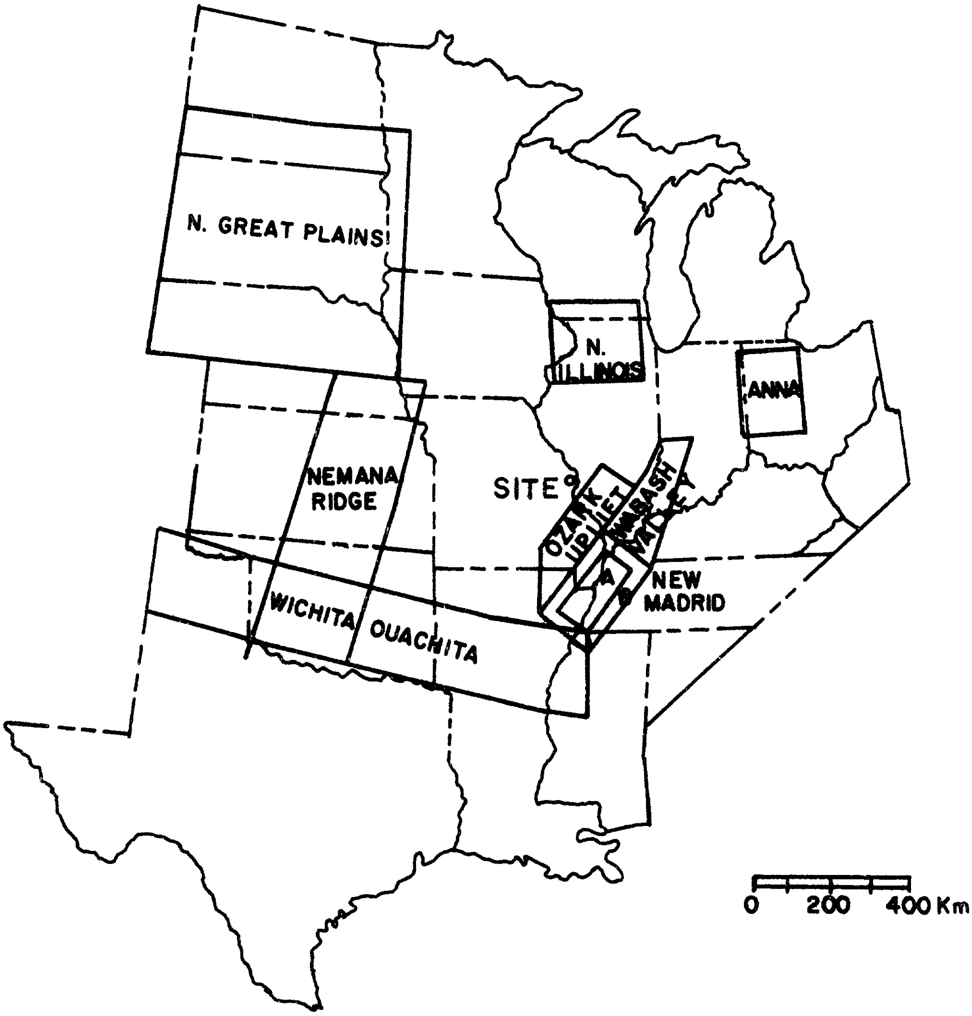

Figure 16. Seismic Source Regions of the Central United States (after Nuttli and Herrmann, 1978).

on the distribution of earthquake epicenters and the tectonic features in the region (Nuttli and Herrmann, 1978). The zonation was based principally on historic seismicity rather than on geologic data because of the difficulty of identifying active faults in the Central United States. However, statistical tests indicate that the seismicity catalog is complete for all earthquakes of m_b greater than five.

The maximum magnitude earthquakes for the source zones within the regional area are listed in Table II. The maximum earthquakes are 1000-year earthquakes and have a 63 percent probability of occurrence in that time interval.

Design Earthquakes.

In the present study, the seismic source zones, maximum magnitude earthquakes, and ground motion equations developed by Nuttli and Herrman (1978) were used to estimate the bedrock motions at Creve Coeur (Table III). Two design earthquakes were selected to model the maximum bedrock motion that could be expected in the study area. The design earthquakes consist of a near field, high frequency, Ozark Uplift earthquake and a far field, low frequency, New Madrid, Region A earthquake. The peak horizontal acceleration, peak horizontal velocity, predominant period, and bracketed duration for both design earthquakes are listed in Table IV.

Selection and Modification of the Design Earthquake Accelerograms.

Ideally, an accelerogram selected for engineering design purposes should have site and source conditions comparable to the location under consideration and similar epicentral distance and predominant frequency characteristics (Seed and Idriss, 1969b; Cornell, 1970; Nuttli, 1973). Selection of the design accelerograms were based as much as possible on these factors. However, because of the

TABLE II

MAXIMUM EARTHQUAKES IN THE SEISMIC SOURCE REGIONS OF THE CENTRAL UNITED STATES

Region	Maximum m_b
New Madrid A	7.5
Ozark Uplift	6.7
Wabash Valley	6.6
New Madrid B	6.5
Northern Illinois	6.1
Residual Events	5.3

TABLE III

PEAK ACCELERATIONS AND VELOCITIES AT CREVE COEUR QUADRANGLE FROM MAXIMUM CREDIBLE EARTHQUAKES IN THE SURROUNDING SEISMIC SOURCE ZONES

Seismic Source Zone	m_b	Distance km	Acceleration cm/sec	Velocity cm/sec
Ozark Uplift	6.7	43	455	140
New Madrid Region A	7.5	202	245	188
Wabash Valley	6.6	144	118	33
New Madrid Region B	6.5	154	97	25
Northern Illinois	6.1	257	36	6
Residual Events	5.3	40	92	6

TABLE IV

GROUND MOTION CHARACTERISTICS AT CREVE COEUR QUADRANGLE

FROM THE DESIGN EARTHQUAKES

	Peak Horizontal Acceleration (%g)	Peak Horizontal Velocity (cm/sec)	Predominant Period (sec)	Bracketed Duration (sec)
Ozark Uplift Earthquake	46	140	0.30	>21
New Madrid Region A Earthquake	25	188	0.82	>10

scarcity of strong motion records in the Central United States, design accelerograms had to be chosen from the world-wide strong motion data base. This, of course, presented the problem of using records from areas of different regional geology and, therefore, different attenuation characteristics (Nuttli and Herrmann, 1978).

Because the response spectra for ground surface motions are very dependent on the frequency characteristics of the base motion, three accelerograms were selected to model each design earthquake. This was done in an effort to allow for possible idiosyncrasies present in individual records and to impart some average spectral properties to each design earthquake.

The initial selection of the records was based on similar site characteristics (hard or intermediate rock) and similar peak accelerations and predominant periods comparable to the design values. The final records were selected to give bracketed durations similar to the design values after the records were scaled to the design predominant period. The design values of the peak horizontal velocity could not be satisfied in the scaled records, but the records were selected so as to approximate the design velocity values.

The selected accelerograms are described in Table V. Because there is a lack of records of strong rock motion, two of the three field records had to be selected from sites on alluvium, but the remainder of the accelerograms were taken from sites on hard or intermediate rock.

The scaling factors for the acceleration amplitude (ordinate) and the predominant period (abscissa) are shown in Table VI. This method of simply scaling the required motions is convenient and satisfactory and makes clear the nature of the modifications involved.

The results of this phase of the study were the selection of

TABLE V

CHARACTERISTICS OF THE SELECTED ACCELERATION TIME-HISTORIES

Ozark Uplift Design Earthquake

CIT File No.	Recording Station	Site Classification *	Date of Earthquake	Instrument Component	Peak Acceleration cm/sec^2	Peak Velocity cm/sec	Epicentral Distance km	Bracketed Duration sec	Predominant Period sec
A001	El Centro Site, Imperial Valley	A	5-18-40	S 00° E	341.7	33.4	9.3	25.9	0.25
B034	Parkfield, CA Earthquake, Cholame Shandon Array # 5	A	6-27-66	N 05° W	347.8	22.5	32.4	6.6	0.30
J144	San Fernando Earthquake, Lake Hughes Array # 12	I	2-09-71	N 21° E	346.2	14.7	23.3	14.0	0.20

*A = alluvium, I = intermediate, and HR = hard rock

TABLE V (Continued)

New Madrid Region A Design Earthquake

CIT File No.	Recording Station	Site Classification *	Date of Earthquake	Instrument Component	Peak Acceleration cm/sec^2	Peak Velocity cm/sec	Epicentral Distance km	Bracketed Duration sec	Predominant Period sec
A008	Eureka Earthquake, Federal Building	I	12-21-54	N 79^{o} E	252.7	29.4	24.0	6.0	0.40
B037	Parkfield, CA Earthquake Temblor # 2	HR	6-27-66	N 65^{o} W	264.3	14.5	31.0	2.9	0.25
F088	San Fernando Earthquake, Municipal Building, Glendale	I	2-09-71	S 70^{o} E	265.7	30.7	34.1	8.0	0.60

*A = alluvium, I = intermediate, and HR = hard rock

TABLE VI

SCALING FACTORS FOR THE ACCELERATION

AMPLITUDE AND PREDOMINANT PERIOD

CIT File No.	Scaling Factors	
	Peak Acceleration	Predominant Period
A001	1.33	1.20
B034	1.31	1.00
J144	1.31	1.50
A008	0.97	2.05
B037	0.93	3.28
F088	0.92	1.37

a near field and a far field design earthquake and the estimation of the resulting bedrock motions at Creve Coeur. In addition, six existing acceleration time-histories (three for each design earthquake) were modified to resemble the design earthquake parameters for the purpose of computer simulation of the predicted ground motion.

Site Geology

A geologic investigation and literature search were performed to develop a comprehensive description of the physiographic, stratigraphic, and structural geologic conditions in the Creve Coeur Quadrangle and the surrounding region.

Physiography.

The portion of the Creve Coeur Quadrangle studied is located in north-central St. Louis County, Missouri. The region consists mainly of gently rolling uplands which become more rugged as the Missouri River is approached. The uplands are characterized by rounded divides approximately 700 feet in elevation. A limited area of low relief exists in the area along the Missouri River, Fee Fee Creek, and Creve Coeur Creek. With the exception of these flood plains, the area is moderately dissected by erosion and is well drained.

Bedrock.

The bedrock formations exposed within the study area are flat-lying sedimentary formations of Mississippian and Pennsylvanian age (Fig. 17). The Pennsylvanian rocks are predominantly shales, siltstones, and sandstones with some limestones and thin layers of coal and clay and are generally found at the higher elevations. Mississippian limestones underlie the remainder of the study area and are much more uniform in thickness and composition than the

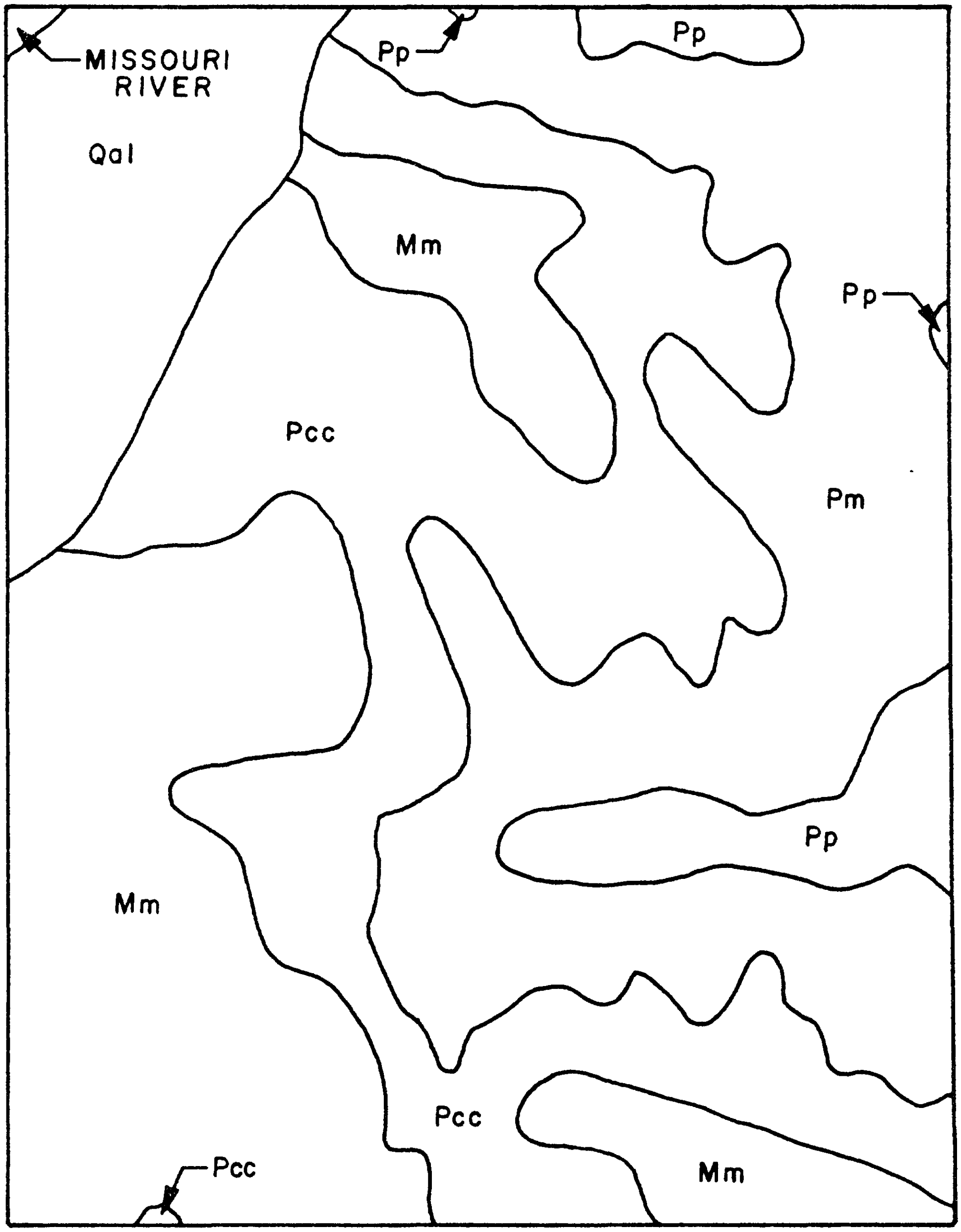

EXPLANATION

Qal Quaternary alluvium

Pennsylvanian System

Missourian Series

Pp Pleasanton group

Desmoinesian Series

Pm Marmaton group

Cherokee group

Pcc Cabaniss subgroup

Mississippian System

Mm Meramecian Series

—— Contact Lines

Figure 17. Geologic Map of Creve Coeur Quadrangle (after Missouri Department of Natural Resources, Division of Geology and Land Survey, 1979).

overlying Pennsylvanian rocks. The limestones have been subject to some solution activity, and limited areas of karst features occur within the study area.

Soils.

The soils overlying the bedrock consist of thick deposits of windblown silt (loess) derived from deposits on the Missouri River flood plain during Pleistocene glaciation. The loess completely mantles the bedrock topography and ranges in thickness from 40 to 95 feet near the river to approximately 10 to 20 feet in the south and eastern sections of the study area. The present land surface generally reflects the bedrock topography despite the relatively thick loess cover.

The Missouri River alluvium along the western part of the study area consists of as much as 100 feet or more of interbedded stratified gravels, sands, silts, and clays. In addition, there are deposits of organic materials included within the alluvium. Significant alluvial deposits also are present along the lower reaches of Fee Fee and Creve Coeur Creeks in the form of flood-plains and alluvial terraces. These consist of stratified sands, silts, and clays.

Evaluation of Ground Response

Ground response as used in this report refers to the reactions of a soil column to earthquake-induced loading from vibratory motion and resulting soil stability. Earthquake vibratory motion is produced by a stress wave emanating from a movement along a fault or from a rupture in the earth's crust. The stress wave is transmitted more rapidly and with less energy loss through firm bedrock than through unconsolidated soils. Therefore, the strong motion travels from the causitive fault movement through the bedrock and then up through the soils to the surface or foundation.

The overlying soils may respond to the bedrock ground motion in a number of different ways. The soils may remain stable, but as the vibratory motion is transmitted through the soil profile the motion undergoes at least some modifications. It is either amplified or attenuated. If the soils are composed of loose, granular materials, however, the soil particles either may compact or densify and cause the surface to subside or, as in the case of saturated sandy or silty soils, may lose their shear strength as a result of liquefaction. A third possibility is that the addition of a seismic force may cause soil slopes to become unstable and slide (Shannon and Wilson, 1972).

The concept that the degree of intensity of ground shaking is, in general, related to the local soil conditions has been accepted since as early as 1908 when Wood (1908) completed his study after the 1906 San Francisco earthquake. He compared the locations of damage from ground shaking with the local geologic setting and concluded that the amount of damage produced by the earthquake in different parts of the San Francisco area depended chiefly on the depth and composition of the underlying materials.

The concept was further strengthened after the 1957 San Francisco earthquake when recordings of ground motion were made at a number of locations. It was apparent from a comparison of the recorded ground motion with the soil columns at the sites that the frequency components of the surface motions at the different sites and the form of the response spectra changed in a reasonably consistent fashion depending on the hardness or softness of the soil conditions (Seed, 1975). Similar variations in ground motion have been recorded in more recent earthquakes, such as the 1971

San Fernando Valley, California, event (Maley and Cloud, 1971).

It also has been demonstrated that there is a variation of dynamic soil properties with the amplitude of the induced motion (Seed and Idriss, 1969b). Thus the strains developed in the deposit also affect the dynamic properties of the soil (shear modulus and damping). Furthermore, the variability of the dynamic soil properties with the amplitude of motion may cause amplification or attenuation of the bedrock motion. Therefore, the thickness and dynamic properties of the soil, as well as the amplitude and frequency of the input motion, determine the modifications of the bedrock motion that will occur (Seed, 1975).

Specific factors affecting dynamic soil behavior are beyond the scope of this report but have been discussed extensively in the literature (Seed, et al., 1973; Seed, 1975; Sherif and Ishibashi, 1978).

Possible approaches to the prediction of soil response from earthquake-induced ground motion have been discussed by Seed (1975). Of these approaches, the analytical ones are generally considered to be the most reliable. The three commonly accepted are the lumped mass model, the wave equation, and the finite element model. These have been reviewed during this project. In general, all the analytical ground response procedures require the same three basic steps (Schabel, et al., 1972): 1) determination of the bedrock motion characteristics underlying the study site; 2) determination of the dynamic soil properties at the site; and 3) analysis through the use of a mathematical model of the dynamic response of the soil column to the bedrock motion. In Phase I of the study, the seismicity, design earthquakes, and their expected bedrock motion in the Creve Coeur area were compiled to satisfy Step 1. The methods and results of the determination of the soil properties and the response analyses for Steps 2 and 3 are discussed below.

Material Properties.

Experimental work was performed in the Geotechnical Engineering Laboratories at the University of Missouri-Rolla and in the field to determine the soil stratigraphy and properties. These data were collected from test borings, a field reconnaissance, laboratory tests, and published and unpublished literature.

Field Exploration. Four borings were drilled to bedrock for the purpose of recovering samples, to identify and establish the stratigraphy, and to determine the competency of the deposits. Three of the borings were located in the deep floodplain deposits and one in the thick loess deposits on the adjacent bluffs. An extensive sampling program was conducted to provide high quality specimens for laboratory analysis. In addition to field classification of the soils, site stratigraphy, relative densities of cohesionless deposits, groundwater conditions, and depth to bedrock were determined by standard field methods. These data were used to establish the average soil properties needed for the response eveluation, to evaluate the potential failure condition, and to define the expected dynamic behavior of the soils.

Laboratory Investigation. Standard laboratory tests were run to determine the soil classifications and index properties as well as the physical and engineering properties of the soils. Tests included grain-size distribution, Atterburg limits, unit weight, and relative densities.

Dynamic triaxial shear tests were conducted to obtain shear moduli and damping for use in the ground response analysis and to evaluate the potential for liquefaction of the cohesionless soils.

This portion of the program was limited in scope by time/budgetary constraints. The amount of testing was, however, considered sufficient for the goal of the pilot study. A discussion of the cyclic testing program is presented in Appendix B. In addition, the shear moduli and damping properties of the soils were compared to data available in related technical publications.

Shear strength data, as well as additional boring logs and soil properties, were obtained through the cooperation of Eugene Brucker of Brucker and Associates in St. Louis, and depths to bedrock were obtained from geologist Ray Linebach of the Missouri State Highway Department.

Soil Profiles. For the purpose of mathematically modeling the ground motion and calculating the associated ground failures, the Creve Coeur study area was divided into seven generalized soil profiles (Fig. 1A, Appendix A) consisting of combinations of six separate soil types. The model profiles were constructed to define differences in the geology, physical properties, thicknesses, and groundwater levels of the soil deposits in Creve Coeur. Dynamic properties based on the test results and available data were assigned to the soil types (Table IA , Appendix A). The model profiles were based primarily on soil borings, existing engineering geologic maps, and field reconnaissance. In addition to soil properties, the profiles show maximum and minimum thicknesses to be expected in the study area.

Profiles A and B pertain to the Missouri River floodplain deposits, which consist of saturated silty fine sands, medium to coarse sands, and some gravels with the depth to ground water being approximately five to six feet. Thickness ranges up to 110 feet. Profiles C and D model the Pleistocene alluvial terrace and floodplain deposits along Fee Fee Creek and Creve Coeur Creek. Limited subsurface data were available in these areas, thus the profiles were developed from existing shallow boring logs and maps. The soils within these deposits are predominantly clayey silts overlying silty fine sands, and the water table is within 12 feet of the surface. The terrace deposits range from 50 to 70 feet in thickness, and the floodplain deposits range from 10 to 40 feet in thickness.

Profiles E, F, and G model the variations in the loess deposits covering the bluffs above the Missouri River flood plain. These deposits have been modified by weathering and generally consist of a clayey silt overlying a medium to stiff clay. The thicknesses for the three profiles range from 10 to 95 feet in the study area. (Individual profiles are divided into narrower ranges.) Borings to bedrock in the loess deposits indicate an irregular bedrock surface as well as a highly variable soil thickness, thus it is difficult to predict the soil thickness at any one location. Because of this, it was necessary to model the area on the range of thicknesses with the understanding that extremes of each type of profile might be encountered at closely spaced sites.

Ground Motion Evaluation.

Analytical Procedure. A survey of existing analytical modeling procedures of ground response was undertaken, and these procedures were evaluated for their applicability to the geologic conditions of the study area. For the Creve Coeur area, it was determined that the SHAKE analysis (Schnabel, *et al.*, 1972) was the most appropriate for the horizontally layered sites.

The SHAKE computer program is based on wave propagation theory. The soils composing each layer within a profile are considered to have uniform viscoelastic properties. In addition, the motion in the underlying bedrock is assumed to consist of a series of sinusoidal motions of different frequencies. The response at the surface of the deposit is then computed for a range of base rock frequencies, which provide a response amplification spectrum. The ground surface motion is then evaluated by multiplying the Fourier spectrum of the base motion by the amplification spectrum. The nonlinear stress-strain characteristics of the soils is accounted for by use of equivalent linear soil properties, and an iterative procedure is used to obtain values for the shear modulus and damping, which are dependent on the strains in each layer (Schnabel, et al., 1972; Seed, 1975).

Input. To determine ground response, the generalized soil profiles, properties, and soil shear moduli and damping vs. strain properties were entered into the SHAKE program. These profiles were then subjected to the three acceleration time-histories representing the near field Ozark Uplift earthquakes and the three acceleration time-histories for the far field New Madrid earthquakes. As mentioned previously, three acceleration time-histories were chosen for each earthquake in an attempt to average idiosyncrasies present in individual records. Because the response spectra for the ground motions are very dependent on the frequency characteristics of the base motion, three acceleration time records with slightly different frequency characteristics should impart an averaging effect on spectral properties and should represent the worse case, i.e., the highest accelerations and greatest strains within the deposits.

Seismic Response of Profiles. The primary objective of the research was to develop mapping procedures that are based on the dynamic response of the local soil columns rather than on a conventional geologic classification. For microzonation, the criteria of major interest are the modification of the bedrock motion by the overlying soil deposits and the resulting surface response. It is the dynamic response that is used as a basis for engineering evaluations of seismic hazards and for evaluations of the potential damaging effects to structures. Classically, microzonation of an area has been based on geologic classifications of the soil units and on the assumption that the seismic response will vary for each unit. However, considering the interrelated effects of the base motion, the dynamic properties of the individual soils composing the deposit, and the thickness of the deposit, geologically different deposits may exhibit very similar dynamic responses. Therefore, geology is not necessarily a valid basis for evaluating relative ground response.

Because engineering evaluations of seismic hazards are based on the dynamic response of the local soil deposits and not necessarily on the geology, the Creve Coeur study area was mapped on the basis of the dynamic response of the model soil profiles.

The seismic response maps constructed for the Creve Coeur area were based on the maximum ground response, or most severe case. As mentioned above, because the dynamic response of a soil deposit for a given base motion depends not only on the dynamic properties of the individual soil types in the deposit but also on the deposit's thickness, a variation in thickness of a given deposit may change the dynamic response significantly. The thicknesses of the soil deposits in the study area tend to vary considerably and are unpredictable because of the irregular bedrock surface. In order to evaluate the most severe ground response, each model soil profile was analyzed by the SHAKE computer program for different possible thicknesses. This was done for the six acceleration time-histories representing the two design earthquakes.

The resulting ground responses, in the form of maximum horizontal accelerations and maximum velocity spectra, were tabulated for each profile and for different thicknesses of each profile. The maximum ground acceleration and velocity response for each model deposit were used as the basis for mapping the dynamic response of the Creve Coeur area for the two design earthquakes.

The resulting response maps do not show different responses for each model deposit on all the maps. In several cases, the horizontal accelerations or velocity responses of the different profiles were similar and were mapped as one unit. This varied for each design earthquake because of the differences in the frequency characteristics of the base motion.

The results of the SHAKE analyses show that maximum bedrock accelerations for all six acceleration time-histories were amplified in all the soil profiles. However, it is of interest to note that in general the greatest intensity of shaking was experienced in the shallower loess deposits. The maximum ground response from the individual acceleration time-histories (in the form of maximum surface accelerations and velocity response spectra) varied somewhat in magnitude and in the profile in which it occurred. However, this was to be expected because of the dependence of the ground response on the frequency characteristics of the base motion and the fundamental frequency of the soil deposits. In general, the amplifying effects of a soil deposit on ground accelerations are greatest when the predominant period of the base motion and the fundamental period of the deposit are similar. It is also important to note that the fundamental period of a deposit will vary somewhat with differences in both frequency and amplitude of the base motions. This is due to the nonlinear behavior of the soils composing the deposit (Seed and Idriss, 1969b; Seed, 1975).

Maps showing the maximum horizontal acceleration response at the ground surface were constructed for the near field and far field design earthquakes and were based on the maximum response from the three acceleration time-histories for each design earthquake (Figs. 18 and 19). These maps were used in the evaluation of slope stability and potential for liquefaction as discussed in the following sections. In addition, the maps also serve as guides to relative ground response.

As mentioned previously, the maximum horizontal ground accelerations were experienced in the shallower loess deposits. For the near field earthquake, the accelerations in the loess deposits ranged from greater than 1.0g in profile F down to 0.73g in profile E. The accelerations experienced in the thicker alluvial deposits tended to follow the same pattern in that the thicker floodplain and terrace deposits ranged between 0.58 and 0.65g, whereas the thinner floodplain deposits along Fee Fee and Creve Coeur Creeks reached a maximum of 0.87g. The maximum ground accelerations experienced for the far field earthquakes followed a similar pattern with slight variations and somewhat lower values. The greatest accelerations experienced in the loess deposits ranged from less than 0.56g in profile F to 0.27g in profile G. Maximum accelerations for the alluvial deposits ranged from a high of 0.50g in the floodplain deposits of Fee Fee and Creve Coeur Creeks (profile D) to a low of 0.41g in the thick floodplain deposits of the Missouri River (profile B).

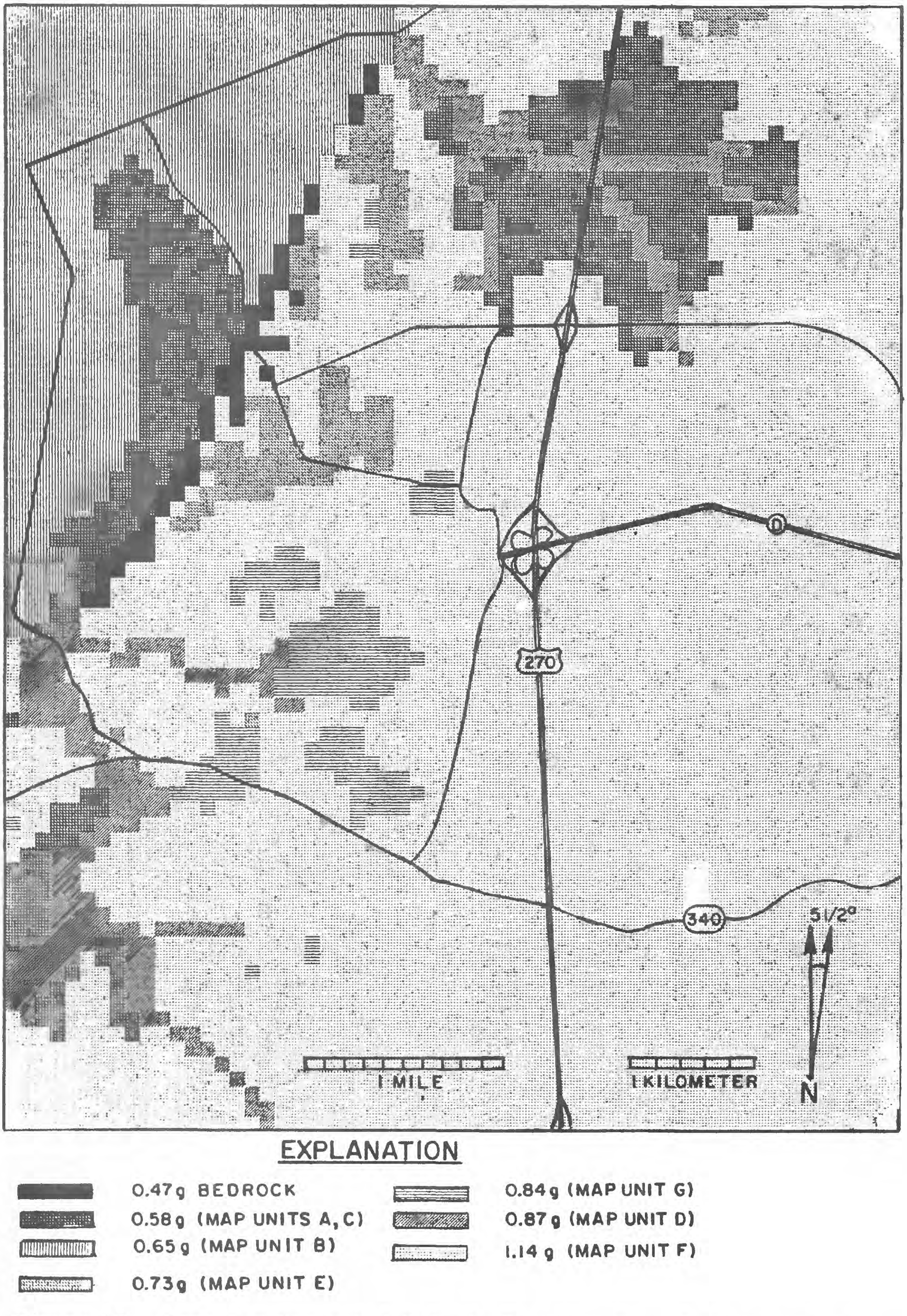

Figure 18. Computer-Generated Seismic Response Map of Maximum Horizontal Accelerations for the Near Field Earthquake, Creve Coeur Quadrangle.

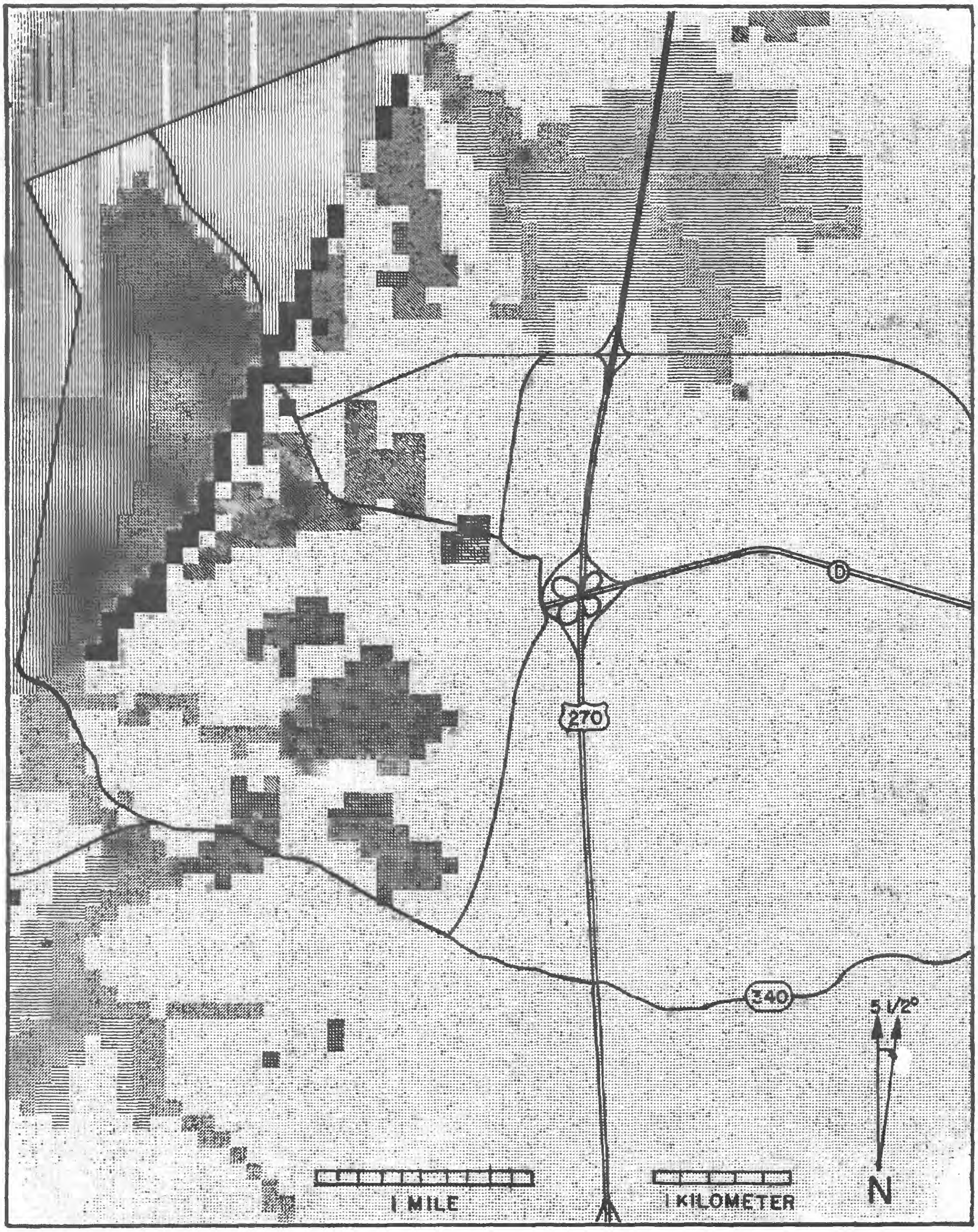

EXPLANATION

- 0.25g (BEDROCK)
- 0.27g (MAP UNIT G)
- 0.41g (MAP UNIT B)
- 0.45g (MAP UNIT A)
- 0.48g (MAP UNIT C)
- 0.50g (MAP UNIT D)
- 0.53g (MAP UNIT E)
- 0.56g (MAP UNIT F)

Figure 19. Computer-Generated Seismic Response Map for Maximum Horizontal Accelerations for the Far Field Earthquake, Creve Coeur Quadrangle.

The trend of relative ground response was as expected because of frequency characteristics of the ground motion and the fundamental period of the deposits. To verify this trend further, Nuttli (personal communication, 1979) has reported experiencing the greatest intensity of shaking in the thinner soil deposits of the St. Louis area during earthquakes. The variations in response of the units to the far field and near field earthquakes were also expected because of the inherent differences in frequency characteristics from attenuation of a far field source.

Evaluation of Slope Stability

The evaluation of the stability of earth slopes is a major problem in seismically active regions. The 1959 Yellowstone earthquake, the 1964 Alaska earthquake, and the 1971 San Fernando, California, earthquake have illustrated the importance of being aware of natural slopes that are susceptible to failure during earthquakes (Seed, 1967) and of the necessity of including aseismic designs for man-made slopes in earthquake prone areas. Because of the potential for property damage and loss of life, most of the seismic slope stability research to date has been devoted to earth dams. The near failure of the lower San Fernando dam during the 1971 earthquake caught the attention of regulatory agencies and design engineers and precipitated a move toward reevaluation of conventional design methods and an increased research effort in developing dynamic slope analyses procedures (Makdisi and Seed, 1978). Many of the results of this research can be applied to the mapping of slope hazards.

For regional seismic hazards mapping, the evaluation of slope stability generally is based on experience, judgment, and qualitative data. It was an objective of this research project to develop a procedure, applicable to regional mapping, that could be used to evaluate seismically induced slope hazards through the calculation of a factor of safety against failure. Slope hazard maps based on engineering analyses would be an improvement over conventional maps, because the magnitude of hazard would be defined. Conventional classifications of relative slope stability are based only on qualitative data.

Areas of potentially unstable slopes within the study area were determined by pseudostatic analyses of generalized slope models for the two design earthquakes.

A field examination was conducted to define slope characteristics, the slope forming deposits, and to look for evidence of past movement. Data concerning soil properties and slope behavior were obtained from published and unpublished technical reports.

It is impractical to analyze each individual slope for regional mapping purposes. Therefore, generalized slope models that represent typical slope conditions were developed. The models included a consideration of the ranges of slope steepness, soil profile, and height so that any slope in the study area would be represented. The ranges of the slope heights were determined from a topographic map. The ranges of the slope angles analysed for each model were based on standard intervals used by the U.S. Geological Survey in its planning and hazards maps. These are:

Flat to very gentle slopes	(Less than 5 percent slope)
Gentle slopes	(5 to 15 percent slope)
Moderate slopes	(15 to 25 percent slope)
Steep slopes	(Greater than 25 percent slope)

The slope models were then constructed on the basis of combinations of slope height, deposit, and range of slope steepness.

A computer slope stability analysis (Wright, 1974) using static, undrained conditions was used to find the most critical failure surface for each of the models for static conditions at various angles of slope and to find the factor of safety against failure. The undrained condition was used to model the worst conditions, i.e., saturated soil after periods of wet weather. By using Newmark's method (1965), critical or yield acceleration was calculated for the slope intervals of each model. This method of analysis is a simplified approach, which permits rapid estimates of slope stability to be made during earthquakes and can be readily applied to regional hazards mapping. By using this procedure, the yield acceleration can be calculated as a steady horizontal force, which acts at the center of gravity of a sliding mass and which will just overcome the stabilizing forces and barely keep the mass in motion after it has started to move or after several pulsations of motion have occurred. For the case of horizontal acceleration, the yield acceleration for a circular sliding surface may be calculated from

$$Ay = (FS-1) \tan \beta \qquad (1)$$

in which

Ay = yield acceleration (expressed in g's)

FS = static factor of safety, and

β = angle between a line that connects the center of gravity of the slide mass with the center of the critical circle and a vertical line intersecting the center of the critical circle.

The resulting yield accelerations and slope intervals were digitized to form a slope data base. The slope hazards were then assessed with a computer by superimposing the maximum acceleration ground response map for each design earthquake upon the slope hazards maps (Figs. 20 and 21), which delineate areas where yield accelerations can be equaled or exceeded, and slope failure is likely during earthquakes with characteristics similar to those of the design earthquakes.

The slopes in the Pleistocene terrace area around Fee Fee and Creve Coeur Creeks generally vary between 30 to 50 feet in relief and have grades up to 35 percent. Yield accelerations, calculated for the slope models that range from moderate to steep, varied from 0.15 to 0.21g for slopes of high relief and from 0.35 to 0.41g for slopes of low relief. Accelerations, which were calculated for the soil profiles by using the SHAKE analysis for both the near field and far field earthquakes, greatly exceeded the yield accelerations. Consequently, the moderate to steep slopes in the terrace deposits were mapped as potential slope hazards.

The thin soil cover of the steeply sloping (greater than 25 percent slope) bluffs of outcropping bedrock that overlook the Missouri River flood plain is presently undergoing soil creep under static conditions. Any ground shaking from an earthquake could further upset this marginal slope stability. Therefore, based on the geologic conditions, the areas occupied by the bluffs were mapped as potentially hazardous for both near field and far field events.

In general, the loess slopes vary in relief from approximately 60 to 100 feet and range in steepness up to 45 percent. Only the yield accelerations for the loess slope models with a greater than 25 percent slope were low enough to present a slope hazard. The yield accelerations for the slopes of high relief

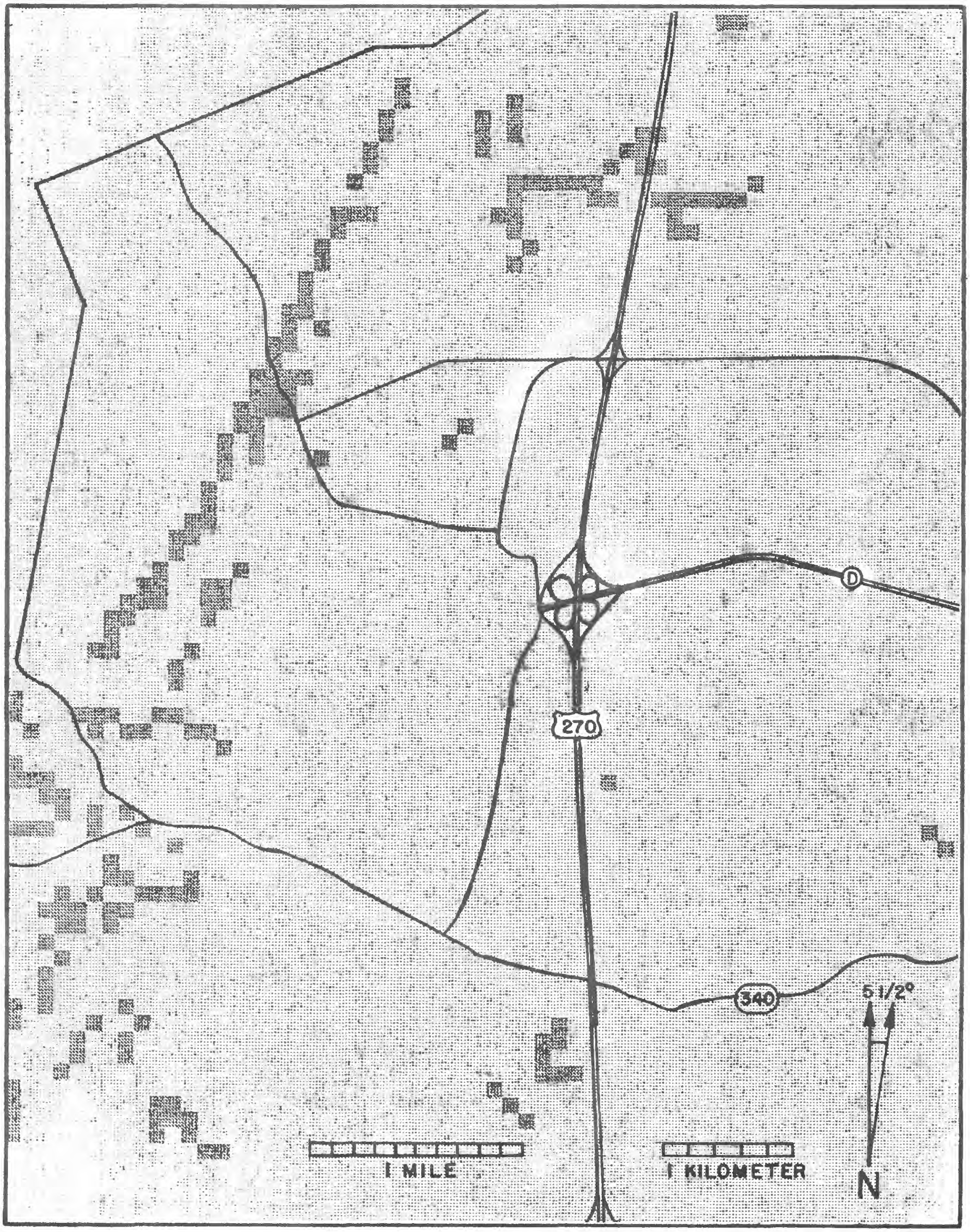

EXPLANATION

SLOPE HAZARD

NO SLOPE HAZARD

Figure 20. Computer-Generated Slope Hazards Map for the Near Field Earthquake, Creve Coeur Quadrangle.

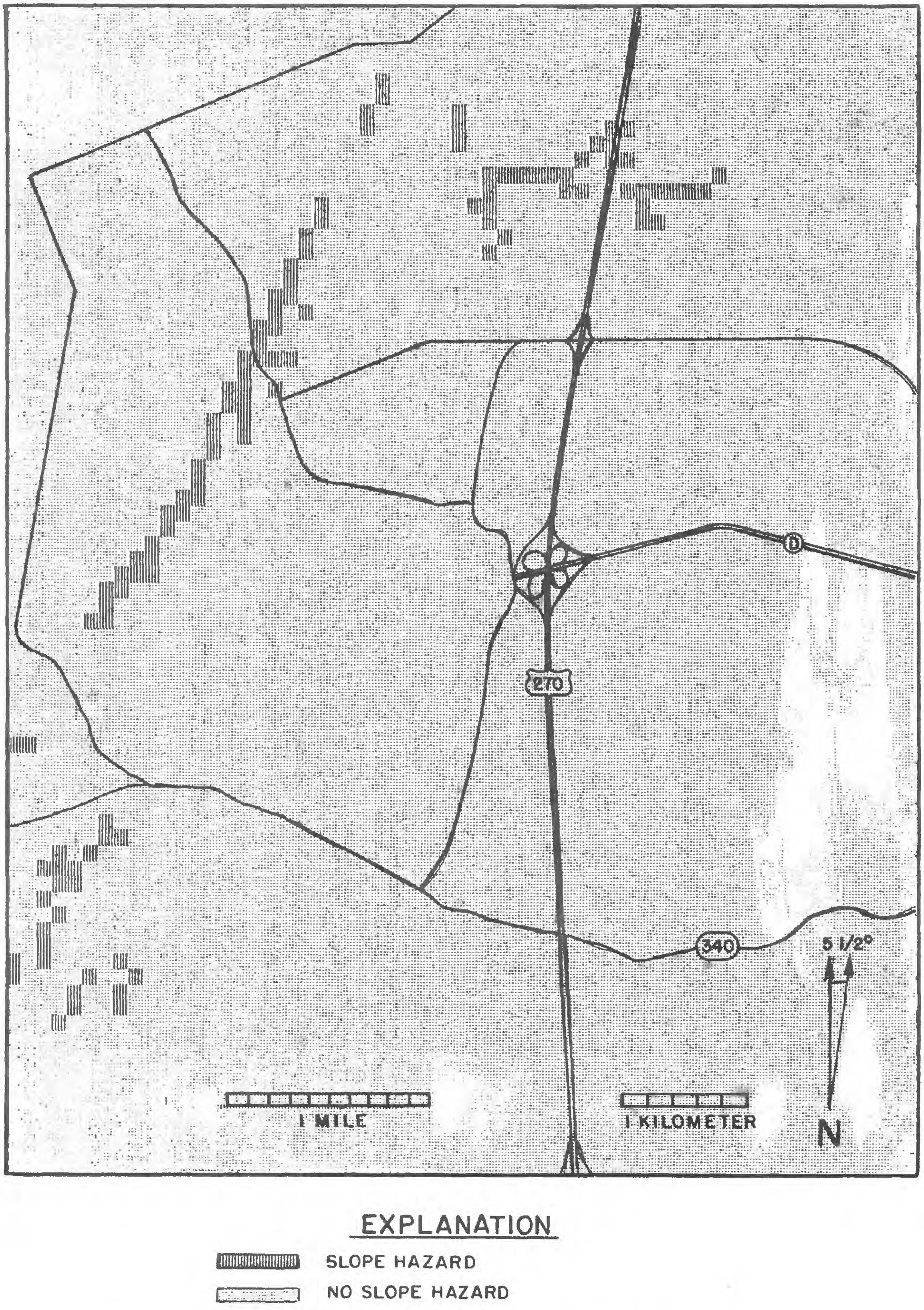

Figure 21. Computer-Generated Slope Hazards Map for the Far Field Earthquake, Creve Coeur Quadrangle.

ranged from 0.61 to 0.64g and for the slopes of low relief from 0.71 to 0.74g. Accelerations in these deposits were predicted to range up to 0.82g for the near field earthquake but only to 0.56g for the far field earthquake. Therefore, loess slopes of greater than 25 percent slope were mapped as potentially hazardous for the near field earthquake only.

Evaluation of Liquefaction Potential

Earthquake-induced liquefaction of saturated soils has been the cause of many catastrophic failures of engineering structures. Major landslides, lateral movement of bridge supports, settling and tilting of building foundations, and failure of waterfront retaining structures have all been documented in recent earthquakes in Alaska and Niigata, Japan, as well as in many other localities (Seed and Idriss, 1971). The potential for liquefaction is therefore a major concern in the design of engineering structures, urban developments, and potentially hazardous structures, such as nuclear power plants. For these reasons, the identification and mapping of geologic deposits susceptible to liquefaction are very important considerations. Although a variety of analytic procedures exist, Seed and Idriss's (1971) simplified procedure was developed to provide a reasonably good means for evaluating liquefaction potential for regional mapping purposes to furnish a base that could readily be supplemented by a ground response analysis to provide an even more definitive evaluation.

The critical acceleration, which is the ground acceleration required to initiate liquefaction, was calculated for the model profiles with high water tables and sand deposits and was digitized to form a data base of liquefaction potential. The liquefaction hazard was then assessed for the two design earthquakes by using the computer to superimpose the liquefaction potential data base on the ground response (maximum horizontal accelerations) data base. The resulting liquefaction hazards maps (Figs. 22 and 23) show the areas where the critical accelerations to initiate liquefaction are equaled or exceeded.

Areas digitized as susceptible to liquefaction include the floodplain deposits of the Missouri River and the terrace and floodplain deposits of the Fee Fee and Creve Coeur Creeks. All these deposits contain thick sands and fine silty sands, a water table close to the surface, and grain-size distributions and relative densities that are within Seed and Idriss's limits of liquefaction susceptibility (Seed and Idriss, 1971). Because of the severe ground motion that could be induced from both the near field and far field earthquakes, the critical accelerations required for liquefaction can be greatly exceeded. Therefore, all the susceptible areas were rated as having a high level of liquefaction hazard. For further studies, in which a less severe ground motion is used, it may be desirable to delineate differences in the liquefaction hazards by using designations of high, moderate, and low (hazard or potential) to reflect the magnitudes of ground accelerations that would exceed the critical acceleration.

Evaluation of Damage Potential

Most documented attempts at producing ground response hazards maps have used either Modified Mercalli Intensities or intensity designations predicted from empirical relations based on historic intensity data (Borcherdt, *et al.*, 1978). Medvedev's (1965) seismic intensity increments, which are based on depth to ground water, have also been used (Bell, *et al.*, 1978). The disadvantages in using this type of approach are many, but probably the greatest

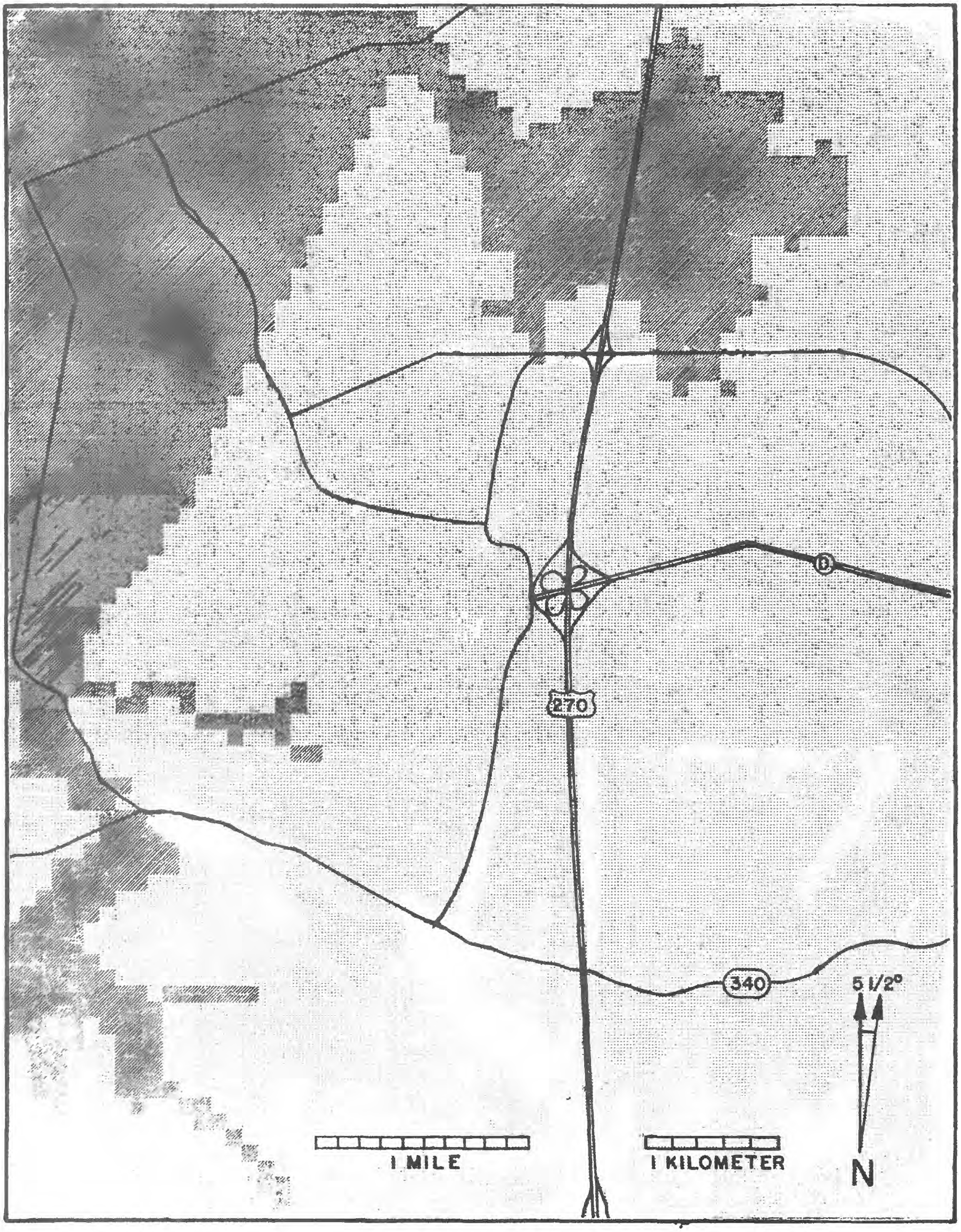

EXPLANATION

HIGH LIQUEFACTION HAZARD

NO LIQUEFACTION HAZARD

Figure 22. Computer-Generated Liquefaction Hazards Map for the Near Field Earthquake, Creve Coeur Quadrangle.

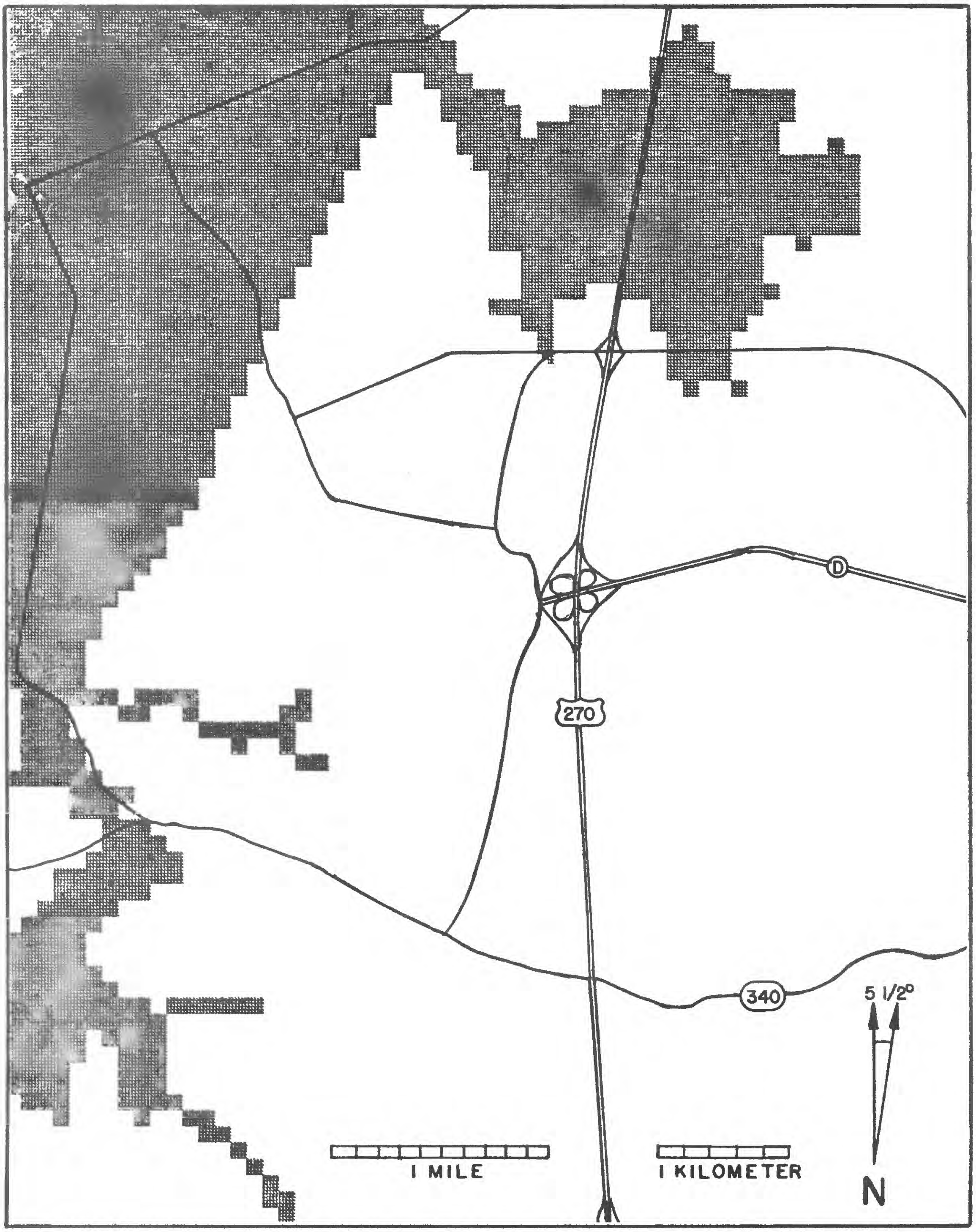

EXPLANATION

HIGH LIQUEFACTION HAZARD

NO LIQUEFACTION HAZARD

Figure 23. Computer-Generated Liquefaction Hazards Map for the Far Field Earthquake, Creve Coeur Quadrangle.

disadvantages are that many of the methods are very empirical, often based too heavily on qualitative judgment, and do not consider the dynamic properties of the local soil column or the frequency characteristics of the ground motion. In addition, it is difficult for the engineer and planner to interpret the potential damage to structures from these intensities. Algermissen and Perkins (1972) suggested that maps of intensity of shaking should be closely related to the use contemplated for the maps. In microzonation, safety against building damage from seismic shaking is of major interest. With this point of view, the significant effects of earthquakes on structures is the inducement of forces into the structures and the effects of these forces on structural performance. For these reasons, a seismic response hazards map or intensity of shaking map should include information not only on the dynamic lateral forces exerted on structures by the ground motion but on the effects of the ground motion on structural performance.

Damage Potential.

The time-history of a ground motion at a specific site with a given soil column is characterized by a response spectrum. The differences in time-histories of motions at different locations are evaluated by comparing the response spectra. An important application of the response spectrum is that it provides a means of evaluating the maximum lateral forces developed in a structure subjected to a given base motion. Design engineers use the acceleration response spectrum (S_a) to approximate the maximum lateral force on a building. This force is approximately equal to the product of the spectral acceleration for the fundamental period of the structure and the weight of the building.

Seed (1975) compared the distribution of spectral accelerations for different period ranges for the 1957 San Francisco earthquake. The distribution of S_a/g varied widely, therefore the lateral force expressed as a proportion of the weight of any building also varied widely for different structures over a small section of the city. Spectral acceleration values are an index of the maximum lateral forces that a structure is subjected to by a given ground motion, but they do not provide information on the length of time a structure is subjected to that force. Therefore, the S_a is not necessarily the best index of the potential damage to a structure. The spectral velocity, S_v, is considered to be a better index of damage potential, because it is based on the S_a and its period. Seed (1975) compared the distribution of S_v to the same cross section and ground motion as discussed previously. The deformation potential, expressed as S_v, varies considerably less than the maximum dynamic lateral force coefficient, S_a/g, because it is influenced less by a strong motion of very short duration.

Damage potential indices have been developed (Seed, 1975) that provide a relative measure of the ability of a structure to withstand a given ground motion. One index is based on the ratio S_a/g, the other on the S_v. Because the S_v is a better index of the damaging effects of a base motion, the damage potential index based on it is considered better and was proven to be quite satisfactory as a basis for analyzing the damage during the 1967 Caracas earthquake.

Ground Response Hazards Map for Creve Coeur.

The maximum S_v response from the three acceleration time-histories for each design earthquake for a period range of 0.1

to 0.2 seconds was used to prepare two maps (Figs. 24 and 25). This range is generally accepted as the upper end of the range of the natural period of the fundamental mode of response for one- and two-story structures. Because S_v is a measure of the potential damaging effect of a base motion, the resulting maps are useful as measures of the ground response hazards that one- and two-story buildings would sustain. For expanded studies, other period ranges may be mapped for multiple story structures when applicable. The map should be useful to engineers and architects for determining the damage potential indices of structures and ascertaining the degree of relative ground shaking and movement of dynamic lateral forces.

As mentioned previously, the maximum ground responses (in the form of maximum accelerations and S_v responses) derived from the individual acceleration time-histories vary somewhat in magnitude and are different in the various deposits in which they occur. Also, the maximum S_v response for the 0.1- to 0.2-second period range does not occur in the same deposit in which the maximum acceleration is experienced. This is due to the fact that the maximum S_v response occurs for a longer period.

The greatest S_v response for the far field earthquake occurred in the thinner loess deposits (profile F). The S_v response is much greater in profile F than it is in the other deposits and even exceeds the maximum response of the deposits to the near field earthquake. This is simply the result of a much more rapid buildup to a peak in S_v in this profile than in the other deposits. The S_v response of profile F ranges from 0.24 to 1.37 feet per second for the design period range, whereas the S_v response of the other thin loess and alluvial deposits did not exceed 0.51

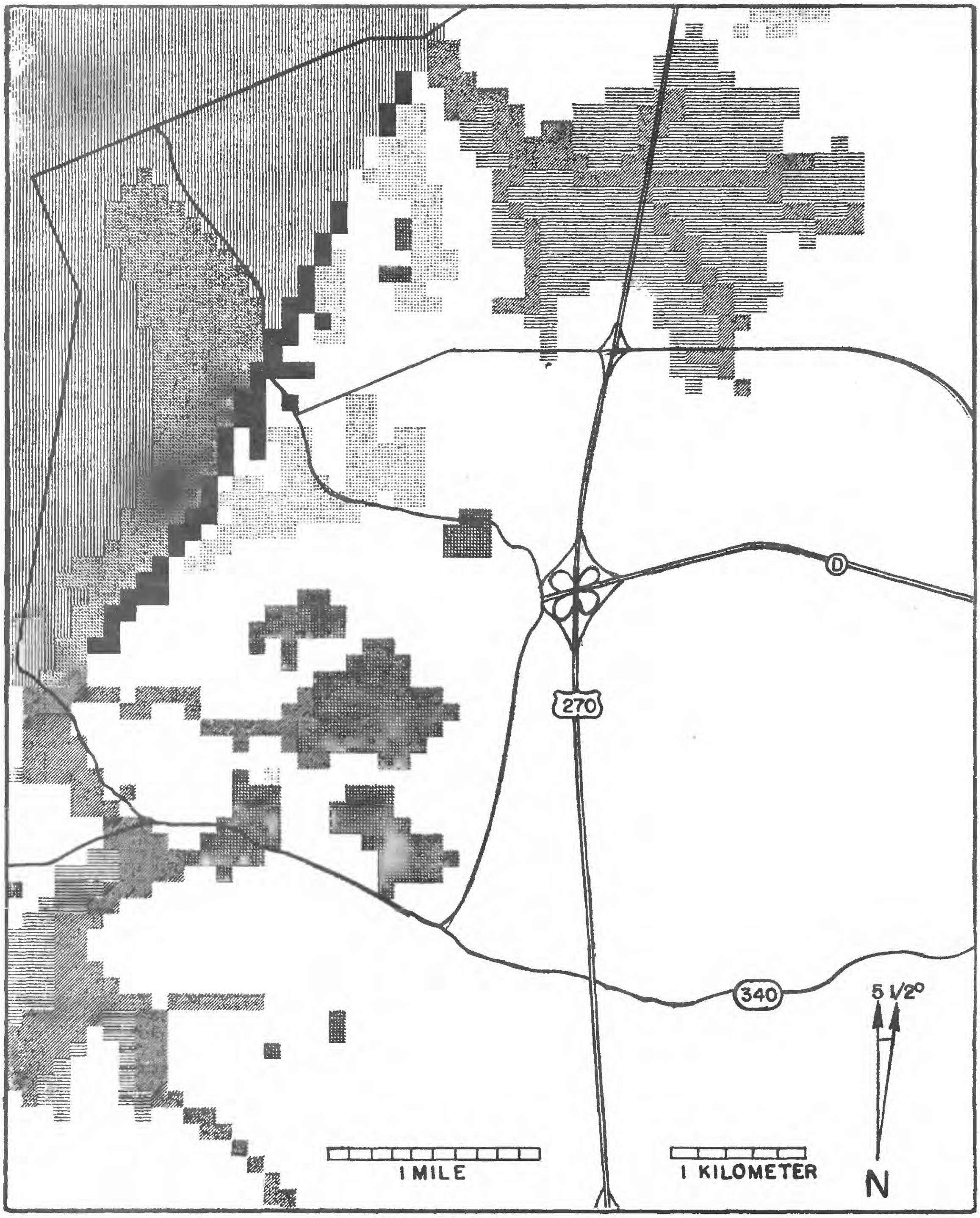

EXPLANATION

SPECTRAL VELOCITY RESPONSE (0.1–0.2 SECOND, 5% DAMPING)

- BEDROCK
- 0.50–1.07 Ft./Sec. (MAP UNIT G)
- 0.13–0.69 Ft./Sec. (MAP UNIT B)
- 0.10–0.58 Ft./Sec. (MAP UNIT A)
- 0.07–0.56 Ft./Sec. (MAP UNIT C)
- 0.40–1.75 Ft./Sec. (MAP UNIT D)
- 0.10–0.46 Ft./Sec. (MAP UNIT E)
- 0.34–1.21 Ft./Sec. (MAP UNIT F)

Figure 24. Computer-Generated Map of Damage Potential for One- to Two-Story Structures for the Near Field Earthquake, Creve Coeur Quadrangle.

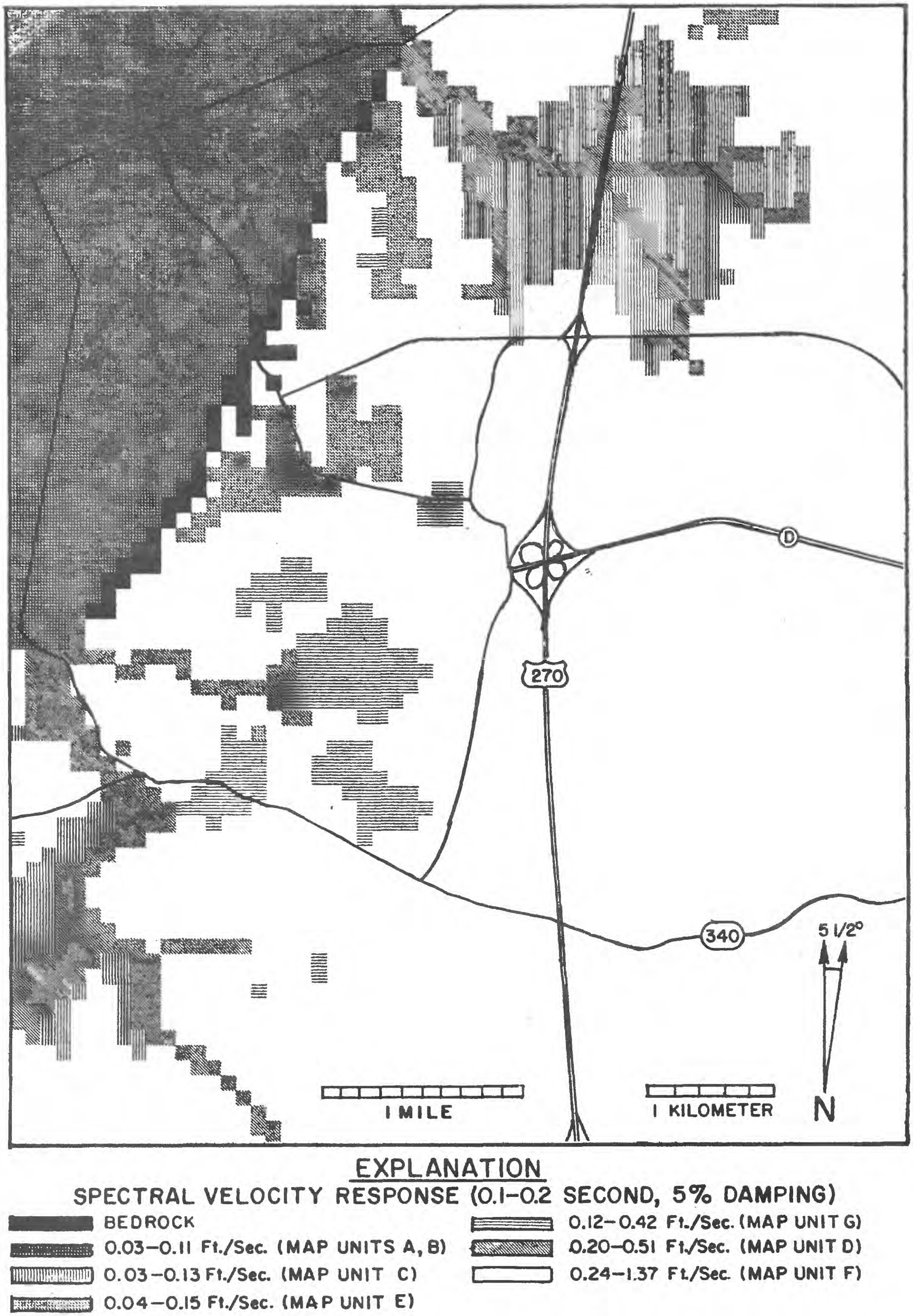

Figure 25. Computer-Generated Map for Damage Potential for One- to Two-Story Structures for the Far Field Earthquake, Creve Coeur Quadrangle.

feet per second. The thicker loess and alluvial deposits did not exceed an S_V of 0.15 feet per second.

The most severe S_V response for the near field earthquake occurred in the floodplain deposits along Fee Fee and Creve Coeur Creeks (profile D) in which the S_V ranged from 0.40 to 1.75 feet per second. The thin loess deposits also experienced strong S_V responses ranging up to a maximum of 1.21 feet per second for profile F and 1.07 feet per second for profile G. The thicker loess and alluvial deposits experienced a much lower S_V response, which did not exceed 0.69 feet per second.

Because the S_V is an index of the damaging effects of a base motion, the highest potential for damage to one- and two-story structures in the Creve Coeur area from the design ground motions would be in the thin loess and alluvial deposits. The potential for damage as a result of ground motion alone would be much less in the thick alluvium and loess deposits.

SUMMARY AND CONCLUSIONS

The primary objective of the research was to develop mapping procedures that would be based on the dynamic response of local soil columns rather than on a conventional geologic classification of soil deposits. Zoning maps based on this concept would be an improvement over existing procedures, because ground response is of primary importance in assessing the potential for damage to structures and the levels of individual seismic hazards.

In addition, an effort was made to develop a method that could be used to evaluate the levels of individual seismic hazards in the form of zoning maps at detailed scales and to assess the significant seismic hazards for a study area. The method would be an improvement over existing procedures, because it would incorporate provisions for both quantitative engineering data and qualitative geologic data, both of which are not generally considered in regional hazard mapping.

The objectives were accomplished through the development of a simple and rational method,which was used to assess the relative levels of seismic hazards applicable to the study area. Assessments of liquefaction and slope hazards were made on the basis of the maximum seismic response of the soil columns and on calculations of factors of safety against failure. State-of-the-art engineering analyses as well as the latest geologic and seismologic information and techniques were applied in these assessments.

The method for the hazard assessment was adapted to the minicomputer-driven Comtal image processing system, which has a display with interactive gridded data base capabilities. Computer-generated, earthquake hazards maps provide the maximum degree of freedom in assessing or delineating each hazard for a given area, because hazard classification may be modified or updated easily for different earthquakes or additional information.

Modified acceleration time-histories were used to represent the two design earthquakes chosen from the seismic source zones close to the St. Louis area. Model soil profiles were developed on the basis of field and laboratory tests and entered along with the earthquake information into the SHAKE (Schnabel, et al., 1972) computer program. The SHAKE analysis was used to calculate the ground motion characteristics for the two design earthquakes in the form of the maximum horizontal accelerations, velocity spectra, and shear stresses developed in the soil profiles.

A seismic response data base was constructed by using a gridded file system covering the geographical area studied. From this data base, computer-generated maps of maximum acceleration and damage potential were constructed. The distribution of maximum acceleration was used to aid in the assessment of liquefaction hazards and slope hazards. The damage potential maps were based on the velocity response spectra of the various soil deposits and served as an index of the relative potential for damage from the two design earthquakes to one- and two-story structures. The liquefaction potential of the saturated sandy deposits was assessed by calculating the critical acceleration that would induce liquefaction and was digitized to form a liquefaction data file. This data file was superimposed on the expected acceleration response data file to assess the liquefaction hazard and to define the hazard area. Slope stability hazards were calculated by using a pseudostatic approach in which the static factor of safety and the failure surface were calculated. The magnitude of acceleration (yield acceleration) required to cause failure of each model slope was calculated and digitized to form a slope data file. The yield accelerations were superimposed upon the maximum horizontal acceleration data file to assess the slope hazard and to delineate areas subject to slope failure.

The resulting set of maps should be of value to engineers, architects, planners, and government officials who make decisions concerning the future development of the Creve Coeur area. In addition, the procedures developed for this study are applicable to any seismic hazards study.

RECOMMENDATIONS

Recommendations drawn from this study are:

1. Future seismic hazard mapping should be based on the dynamic response of local soil deposits rather than on conventional geologic classifications. The dynamic response is of primary importance in quantitative assessments of the potential for damage to structures and of the levels of individual seismic hazards.

2. Considering the proximity of the St. Louis area to active seismic regions and the broad areas defined by this study that have a high level of potential seismic hazard, it is recommended that the pilot study be expanded to include all of the St. Louis metropolitan area. Earthquake hazards maps are essential to effective planning and design in a seismically active metropolitan area.

3. Different design earthquakes may be chosen for an expanded study. The hazard assessment and mapping procedure was developed by using maximum earthquakes (1,000-year earthquakes, which have a 63 percent probability of occurrence in that time interval). This decision on earthquake selection should be based on the life

expectancies of structures and the completeness and reliability of the seismicity records for earthquakes with shorter return periods.

4. A more precise evaluation of the liquefaction hazard and dynamic soil properties could be developed with more sophisticated testing equipment.

5. The procedures of earthquake hazard evaluation developed from this study are applicable to any seismic hazards study outside the St. Louis area and may be easily modified to add or delete data applicable to any hazard assessment.

6. A more sophisticated evaluation of the slope stability analysis that utilizes the amount of displacement as a criterion for failure should be considered. Because of the pulsating nature of earthquake-induced forces, calculations of slope stability using a constant inertial force result in conservative estimates of deformation and do not predict liquefaction failures.

BIBLIOGRAPHY

Algermissen, S. T., Stepp, J. C., Rinehart, W. A., and Arnold, E. P., 1969, Studies in seismicity and earthquake damage statistics: U.S. Dept. of Commerce, E.S.S.A., Appendix B.

Algermissen, S. T., and Perkins, D. M., 1972, A technique for seismic zoning: General considerations and parameters: Proceedings, International Conference on Microzonation, Seattle, Wash., pp. 865-878.

Bauhof, F. C., 1979, Geology, seismicity, and anticipated earthquake ground motions in Creve Coeur Quadrangle, St. Louis County, Missouri: Unpublished Masters Thesis, University of Mo.-Rolla, Rolla, Mo.

Bell, E. J., Trexler, D. T., and Bell, J. W., 1978, Computer-simulated composite earthquake hazard model for Reno, Nevada: Proceedings, Second International Conference on Microzonation, San Francisco, Calif., pp. 471-484.

Bingler, E. C., 1974, Earthquake hazards map, Reno folio: Nevada Bur. of Mines and Geology, Environmental Series, Map 4A.

Bishop, E. E., Eckel, E. B., and others, 1978, Suggestions to authors of the reports of the United States Geological Survey, 6th ed.: U.S. Government Printing Office, Washington, D.C.

Borcherdt, R. D., 1975, Studies for seismic zonation of the San Francisco Bay region: U.S. Geological Survey Prof. Paper 941-A.

Borcherdt, R. D., Gibbs, J. F., and Lajoie, K. R., 1975, Prediction of maximum earthquake intensity in the San Francisco Bay region, California, for large earthquakes on the San Andreas and Hayward Faults: U.S. Geological Survey, MF-709.

Borcherdt, R. D., Gibbs, J. F., and Fumal, T. E., 1978, Progress on ground motion predictions for the San Francisco Bay region, California: Proceedings, Second International Conference on Microzonation, San Francisco, Calif., pp. 241-254.

Brabb, E. E., Pampeyan, E. H., and Bonilla, M. G., 1972, Landslide susceptibility in San Mateo County, California: U.S. Geological Survey Misc. Field Studies Map, MF-360.

Brown, R. D., Jr., 1972, Active faults, probable active faults, and associated fracture zones, San Mateo County, California: U.S. Geological Survey Misc. Field Studies Map, MF-355.

Castro, G., 1969, Liquefaction of sands: Harvard Soil Mechanics Series. No. 81, Harvard University, Cambridge, Massachusetts.

Clough, R. W., and Chopra, A. A., 1966, Earthquake stress analysis in earth dams: Jour. of the Engineering Mechanics Div., A.S.C.E., Vol. 92, No. EM2, Proc. Paper 4793, pp. 197-212.

Cornell, C. A., 1970, Design seismic inputs: in Hansen, R. J., ed., Seismic design for nuclear power plants: M.I.T. Press, Cambridge, Mass.

Dibblee, T. W., Jr., 1973, Regional geologic map of the San Andreas and related faults in Carrizo Plain, Temblor, Caliente, and La Danza Ranges and vicinity, California: U.S. Geological Survey Misc. Geol. Inv. Map, I-757.

Finn, W. D. L., 1967, Static and seismic analysis of slopes: Rock Mechanics and Engineering Geology, Jour. of International Society of Rock Mechanics.

Finn, W. D. L., 1972, Liquefaction of sands: Proceedings, International Conference on Microzonation, Seattle, Wash., pp. 87-111.

Finn, W. D., Bransby, P. L., and Pickering, D. J., 1970, Effect of Strain History on Liquefaction of Sand, Journal of the Soil Mechanics and Foundation Div., A.S.C.E., Vol. 96, SM6, pp. 1917-1937.

Fuller, M. L., 1912, The New Madrid earthquake: U.S. Geological Survey Bull. 494.

Gaus, M. P., and Sherif, M.A., Co-Chairmen, 1972, Proceedings, International Conference on Microzonation, Seattle, Wash.

Gaus, M. P., and Sherif, M. A., 1972, Zonation and microzonation: Proceedings, International Conference on Microzonation, Seattle, Wash., pp. 3-12.

Goodfield, A. G., 1965, Pleistocene and surficial geology of the City of St. Louis and the adjacent St. Louis County, Missouri: Unpublished Ph.D. Dissertation, Univ. of Ill., Urbana, Ill.

Hadley, J. B., and Devine, J. F., 1974, Seismotectonic map of the eastern United States: U.S. Geological Survey Misc. Field Studies Map, MF-620.

Hays, W. W., Algermissen, S. T., Miller, R. D., and King, K. W., 1978, Preliminary ground response maps for the Salt Lake City, Utah, area: Proceedings, Second International Conference on Microzonation, San Francisco, Calif., pp. 497-508.

Idriss, I. M., and Seed, H. B., 1966, Response of earth banks during earthquakes: Report, Soil Mechanics and Bituminous Laboratory, Univ. of Calif., Berkeley, Calif., April.

Idriss, I. M., Dobry, R., and Singh, R. D., 1966, Nonlinear Behavior of Soft Clays during Cyclic Loading, Journal of the Geotechnical Engineering Div., A.S.C.E., Vol. 104, No. GT12, pp. 1427-1447.

Keefer, D. K., Wieczorek, G. F., Harp, E. L., and Tuel, D. H., 1978, Preliminary assessment of seismically induced landslide susceptibility: Proceedings, Second International Conference on Microzonation, San Francisco, Calif., pp. 279-290.

Kochelman, W. J., and Brabb, E. E., 1978, Examples of seismic zonation in the San Francisco Bay region: Proceedings, Second International Conference on Microzonation, San Francisco, Calif., pp. 303-314.

Ladd, R. S., 1976, Specimen Preparation and Cyclic Stability of Sands, Journal of the Geotechnical Engineering Div., A.S.C.E., Vol. 103 No. GT6, pp. 535-548.

Lawson, A. C., et al., 1908, The California earthquake of April 18, 1906: Report of the State Earthquake Investigation Commission, Carnegie Institution of Wash., Wash., D.C., Pub. No. 87.

Lee, K. L., 1974, Seismic permanent deformations in earth dams: Report no. UCLA-ENG-7497, School of Engineering and Applied Science, Univ. of Calif. at Los Angeles, Los Angeles, Calif.

Lee, K. L., and Seed, H. B., 1967, Cyclic Stress Conditions Causing Liquefaction of Sands, Jour. of the Soil Mechanics and Foundations Div., A.S.C.E., Vol. 93, No. SM1, pp. 689-707.

Liu, B. C., and Hsieh, C. T., 1979, Earthquake risk and damage estimates for New Madrid: Proceedings, National Conference of Earthquake Engineering, Stanford, Univ.

Makdisi, A. M., and Seed, H. B., 1978, Simplified procedure for estimating dam and embankment earthquake-induced deformations: Jour. of the Geotechnical Engineering Div., A.S.C.E., No. GT7, Proc. Paper 13898, pp. 849-866.

Maley, R. P., and Cloud, W. K., 1971, Preliminary strong-motion results from the San Fernando earthquake of February 1971, in The San Fernando, California earthquake of February 9, 1971: U.S. Geological Survey Prof. Paper 733, pp. 163-176.

Marcusson, W. F., III, Chairman, 1978, Definition of terms related to liquefaction: Jour. of the Geotechnical Engineering Div., A.S.C.E., GT9, pp. 1197-1200.

Medvedev, A. V., 1965, Engineering seismology: National Technical Information Service, NTIS No. TT65-50011.

Missouri Department of Natural Resources, Division of Geology and Land Survey, 1979, Geologic map of Missouri.

National Academy of Sciences, 1971, The great Alaska earthquake of 1964: Wash., D.C.

Newmark, N. M., 1965, Effects of earthquakes on dams and embankments: Geotechnique, Vol. XV, No. 2, June, pp. 139-160.

Nilsen, T. H., and Brabb, E. E., 1975, Landslides: Studies for seismic zonation of the San Francisco Bay region: U.S. Geological Survey Prof. Paper 941-A, pp. A75-A87.

Nuttli, O. W., 1972, Magnitude, intensity, and ground motion relations for earthquakes in the central United States: Proceedings, International Conference on Microzonation, Seattle, Wash., pp. 307-318.

Nuttli, O. W., 1973, State-of-the-art for assessing earthquake hazards in the United States, report I, design earthquakes for the central United States: U.S. Army Corps of Engineers Waterways Experiment Station, Vicksburg, Miss.

Nuttli, O. W., 1979, Personal communication.

Nuttli, O. W., and Herrmann, R. B., 1978, State-of-the-art for assessing earthquake hazards in the United States: Credible earthquakes for the central United States: Misc. Paper S-73-1, Report 12, U.S. Army Waterways Experiment Station, Vicksburg, Miss.

Olsen, P. G., 1972, Seismic microzonation in the City of Santa Barbara, California: Proceedings, International Conference on Microzonation, Seattle, Wash., pp. 395-408.

Prater, E. G., 1979, Yield acceleration for seismic stability of slopes: Jour. of the Geotechnical Engineering Div., A.S.C.E., No. GT5, May, pp. 682-687.

Pyke, R., 1978, Some Effects of Test Configurations on Measured Soil Properties Under Cyclic Loading, & Geotechnical Testing Journal, A.S.T.M., Vol. 1, No. 3, pp. 125-133.

Radbrush-Hall, D. H., 1974, Examples of engineering geologic mapping in seismically active areas of the United States: Bull. of the International Association of Engineering Geology, Dec., pp. 15-25.

Richter, C. F., 1959, Seismic regionalization map of the United States: Proceedings, International Conference on Microzonation, 1972, Seattle, Wash., p. 201.

Rockaway, J. D., and Lutzen, E. E., 1970, Engineering geology of the Creve Coeur Quadrangle, St. Louis County, Missouri: Missouri Geological Survey and Water Resources, Engineering Geology Series, No. 2.

Santa Cruz County Board of Supervisors, 1975, Seismic safety element, an element of the Santa Cruz County general plan: Santa Cruz Planning Dept., Santa Cruz, Calif.

Sarma, S. K., 1973, Stability analysis of embankments and slopes: Geotechnique, Vol. 23, No. 3, pp. 423-433.

Schell, B. A., 1978, Seismotectonic microzoning for earthquake risk reduction: Proceedings, Second International Conference on Microzonation, San Francisco, Calif., pp. 571-586.

Schnabel, P. B., Lysmer, J., and Seed, H. B., 1972, SHAKE, a computer program for earthquake response analysis of horizontally layered sites: Earthquake Engineering Research Center Report No. EERC72-12, Univ. of Calif., Berkeley, Calif.

Seed, H. B., 1966, A method for earthquake-resistant design of earth dams: Jour. of the Soil Mechanics and Foundations Div., A.S.C.E., Vol. 92, No. SM1, Proc. Paper 4616, Jan., pp. 13-41.

Seed, H. B., 1967, Slope stability during earthquakes: Jour. of the Soil Mechanics and Foundations Div., A.S.C.E., Vol. 93, No. SM4, Proc. Paper 5319, July, pp. 299-323.

Seed, H. B., 1975, Earthquake effects on soil foundation systems, in Winterhorn, H. F., and Fang, H., eds., Foundation engineering handbook, Van Nostrand Reinhold Co., N.Y., pp. 700-732.

Seed, H. B., et al., 1973, Analysis of the slides in the San Fernando Dams during the earthquake of February 9, 1971: Report No. EERC73-2, Earthquake Engineering Research Center, Univ. of Calif., Berkeley, Calif., June.

Seed, H. B., and Idriss, I. M., 1967, Analysis of soil liquefaction: Niigata earthquake: Jour. of the Soil Mechanics and Foundations Div., A.S.C.E., Vol. 93, No. SM3, Proc. Paper 4233, May, pp. 83-108.

Seed, H. B., and Idriss, I. M., 1969a, Characteristics of rock motions during earthquakes: Jour. of the Soil Mechanics and Foundations Div., A.S.C.E., Vol. 95, No. SM5, Sept., pp. 1199-1218.

Seed, H. B., and Idriss, I. M., 1969b, Influence of soil conditions on ground motions during earthquakes: Jour. of the Soil Mechanics and Foundations Div., A.S.C.E., Vol. 95, No. SM1, pp. 99-137.

Seed, H. B., and Idriss, I. M., 1970, Soil moduli and damping factors for dynamic response analyses: Report No. EERC70-10, Univ. of Calif., Berkeley, Calif.

Seed, H. B., and Idriss, I. M., 1971, Simplified procedure for evaluating soil liquefaction potential: Jour. of the Soil Mechanics and Foundations Div., A.S.C.E., Vol. 97, No. SM9, pp. 1249-1273.

Seed, H. B., and Martin, G. R., 1966, The seismic coefficient in earth dam design: Jour. of the Soil Mechanics and Foundations Div., A.S.C.E., Vol. 92, No. SM3, Proc. Paper 424, May, pp. 25-58.

Seed, H. B., and Schnabel, P. B., 1972, Soil and geologic effects on site response during earthquakes: Proceedings, International Conference on Microzonation, Seattle, Wash., pp. 61-86.

Seed, H. B., and Whitman, R., 1972, Soil Conditions and building damage in the 1967 Caracas earthquake: Jour. of the Soil Mechanics and Foundations Div., A.S.C.E., No. SM8, August.

Seed, H. B., and Wilson, S. D., 1967, The Turnagain Heights landslide, Anchorage, Alaska: Jour. of the Soil Mechanics and Foundations Div., A.S.C.E., Vol. 93, No. M4, July, pp. 325-353.

Seed, H. B., Makdisi, F. I., and DeAlba, P., 1978, Performance of earth dams during earthquakes: Jour. of the Geotechnical Engineering Div., A.S.C.E., No. GT7, Proc. Paper 13870, July, pp. 967-984.

Serff, N., et al., 1976, Earthquake induced deformations of earth dams: Report No. EERC76-4, Earthquake Engineering Research Center, Univ. of Calif., Berkeley, Calif., Sept.

Shannon and Wilson, Inc., 1972, Soil behavior under earthquake loading conditions: Report for U.S. Atomic Energy Commission, Jan.

Sherif, M. A., Wu, M. J., and Bostrom, R. C., 1972, Reduction in soil strength due to dynamic loading: Proceedings, International Conference on Microzonation, Seattle, Wash., pp. 439-454.

Sherif, M. A., Chairman, 1978, Proceedings, Second International Conference on Microzonation, San Francisco, Calif.

Sherif, M. A., and Ishibashi, I., 1978, Soil dynamics considerations for microzonation: Proceedings, Second International Conference on Microzonation, San Francisco, Calif., pp. 81-110.

Silver, M. L., 1977, Laboratory Triaxial Testing Procedures to Determine the Cyclic Strength of Sands, U.S. Nuclear Regulatory Commission NUREG-0031, NRC6.

Silver, M. L., and Park, T. K., 1975, Testing Procedure Effects on Dynamic Soil Behavior, Jour. of the Geotechnical Engineering Div., A.S.C.E., Vol. 101, No. GT10, pp. 1061-1083.

Silver, M. L., and Seed, H. B., 1971, Deformation Characteristics of Sands under Cyclic Loading, Jour. of the Soil Mechanics and Foundation Div., A.S.C.E., Vol. 97, SM8, pp. 1081-1097.

Simac, M., 1979, Acquisition and application of cyclic triaxial test data: Unpublished Masters Thesis, University of Mo.-Rolla, Rolla, Mo.

Spencer, E., 1978, Earth slopes subject to lateral acceleration: Jour. of the Geotechnical Engineering Div., A.S.C.E., No. GT12, December, pp. 1489-1500.

Taylor, P. W., and Larkin, T., 1978, Seismic Site Response of Nonlinear Soil Media, Jour. of the Geotechnical Engineering Div., A.S.C.E., Vol. 104, No. GT3, pp. 369-383.

Time, 1979, Middle America's fault: Nov. 19, pp. 66-67.

Union Electric Company, 1973, Callaway Nuclear Power Plant preliminary safety analysis report: Vol. 2, Section 5, Docket Nos. 50-448 and 50-486.

U.S. Geological Survey, 1971, The San Fernando, California, earthquake of February 9, 1971: Prof. Paper 733.

U.S. Geological Survey, 1979, Discovery of fault zone in Arkansas may solve quake puzzle: Dept. of Interior News Release, Oct. 19.

Van Horn, R., and Van Driel, J. N., 1977, Computer composite map showing inferred relative stability of the land surface during earthquakes, Sugar House Quadrangle, Salt Lake County, Utah: U.S. Geological Survey Misc. Inv. Series, I-766-0.

Wentworth, C. M., Ziony, J. I., and Buchanan, J. M., 1970, Preliminary geologic environmental map of the greater Los Angeles area, Calif.: U.S. Geological Survey, published as Atomic Energy Commission Division of Technical Information Extension TID 25363.

Wieczorek, G. F., Wilson, R. C., and Harp, E. L., 1979, An experimental seismic slope stability map of the La Honda Quadrangle, San Mateo County, California: abs., Geological Society of America Annual Meeting, San Diego, Calif.

Wilson, R. C., 1979, Numerical simulation of the interaction of strong ground motion with seismically induced landslides: abs., Seismological Society of America Annual Meeting, Golden, Colorado, May 21-23.

Wilson, R. C., Wieczorek, G. F., and Harp, E. L., 1979, Development of criteria for regional mapping of seismic slope stability: abs.; Geological Society of America Annual Meeting San Diego, California.

Wood, H. D., 1908, Distribution of apparent intensity in San Francisco: The California earthquake of April 18, 1906: Report of the State Earthquake Investigation Commission, Carnegie Institution of Wash., Wash., D.C.

Wright, S. G., 1974, SSTAB1-A general computer program for slope stability analyses: Research Report No. GE-74-1, Dept. of Civil Engineering, University of Texas at Austin.

Yen, B. C., and Trotter, J. R., 1978, Shallow slides due to 1971 San Fernando earthquake: Proceedings, Earthquake Engineering and Soil Dynamics Conference, A.S.C.E., Vol. II, pp. 1076-1096.

Yoshikawa, S., Iwasaki, Y. T., and Tai, M., 1978, Microzoning of the Osaka region: Proceedings, Second International Conference on Microzonation, San Francisco, Calif., pp. 445-456.

Youd, T. L., and House, S. N., 1976, Liquefaction during the 1906 San Francisco earthquake: Jour. of the Geotechnical Engineering Div., A.S.C.E., Vol. 102, No. GT5, pp. 425-439.

Youd, T. L., and Perkins, D. M., 1978, Mapping Liquefaction-induced ground failure potential: Jour. of the Geotechnical Engineering Div., A.S.C.E., No. GT4, pp. 433-446.

Youd, T. L., Tinsley, J. C., Perkins, D. M., King, E. J., and Preston, R. F., 1978, Liquefaction potential map of San Fernando Valley, California: Proceedings, Second International Conference on Microzonation, San Francisco, Calif., pp. 267-278.

APPENDIX A

MODEL SOIL PROFILES AND PROPERTIES

FOR CREVE COEUR

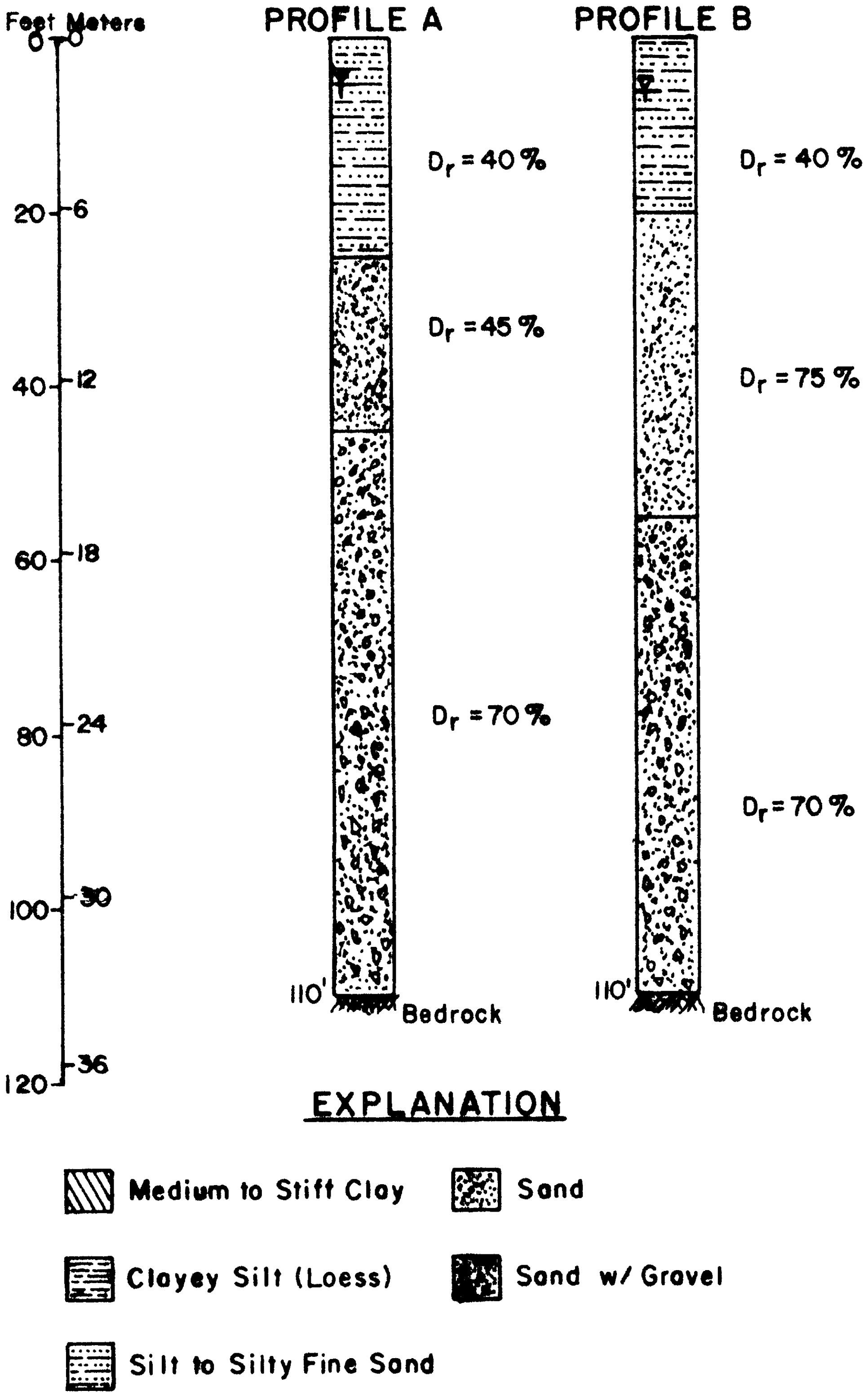

Figure 1A. Model Soil Profiles for the Creve Coeur Area.

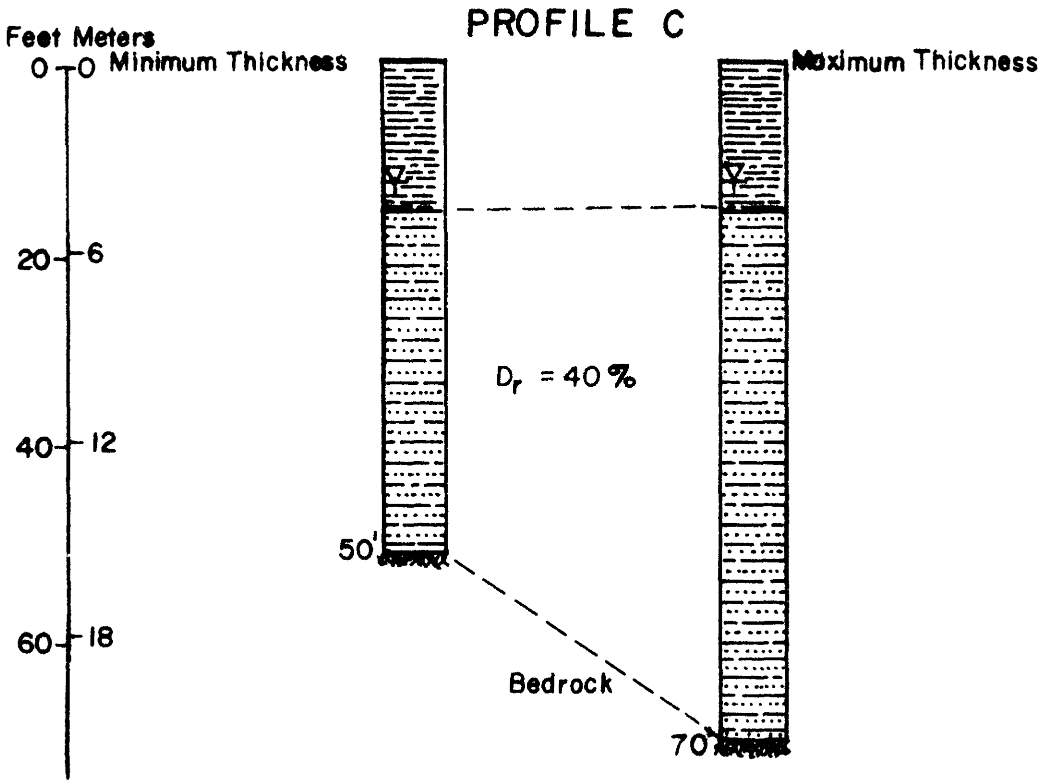

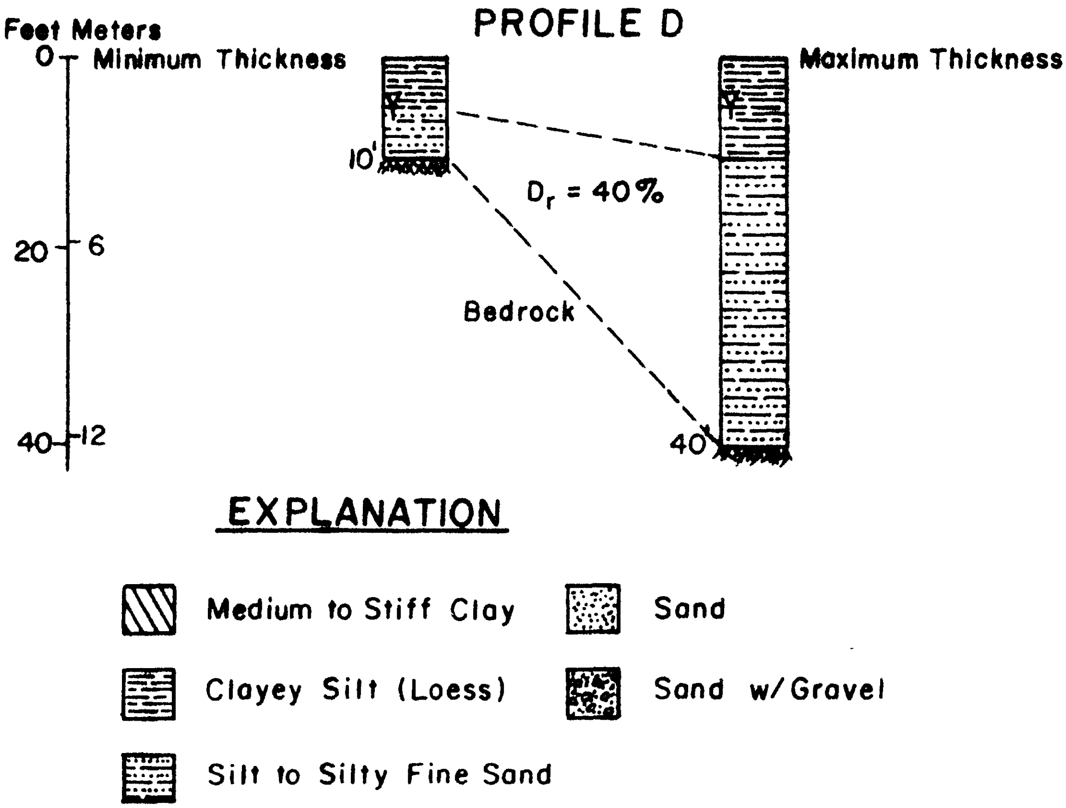

Figure 1A. Continued.

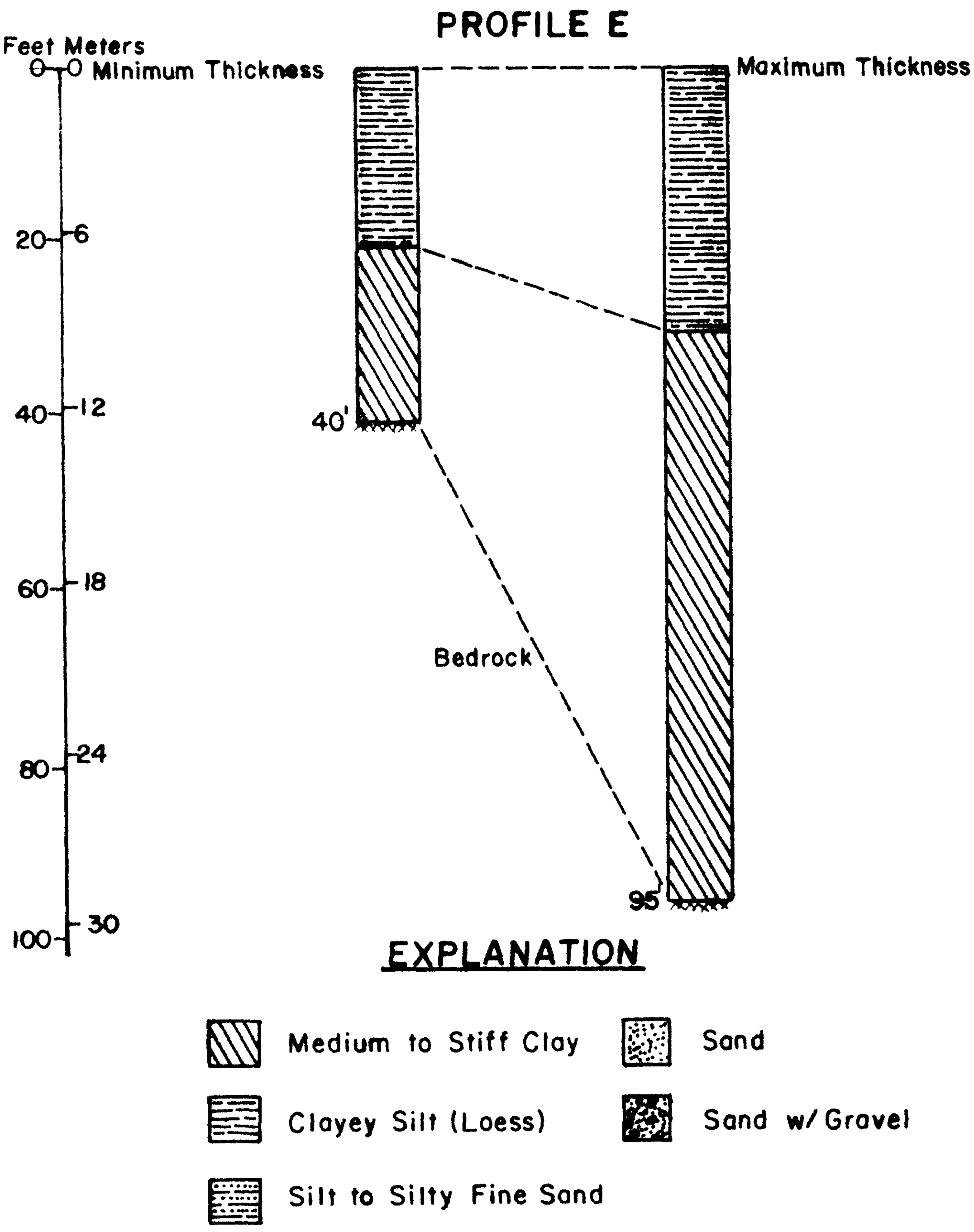

Figure 1A. Continued.

PROFILE F

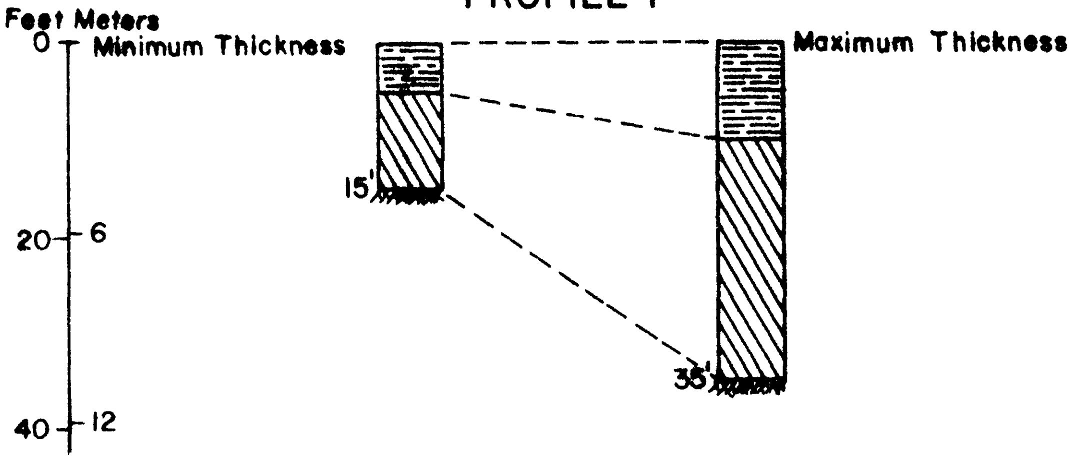

PROFILE G

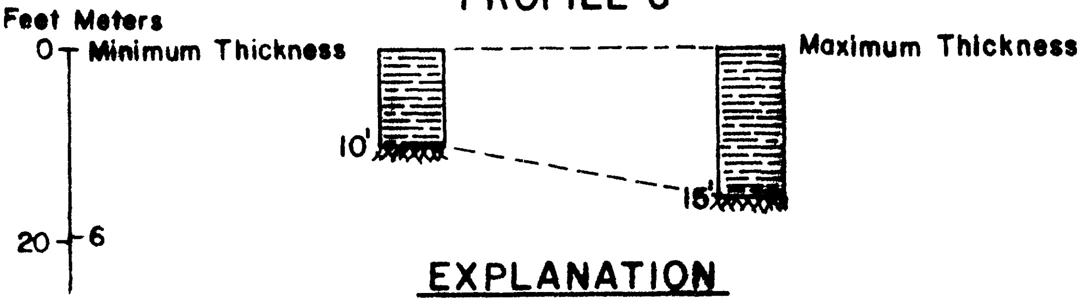

EXPLANATION

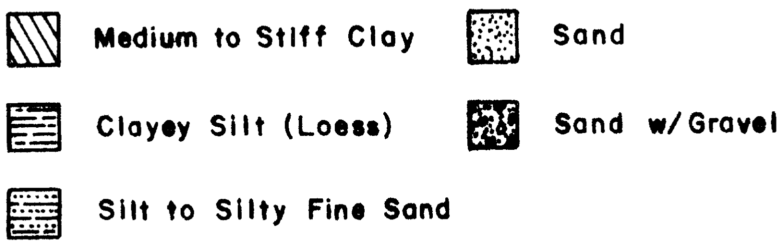

Figure 1A. Continued.

TABLE IA

GENERALIZED SOIL PROPERTIES FOR CREVE COEUR

Silt and Silty Fine Sand (D_r = 40%)

G_s = 2.67	γd_{40} = 81.6 pcf	vane shear = 1.0 ksf
e_{40} = 1.04	γ_{moist} = 95.0 pcf	
D_{50} = 0.085mm	γ_{sat} = 113.0 pcf	

Fine to Medium Sand with Gravel (D_r = 45%)

G_s = 2.65	γd_{45} = 102.2 pcf	D_{50} = 0.28mm
e_{45} = 0.62	γ_{sat} = 126.0 pcf	

Fine to Medium Sand with Gravel (D_r = 75%)

G_s = 2.65	γd_{75} = 106.8 pcf	D_{50} = 0.28mm
e_{75} = 0.55	γ_{sat} = 129.0 pcf	

Medium to Coarse Sand with Gravel (D_r = 70%)

G_s = 2.68	γd_{70} = 128.0 pcf	D_{50} = 1.0mm
e_{70} = 0.31	γ_{sat} = 135.0 pcf	

Silty Clay

G_s = 2.70	PL = 21	γ_{moist} = 123.0 pcf
LL = 37	γd = 104.4	vane shear = 1.25 ksf

Medium to Stiff Clay

G_s = 2.72	PL = 19	γ_{moist} = 127.0 pcf
LL = 42	γd = 106.0 pcf	vane shear = 2.6 ksf

APPENDIX B

CYCLIC TRIAXIAL TESTING OF CREVE COEUR AREA SOILS

CYCLIC TRIAXIAL TESTING OF CREVE COEUR AREA SOILS

INTRODUCTION

The use of cyclic triaxial tests to determine dynamic soil properties is an accepted procedure among practicing geotechnical engineers. As a part of this project, a closed loop servohydraulic test, data acquisition, and presentation system was developed for cyclic triaxial soil testing.

The complete test system consists of an MTS, Inc. supplied load frame, actuator, hydraulic pump, and control package. Additional system components include a digital voltmeter, x-y recorder, computer terminal, and a Nova minicomputer.

The electronic control package consists of the control panel, signal function generator, and counter panel. The signal function generator supplies command signals to the servocontroller in a variety of waveforms, i.e., sine or square wave. The counter panel may be used to terminate a test after a specific number of cycles. The control panel consists of amplifiers and conditioners to coordinate the closed loop operation on each of the three possible selections for the controlled variable.

Recording of all specimen behavior information was accomplished by programming a NOVA 3 minicomputer, manufactured by Data General Corporation, to read and store the data on disks. The computer terminal allowed the test operator to interact with the computer and que the computer as to when the acquisition of test data was to commence. Any x-y recorder by Houston Instruments was used to monitor specimen behavior during the test. The digital voltmeter indicated the amount of load being applied to the sample. This voltmeter was extremely valuable in controlling the load applied during the saturation and consolidation phases of the test by providing a continuous monitoring of the load.

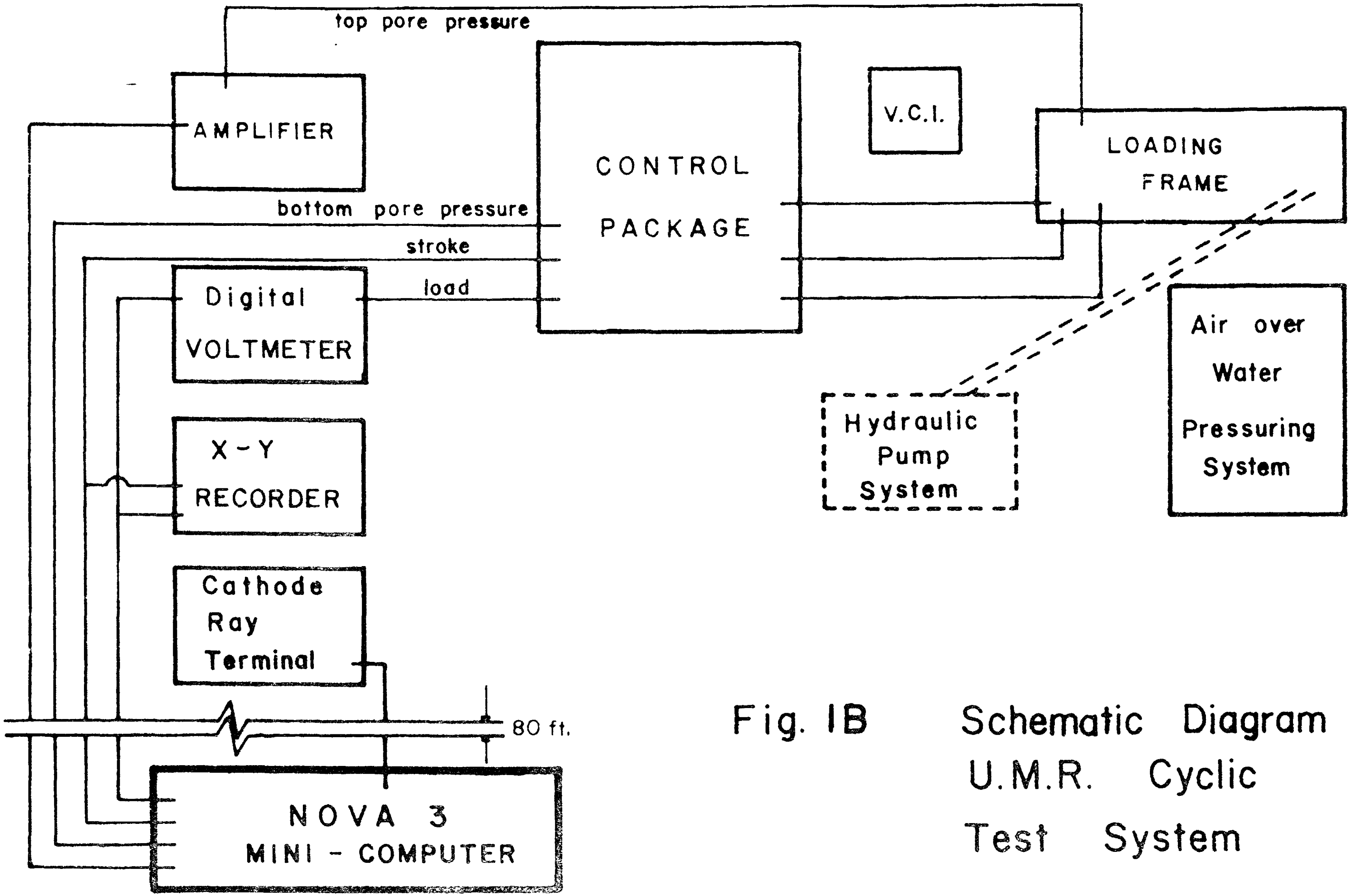

Fig. IB Schematic Diagram U.M.R. Cyclic Test System

SAMPLE PREPARATION

Representative disturbed and undisturbed soil samples were obtained from a test boring and subsurface sampling program conducted in the study area. Subsurface samples of cohesionless soils were taken with a split spoon sampling tool. Cohesive soil samples were obtained with a fixed piston (Osterberg) sampler.

Variations in the methods of sample preparation have been known to affect the dynamic behavior of reconstituted soil specimens significantly (Castro, 1969; Lee and Seed, 1967); however, the major difficulty arises in reconstituting test samples of cohesionless soils to a uniform density. Possible sample formation techniques include pluviating saturated samples, moist and dry vibration, and moist and dry tamping.

Ladd (1976) developed a moist tamping procedure for coarse grained soil specimens that produces samples that have a relatively uniform density throughout and minimizes the tendency for particle segregation. With this procedure, one can recognize and make corrections for the fact that in compacting a material in layers, each succeeding layer densifies the material in the layers below it.

Basically, the compactive effort put into each equal weight layer is controlled by the predetermined height to which each layer is compacted. The heights of the layers are greater at the bottom and smaller at the top at the start of the sampling operation but are all equal at the end of compaction.

This procedure, known as under compaction, was used to reconstitute all the cohesionless soil samples tested in cyclic shear.

CYCLIC STRENGTH TESTS

All the cyclic strength, liquefaction tests were run with a performance specification published by Silver (1977). The loading mechanism, triaxial cell, recording equipment, and measuring instruments all matched or exceeded the minimum requirements for accuracy, reliability, and repeatability required to measure the resistance of a soil to liquefaction.

During each of these stress controlled tests, the load, deformation, and pore pressure at the top and bottom platens were recorded versus time by a NOVA minicomputer. Each test, run at 1 Hz, was taken to a 100 percent pore pressure response with a double amplitude strain of 20 percent, or 500 cycles, whichever came first. This allowed the number of cycles to 100 percent pore pressure response and 100 percent pore pressure response with 5, 10, and 20 percent double amplitude strain to be determined.

For each material type defined in a given soil profile analyzed, a material curve had to be determined for a desired appropriate failure criterion. The stress ratios chosen so that the material curve could be defined by three points or tests were 0.48, 0.35, and 0.275. The maximum stress ratio, which could be applied in the tests, is 0.5. Any stress ratio greater than that would cause the pulsating deviator stress, σ_{dp}, to be larger than the effective confining pressure, thus placing a tensile load on the sample. Because cohesionless samples cannot resist tension, the sample would tend to neck at the top (Castro, 1969).

To verify the results obtained from this testing procedure and equipment, material curves for Monterey No. 0 sand at 60 percent relative density were determined and compared to published results. The results from this test equipment were consistent with the expected values.

MODULUS AND DAMPING TESTS

Strain controlled cyclic tests, run with the same procedures outlined for stress controlled tests, were used for inducing small shear strains in saturated and unsaturated soil samples to determine the shear modulus and damping of the material. Cohesive and cohesionless samples were usually tested at 0.5 Hz in a stage technique to minimize the number of tests performed.

Equivalent linear soil property theory was used for defining the shear modulus and damping parameters of anisotropic, nonlinear, hysteretic behavior of soils. The major assumption of this theory is that on any one particular loading cycle the stress-strain behavior can be considered isotropic, linear, and elastic. This allows shear strain, γ_o, to be defined in terms of the axial strain, ε_{ax}, as follows:

$$\gamma_o = \varepsilon_{ax} - \varepsilon_{radial} \tag{B1}$$

$$\gamma_o = (1 + \mu)\varepsilon_{ax} \tag{B2}$$

In these equations, μ is Poisson's ratio.

Relatively little inquiry into the reasonable values for Poisson's ratio of soils has been published; however, several publications contain good approximations of Poisson's ratio for different soils under different conditions. Once Poisson's ratio is determined, Young's modulus, E, can be determined from triaxial testing and related to the shear modulus, G, by using

$$G = E/(2(1 + \mu)) \tag{B3}$$

The three most important parameters affecting moduli are strain amplitude, mean effective confining stress, and relative density. Seed and Idriss (1970) presented the following formula:

$$G = 1000\ K_2(\sigma'_m)^{1/2} \tag{B4}$$

in which σ'_m is the effective confining pressure, and K_2 is the factor dependent on relative density and strain amplitude.

For any soil profile, the relative density of a material will already be determined, therefore only the values of the moduli at various strain levels need be obtained to complete the constitutive relation. Damping is less sensitive to changes in confining pressure, and, therefore, needs only be defined for various strain amplitudes.

STAGE TESTING

The stage testing technique consists of initially saturating and consolidating a specimen before the first cycling of strain. Starting at the smallest desired induced shear strain, 11 cycles of strain are applied to the specimen, while load, deformation, and pore pressure are recorded versus time. After cycling has terminated, the sample is reconsolidated until the residual pore pressures are reduced to zero. The changes in volume and height are recorded during the process. Then the next higher strain level is applied, with the same sequence of events being repeated until all the desired strain levels have been tested (Silver and Park, 1975). If the volume change of the sample exceeds five percent of the initial relative density, the values for shear modulus should be corrected accordingly.

The value and number of strain levels needed to define the curve in Figure 2B were determined through past experience. Taylor and Larkin (1978) suggested that the shear strain levels be evenly spaced along the semilog plot to allow the minimum number of levels to be tested. They suggested levels of 0.0001, 0.0002, 0.0005, 0.001, 0.002, 0.005, 0.01, 0.02, 0.05, 0.1, 0.2, and 0.5 percent shear strain. Fortuitously, these points will probably give the best piecewise linear idealization of the curve, presented in Figure 2B, for the input into the ground response computer program, SHAKE.

Behavior cited in the literature shows that during the cyclic loading of dry sands the modulus tends to increase, whereas for saturated sands the modulus tends to decrease as additional cycles of loading are applied. Cohesive soils, especially soft clays, behave in much the same manner as saturated sands in this respect (Idriss, et al., 1966). Silver and Seed showed in 1971 that the most drastic change in modulus occurs in the first ten cycles for both dry and saturated sands. Finn, et al. (1970) felt that when either 15 cycles of load are applied or a pore pressure response of 50 percent of the effective confining pressure is incurred the most drastic change in properties takes place in saturated sands. Values taken for modulus and damping on the fifth or tenth cycle was reported by Pyke (1978) as common practice.

Based on the above evidence, the value of the modulus and damping on the tenth cycle was adopted as being indicative of any cycle at that strain level. With most of the drastic changes in modulus occurring by the tenth cycle, if an earthquake endures for 30 significant cycles, the modulus is not affected greatly.

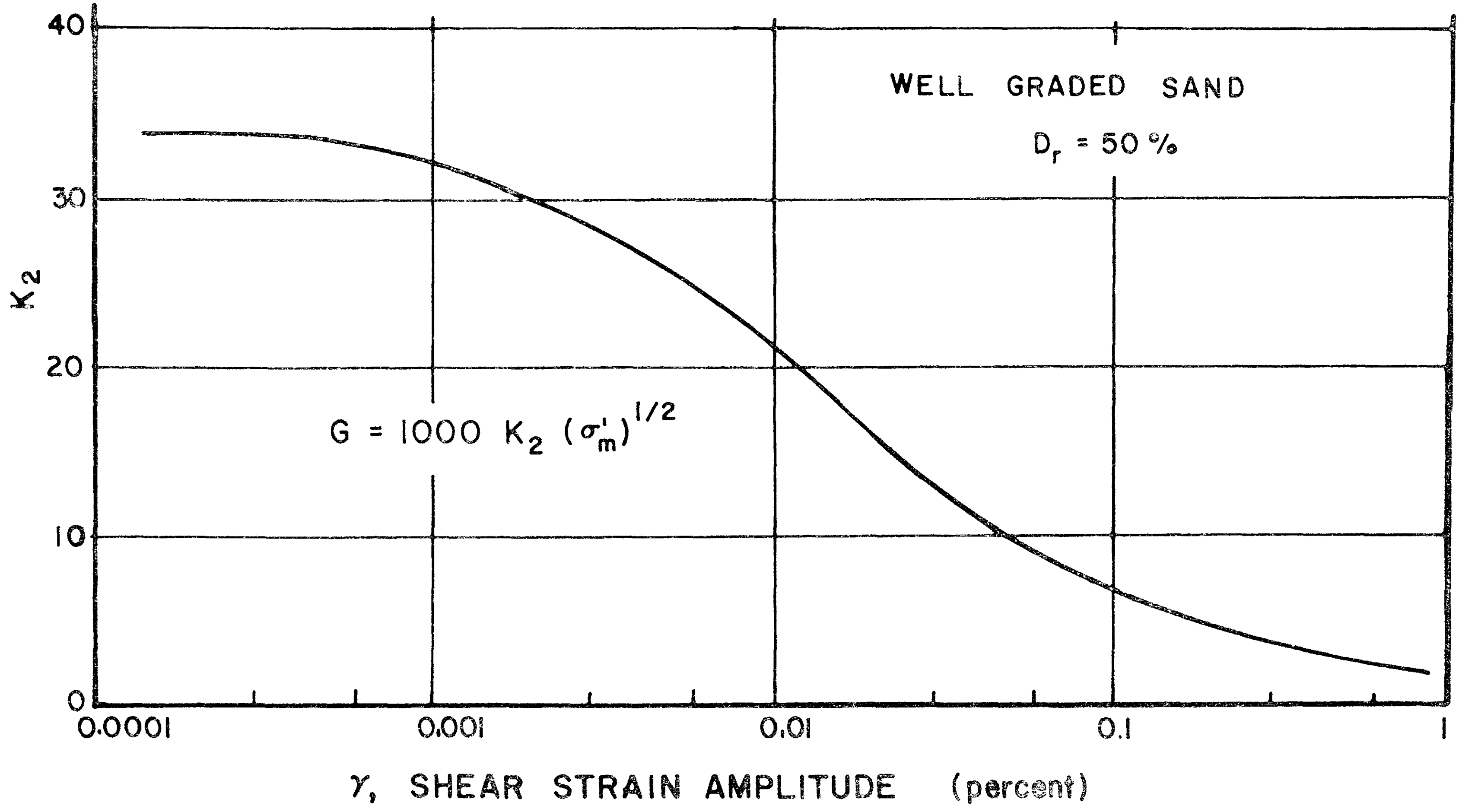

Fig. 2B Shear Modulus Curve for Sands

This also defines the worst case or least modulus in the most common occurrence of saturated sands and cohesive soils in a ground response analysis.

The effects of the stage testing technique on the values obtained for modulus and damping were evaluated by Silver and Park (1975). During the testing of dry and moist samples, the stage testing technique gives excellent results. For saturated sands, the stage technique is only valid up to a shear strain level of 0.1 percent (Figure 3B). At strain levels greater than this, a significant increase in relative density is noted along with stronger resistance to pore pressure buildup upon reloading thereby increasing the modulus measured above that obtained in fresh tests at the same strain level.

In an attempt to test all the saturated sands in the response area economically, the following procedure with which the shear modulus and damping of a material is determined for those shear strain levels greater than 0.1 percent was adopted.

1. A material type, which seemed representative of the other saturated sands in the response area in terms of relative density and grain characteristics, was selected as the matching material.
2. The matching material had one sample stage tested through all the desired shear strain levels. Also, an additional fresh sample was tested singularly at each strain level greater than 0.1 percent.
3. The change in modulus from the previous strain level to the present was determined for each strain level greater than 0.1 percent.
4. The matching strain was defined as that strain level which

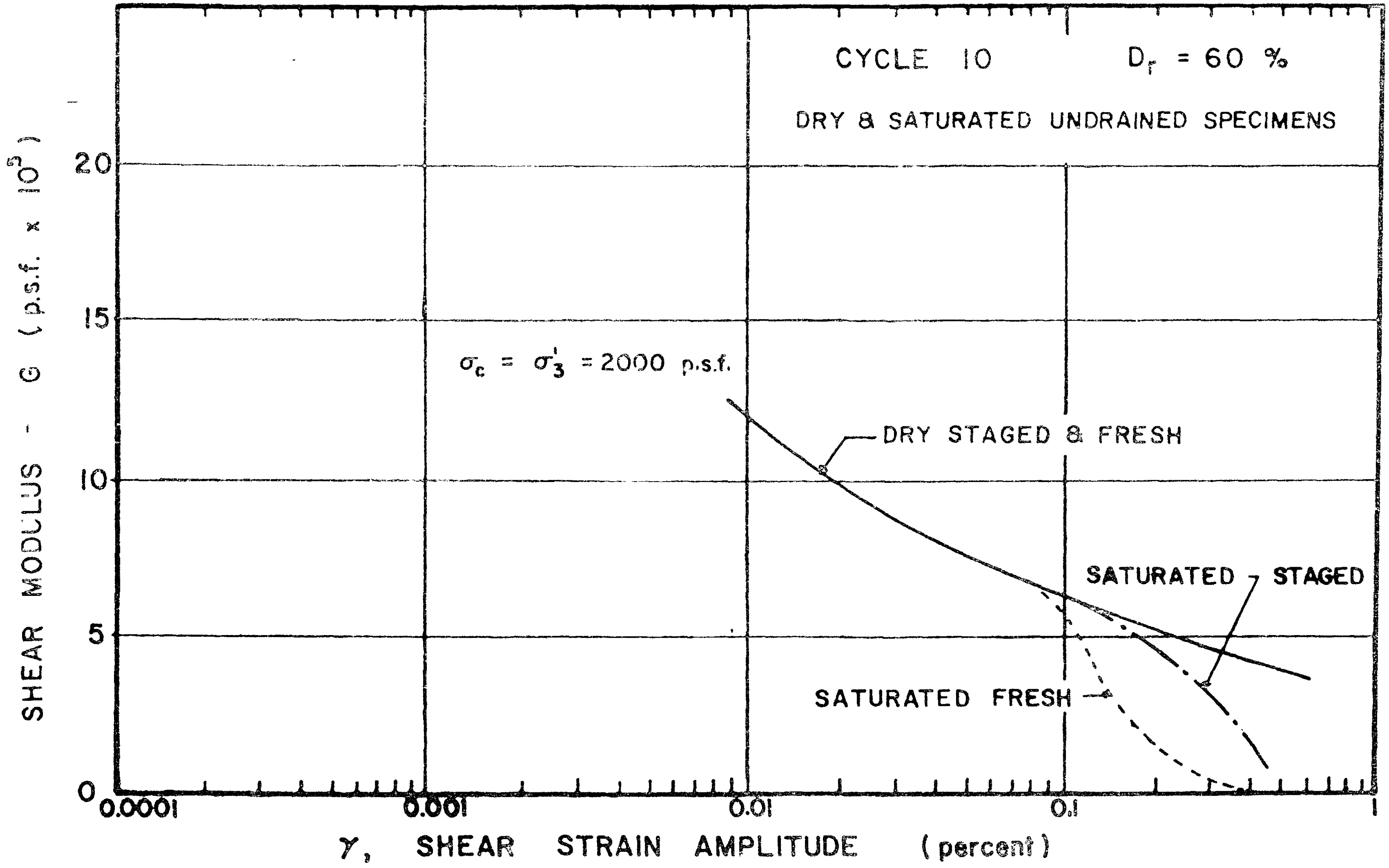

Fig. 3B Differences in Measured Shear Modulus depending on Testing Technique (after SILVER & PARK (1975)) causes the largest decrease in modulus.

5. Each unique saturated sand was then tested by running one sample through the staged testing technique up to a shear strain level of 0.1 percent and performing an additional test on a fresh sample at the matching strain.
6. When interpreting test results from step 5, extrapolation of the shear modulus and damping at the strain levels that were not tested was made by drawing a curve from the stage test results through the matching strain test result parallel to the matching material's curve, step 2.

It is also believed that all cohesive soils can be entirely stage tested. The factors, which cause saturated sands problems, i.e., pore pressure buildup and increased relative density, are very rare occurrences in cyclic loading of cohesive soils, they, therefore, should be ignored.

The accuracy with which cyclic triaxial laboratory data represents field conditions is usually marginal. This is basically due to sampling disturbance especially for soils with high modulus values, i.e., cohesive soils. Maximum laboratory moduli are always less than field determined maximum moduli by 23 to 96 percent for all soils and 185 to 250 percent for sensitive soils.

Taylor and Larkin (1978) presented a method, which is shown in Figure 4B, for increasing the laboratory curve to field values. The correction is based on correlating G_{max} values from in situ shear wave velocity tests to those measured in the laboratory program. Most corrections to field values are based upon G_{max} from shear wave velocity tests.

Because of the limited exploration program and the unavailability of testing equipment, the shear wave velocity data necessary

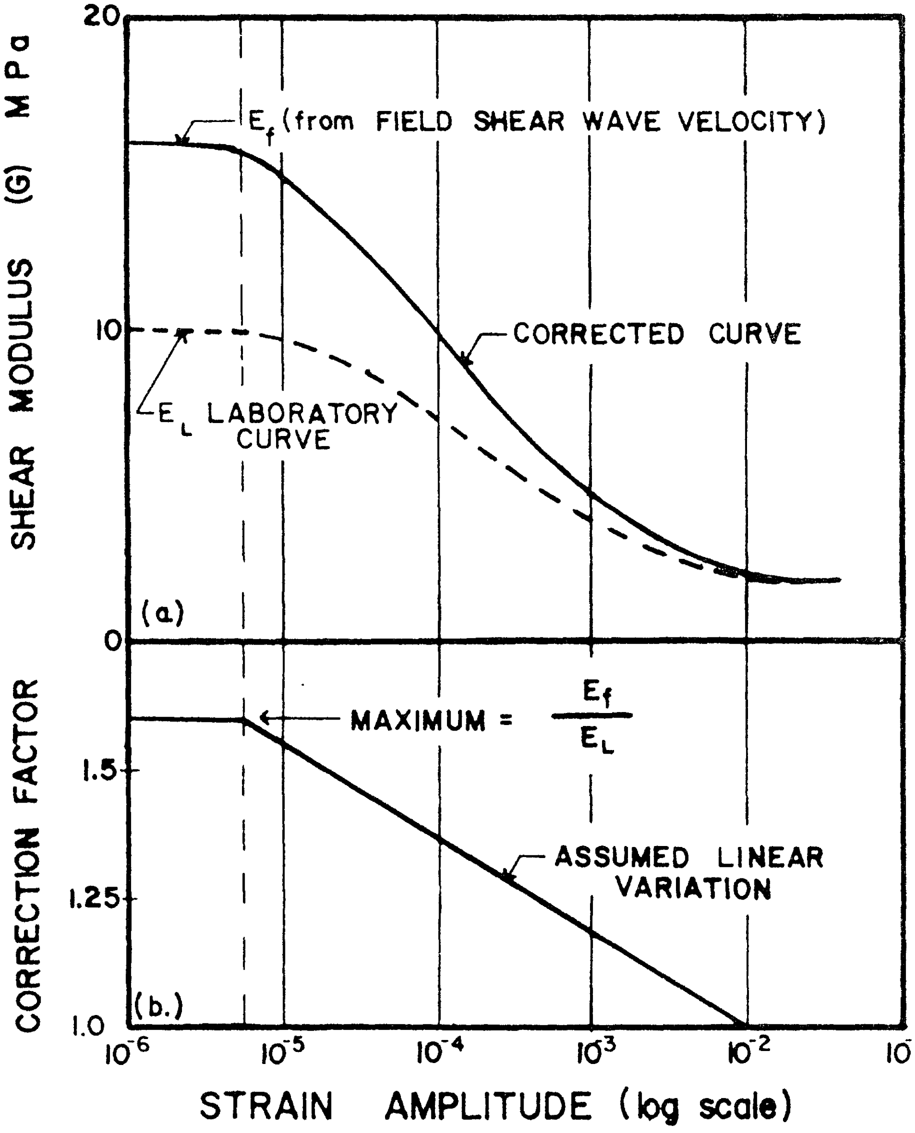

Fig. 4B Correction Procedure for Laboratory Data to Field Values

(after Taylor & Larkins (1978))

to apply the correction on the materials tested was not obtained. To account for the field behavior, the values obtained for G_{max} in the laboratory testing program for saturated cohesive soils were increased by 100 percent, unsaturated cohesive soils by 150 percent, and cohesionless soils by 30 percent, and then the Taylor-Larkin correction was applied. Typical results of this testing program are shown in Figures 5B through 15B.

10TH CYCLE OF LOADING SHEAR STRAIN LEVEL = 0.5000%
SAMPLE #: TEST 17 UNIFORM GREY SAND
BORING #: 2 DEPTH : 35.0 FT. D_R = 85.4 %
EFFECTIVE CONFINING PRESSURE:25.0 P.S.I.

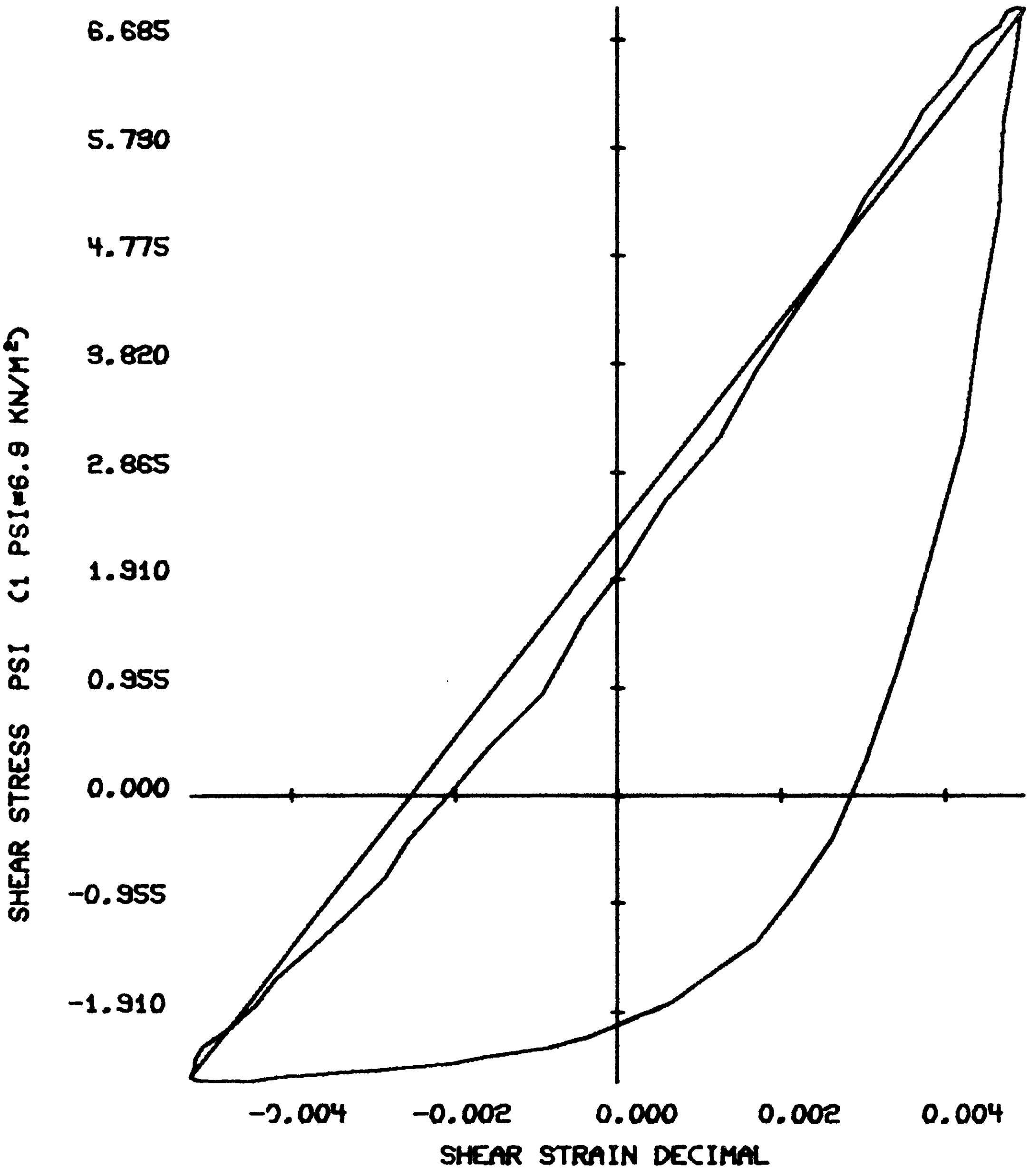

G = 926.1 P.S.I.
D = 16.98 %
SHEAR STRAIN = 0.52947 %

FIG. 5B

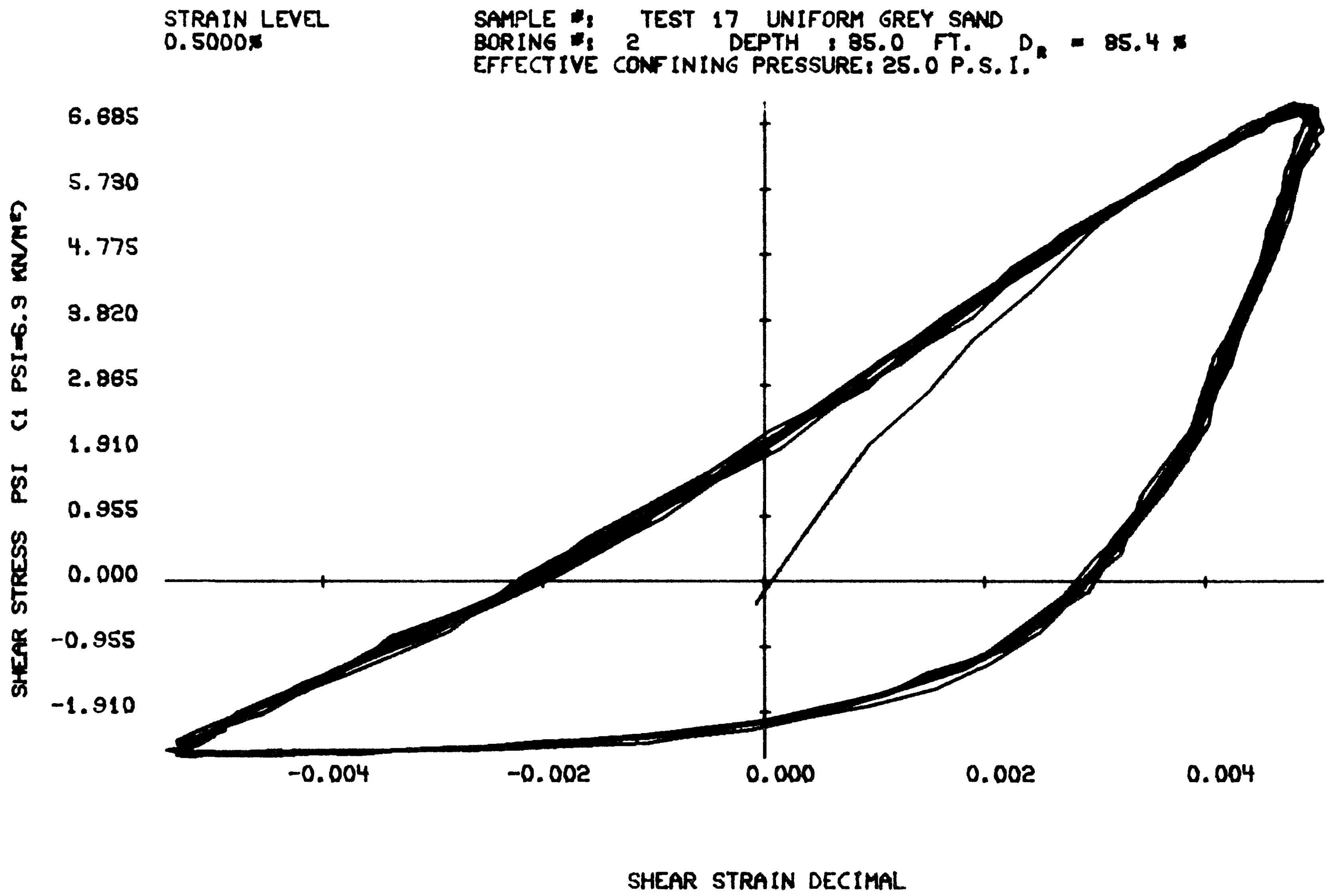
STRAIN LEVEL
0.5000%
SAMPLE #: TEST 17 UNIFORM GREY SAND
BORING #: 2 DEPTH : 85.0 FT. D_R = 85.4 %
EFFECTIVE CONFINING PRESSURE: 25.0 P.S.I.
6.685
5.730
4.775
3.820
2.865
1.910
0.955
0.000
-0.955
-1.910
SHEAR STRESS PSI (1 PSI=6.9 KN/M²)
-0.004
-0.002
0.000
0.002
0.004
SHEAR STRAIN DECIMAL

FIG. 6B

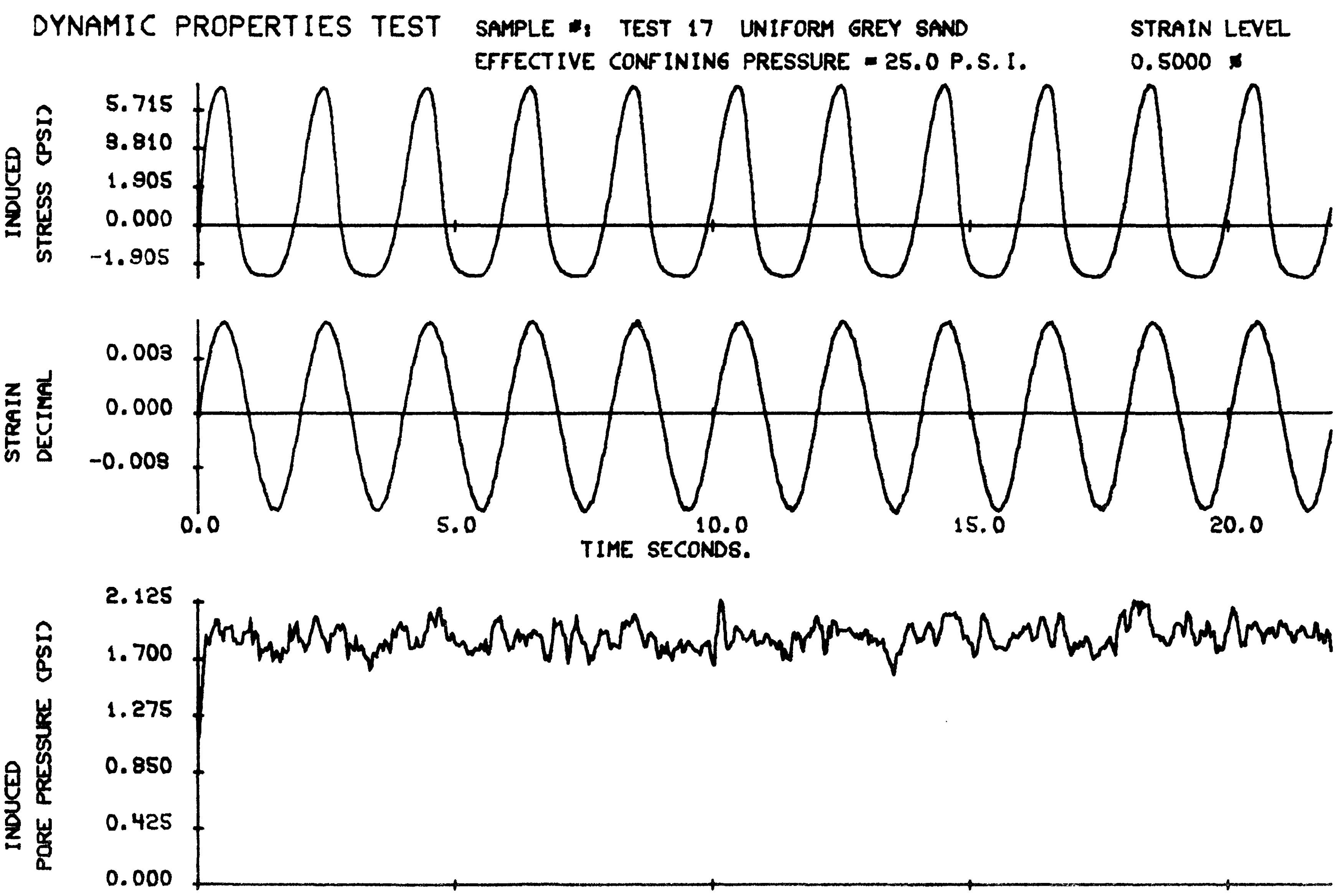
DYNAMIC PROPERTIES TEST
SAMPLE #: TEST 17 UNIFORM GREY SAND
EFFECTIVE CONFINING PRESSURE = 25.0 P.S.I.
STRAIN LEVEL
0.5000 %
INDUCED
STRESS (PSI)
5.715
3.810
1.905
0.000
-1.905
STRAIN
DECIMAL
0.003
0.000
-0.003
0.0
5.0
10.0
15.0
20.0
TIME SECONDS.
INDUCED
PORE PRESSURE (PSI)
2.125
1.700
1.275
0.850
0.425
0.000

FIG. 7B

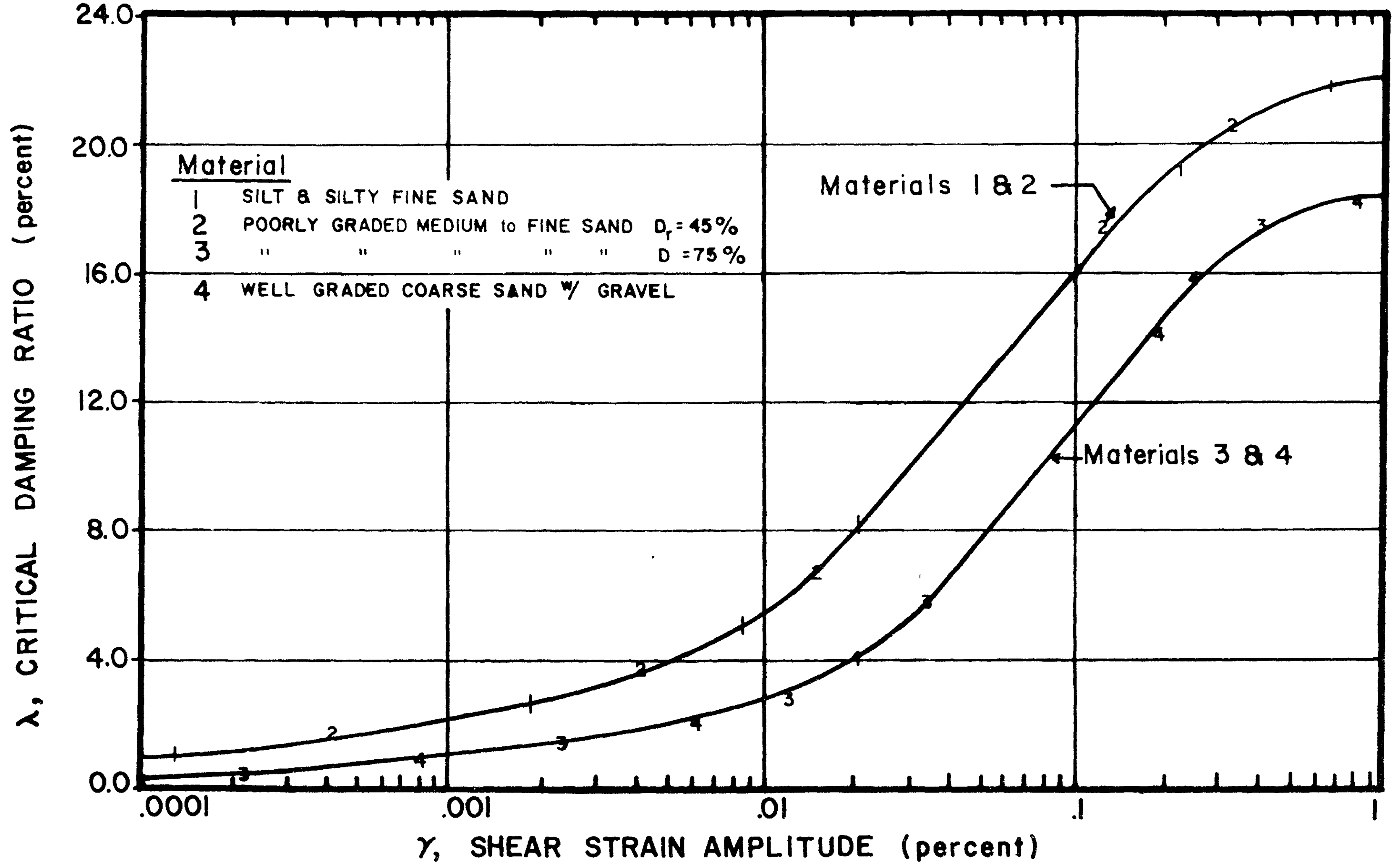
λ, CRITICAL DAMPING RATIO (percent)
24.0
20.0
16.0
12.0
8.0
4.0
0.0
.0001
.001
.01
.1
1
γ, SHEAR STRAIN AMPLITUDE (percent)
Material
1 SILT & SILTY FINE SAND
2 POORLY GRADED MEDIUM to FINE SAND D_r = 45%
3 " " " " " D = 75%
4 WELL GRADED COARSE SAND W/ GRAVEL
Materials 1 & 2
Materials 3 & 4

Fig. 8B

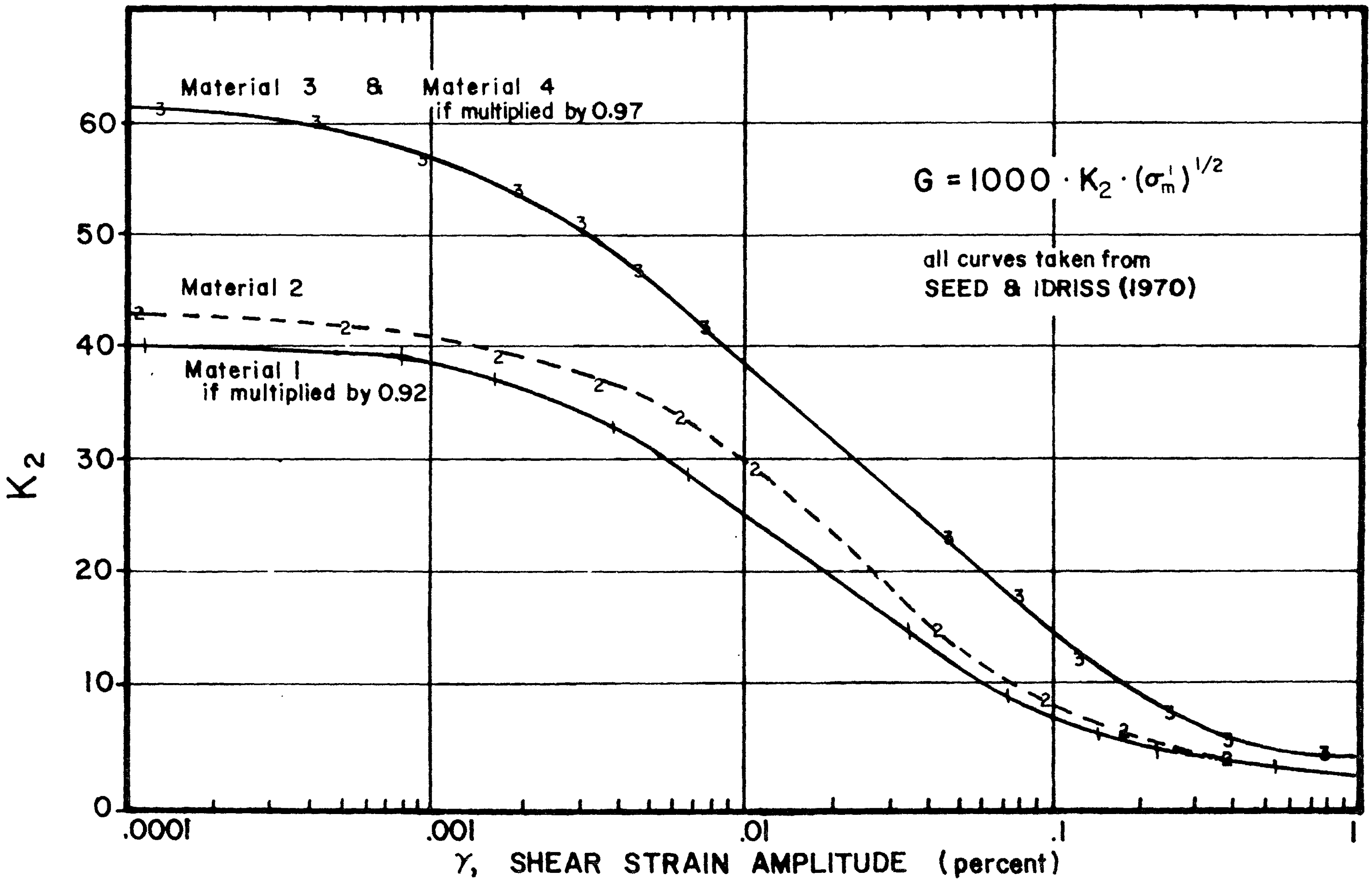

Material 3 & Material 4
if multiplied by 0.97
Material 2
Material 1
if multiplied by 0.92
$G = 1000 \cdot K_2 \cdot (\sigma'_m)^{1/2}$
all curves taken from
SEED & IDRISS (1970)
K_2
60
50
40
30
20
10
0
.0001
.001
.01
.1
1
γ, SHEAR STRAIN AMPLITUDE (percent)

Fig. 9B

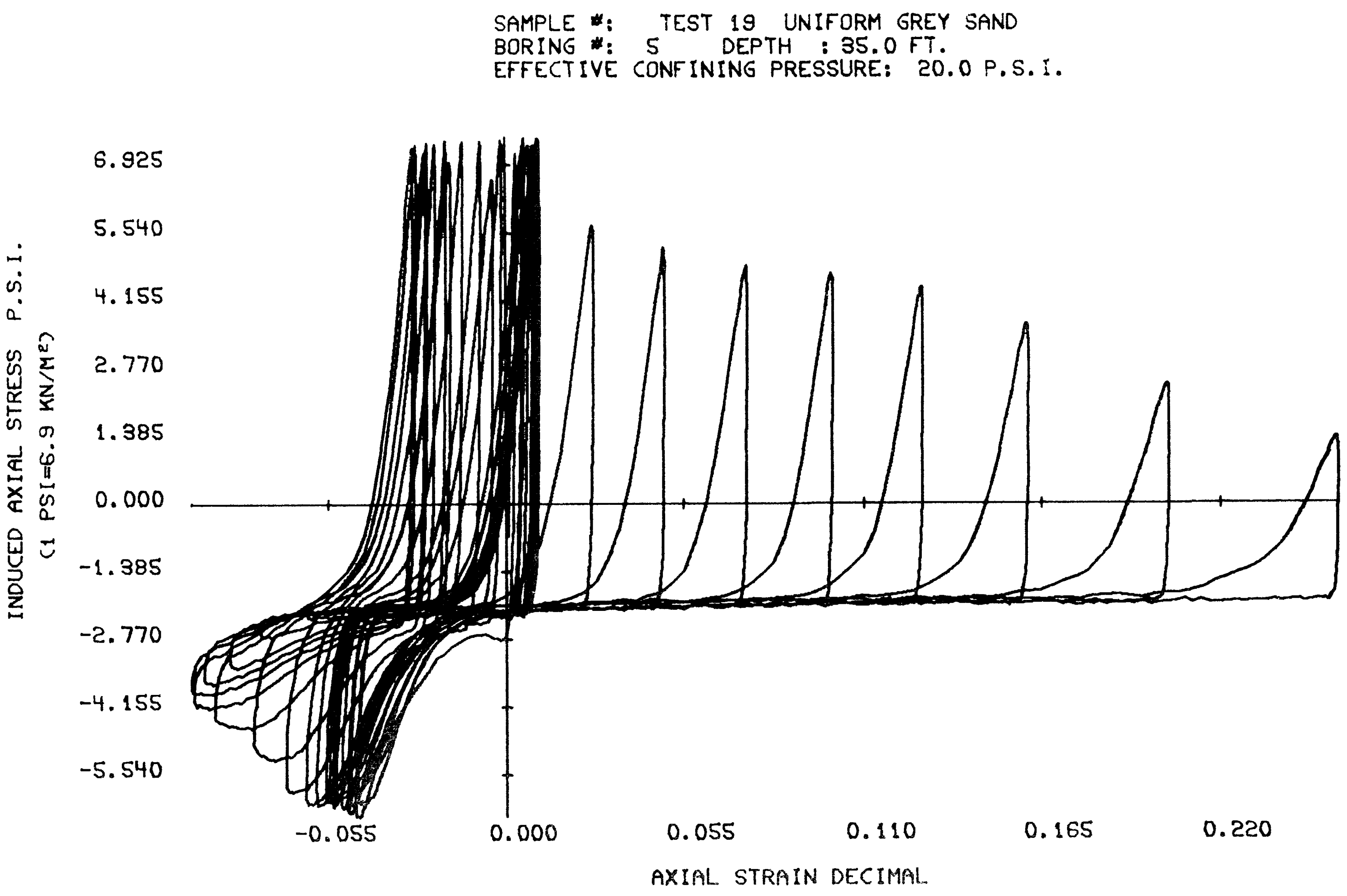
SAMPLE #: TEST 19 UNIFORM GREY SAND
BORING #: S DEPTH : 35.0 FT.
EFFECTIVE CONFINING PRESSURE: 20.0 P.S.I.
INDUCED AXIAL STRESS P.S.I.
(1 PSI=6.9 KN/M²)
6.925
5.540
4.155
2.770
1.385
0.000
-1.385
-2.770
-4.155
-5.540
-0.055
0.000
0.055
0.110
0.165
0.220
AXIAL STRAIN DECIMAL

FIG. 10B

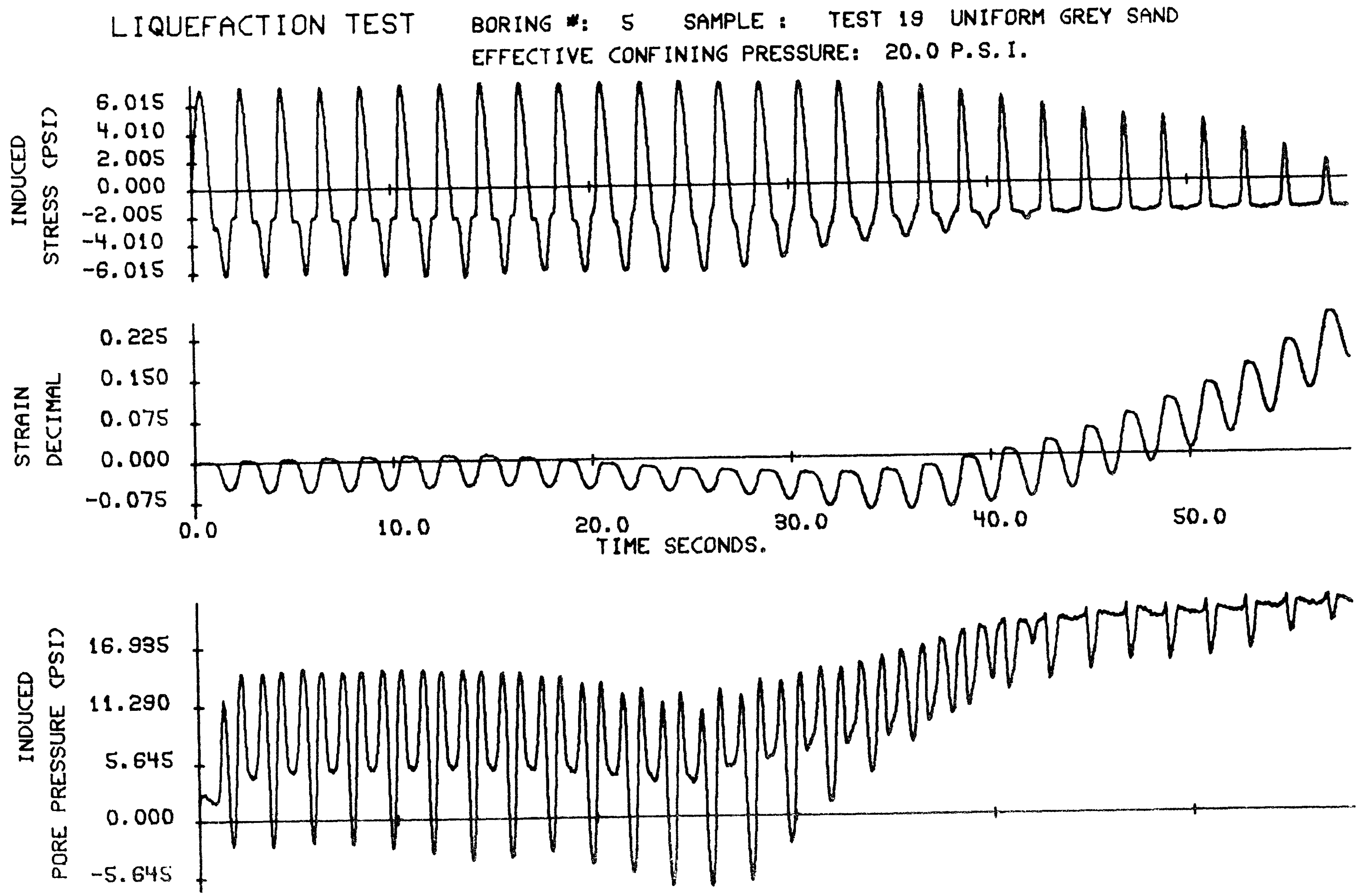
LIQUEFACTION TEST
BORING #: 5 SAMPLE : TEST 19 UNIFORM GREY SAND
EFFECTIVE CONFINING PRESSURE: 20.0 P.S.I.
INDUCED STRESS (PSI)
6.015
4.010
2.005
0.000
-2.005
-4.010
-6.015
STRAIN DECIMAL
0.225
0.150
0.075
0.000
-0.075
0.0
10.0
20.0
30.0
40.0
50.0
TIME SECONDS.
INDUCED PORE PRESSURE (PSI)
16.935
11.290
5.645
0.000
-5.645

FIG. 11B

SAMPLE #: TEST 19 UNIFORM GREY SAND
BORING #: 5 DEPTH : 35.0 FT.
EFFECTIVE CONFINING PRESSURE: 20.0 P.S.I.

X = AVERAGE PORE PRESSURE ACROSS THE SAMPLE
B = PORE PRESSURE BOTTOM OF SAMPLE
T = PORE PRESSURE TOP OF THE SAMPLE

TIME HISTORY OF PORE PRESSURE

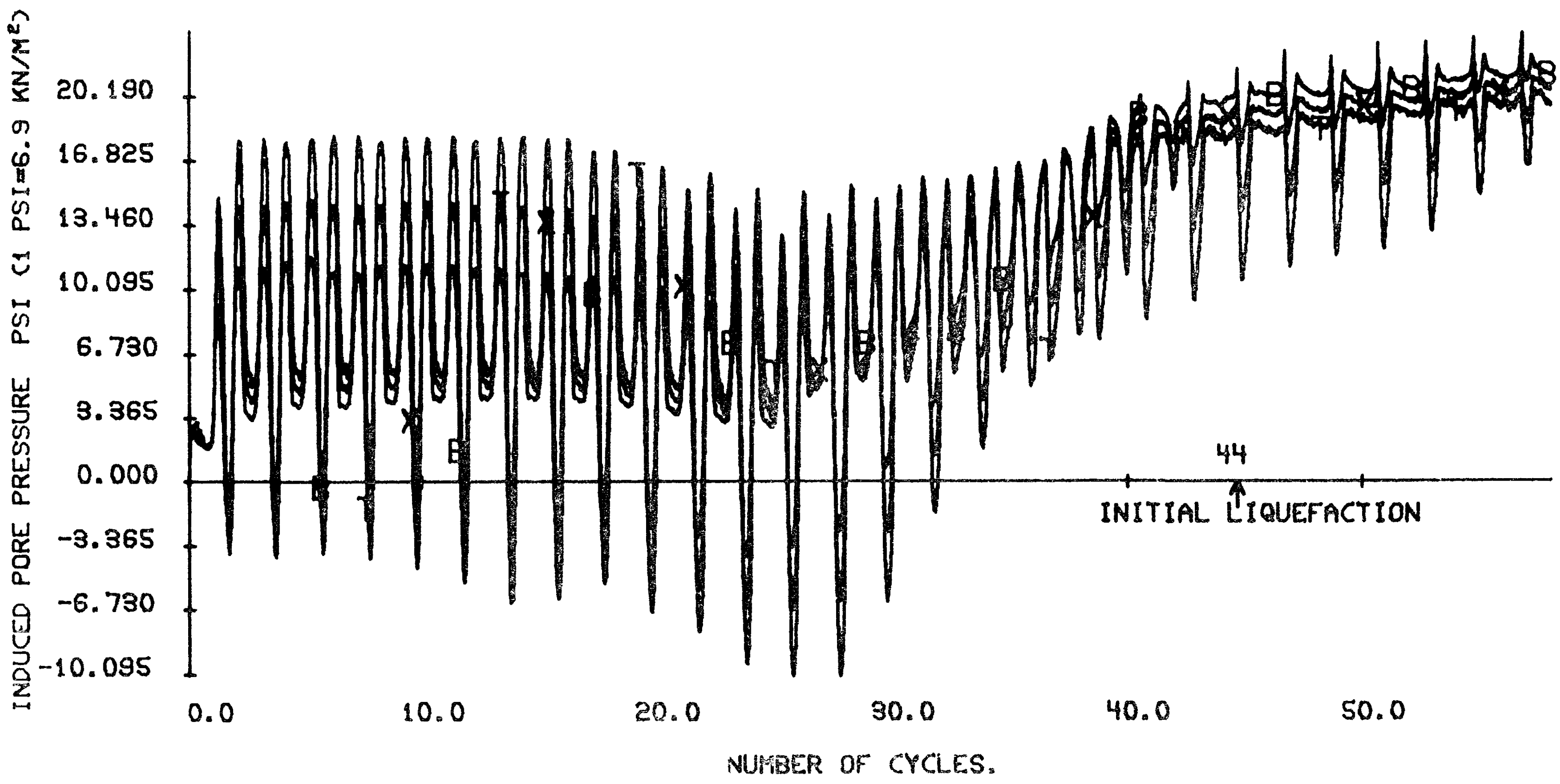

FIG. 12B

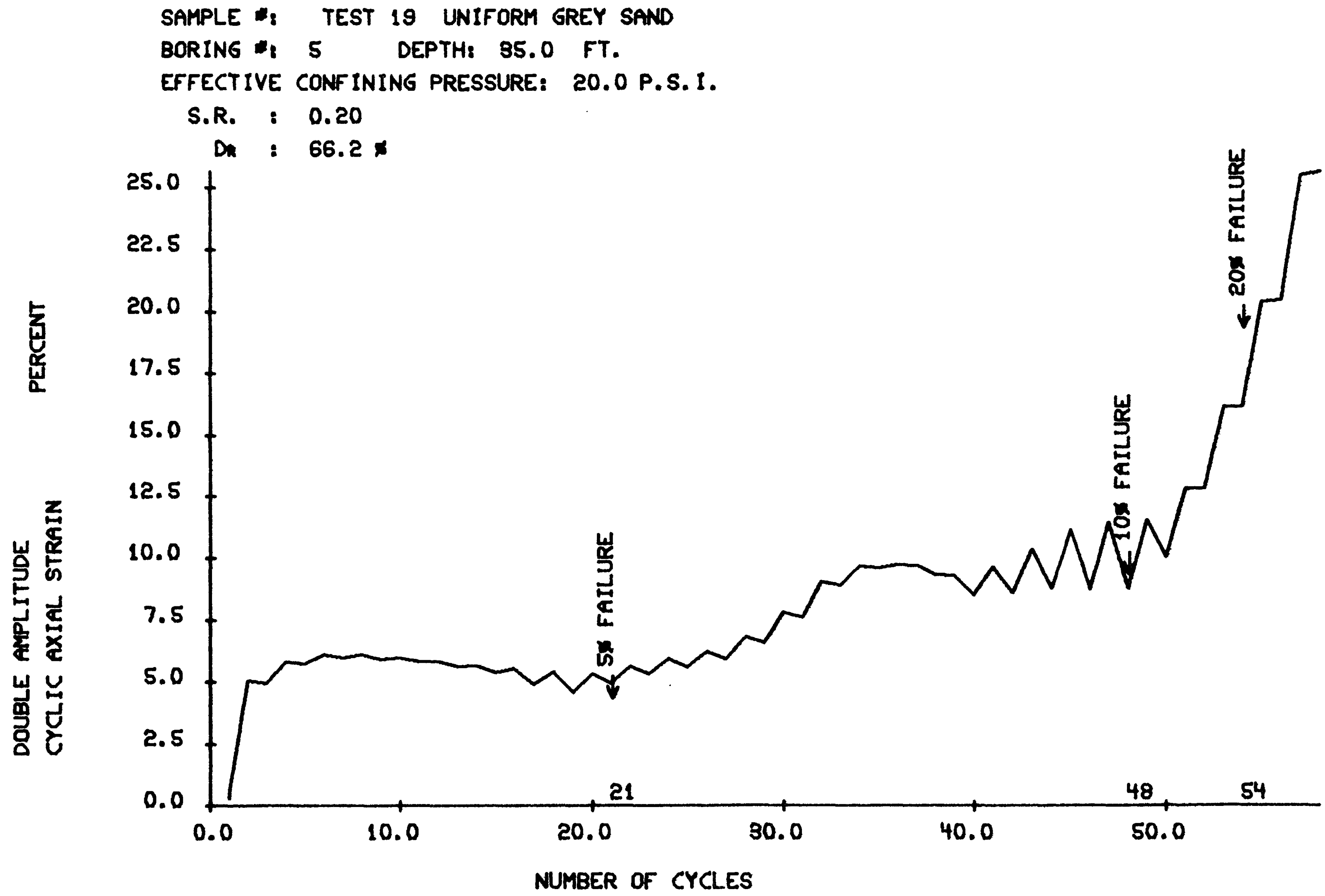
SAMPLE #: TEST 19 UNIFORM GREY SAND
BORING #: 5 DEPTH: 85.0 FT.
EFFECTIVE CONFINING PRESSURE: 20.0 P.S.I.
S.R. : 0.20
Dr : 66.2 %
DOUBLE AMPLITUDE
CYCLIC AXIAL STRAIN
PERCENT
25.0
22.5
20.0
17.5
15.0
12.5
10.0
7.5
5.0
2.5
0.0
5% FAILURE
10% FAILURE
20% FAILURE
21
48
54
0.0
10.0
20.0
30.0
40.0
50.0
NUMBER OF CYCLES

FIG. 13B

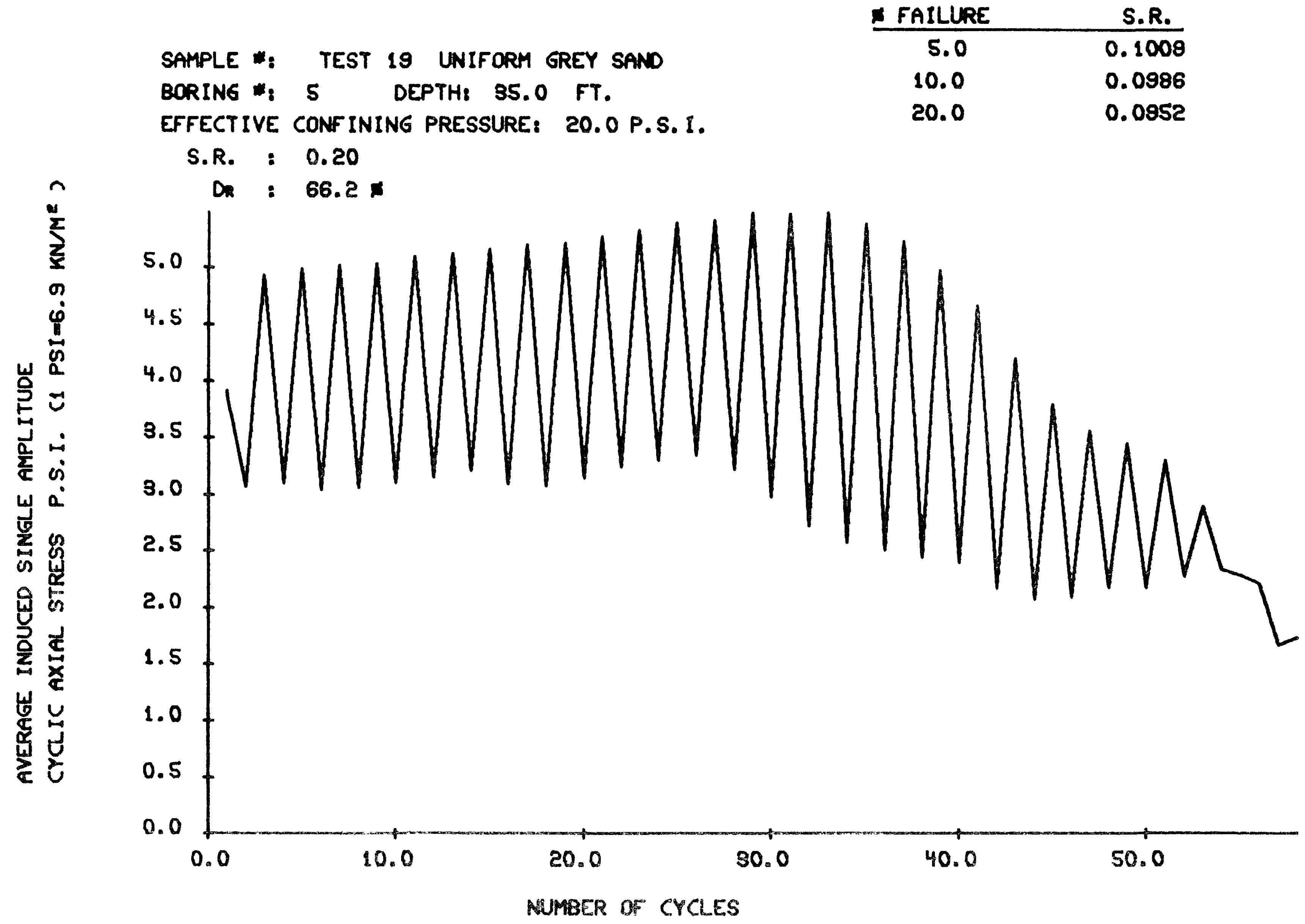
SAMPLE #: TEST 19 UNIFORM GREY SAND
BORING #: 5 DEPTH: 35.0 FT.
EFFECTIVE CONFINING PRESSURE: 20.0 P.S.I.
S.R. : 0.20
Dr : 66.2 %
% FAILURE S.R.
5.0 0.1008
10.0 0.0986
20.0 0.0952
AVERAGE INDUCED SINGLE AMPLITUDE
CYCLIC AXIAL STRESS P.S.I. (1 PSI=6.9 KN/M²)
0.0
0.5
1.0
1.5
2.0
2.5
3.0
3.5
4.0
4.5
5.0
0.0
10.0
20.0
30.0
40.0
50.0
NUMBER OF CYCLES

FIG. 14B

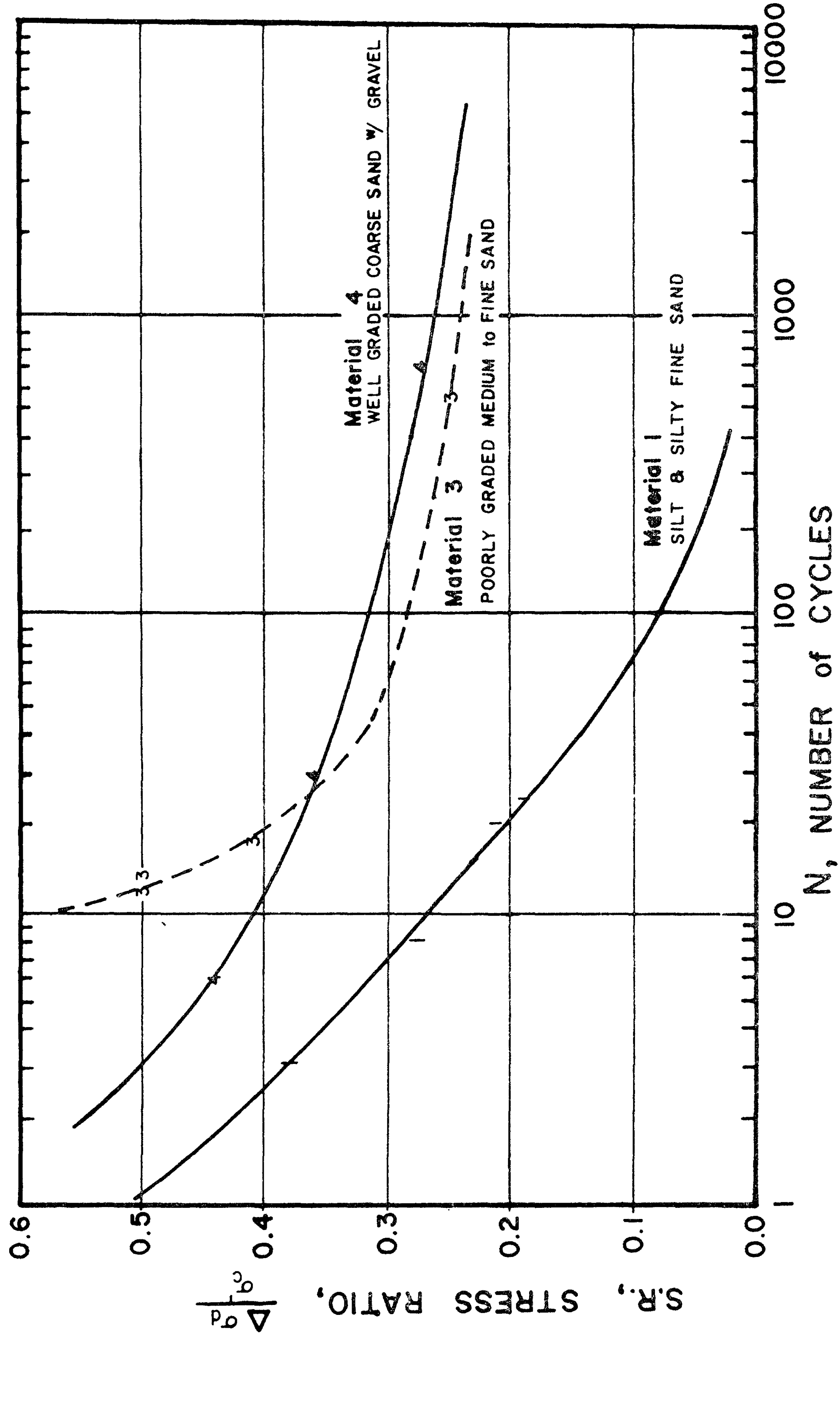
Material 4
WELL GRADED COARSE SAND w/ GRAVEL
Material 3
POORLY GRADED MEDIUM to FINE SAND
Material 1
SILT & SILTY FINE SAND
S.R., STRESS RATIO, $\frac{\Delta q_d}{q_c}$
N, NUMBER of CYCLES
0.0
0.1
0.2
0.3
0.4
0.5
0.6
1
10
100
1000
10000

Fig. 15B